

Novel applications of Cardiovascular Magnetic Resonance in acute myocardial injury

A dissertation for the degree of Doctor of Philosophy

Dr Mayooran Shanmuganathan, BSc, MBBS, MRCP

Lady Margaret Hall, University of Oxford

Oxford Centre for Clinical Magnetic Resonance Research (OCMR)

Acute Vascular Imaging Centre (AVIC)

Radcliffe Department of Medicine | Division of Cardiovascular Medicine

Thesis submission: 21st April 2023

Thesis upload (to Oxford University research archive): 31st October 2023

Supervisors

Professor Vanessa Ferreira, Professor of Cardiovascular Medicine

Professor Keith Channon, Professor of Cardiovascular Medicine

Professor Stefan Piechnik, Professor of Biomedical Imaging

Acknowledgements

I will forever be grateful to all three of my supervisors; Professors Vanessa Ferreira, Keith Channon and Stefan Piechnik, for placing their trust in me, taking me under their wings and providing excellent mentorship, guidance and academic teaching throughout my studies. I am indebted to Professor Ferreira for her teachings and the patience and persistence she showed in allowing me to develop my research skills and projects and being a very responsive and supportive supervisor. I am honoured to have been supervised by Professor Channon who, not only provided the necessary academic support and research infrastructure for this DPhil, but also offered me many words of wisdom and support during harder times to help guide me achieve success throughout the past four years. Professor Piechnik' s immense support during the discovery phase of Chapter 6 was undoubtedly the cornerstone for its success. I am grateful to his astute comments and feedback on all my research findings and his friendly support throughout the years. I am convinced that the experience I have gained from the time with the supervisors will shape my scientific thinking and professional practice for the rest of my life.

I was fortunate to be supported by a large team of scientists, clinicians and others in Acute Vascular Imaging Centre (AVIC), Oxford Centre for Magnetic Resonance Research (OCMR) and the Oxford Heart Centre in John Radcliffe Hospital. Amongst them are the Oxford Acute Myocardial Infarction (OxAMI) study investigators, research fellows and research nurses and co-ordinators without whom I could not have performed my research projects. In particular, I would like to reserve special gratitude to Alison Fletcher, Peter Manley, Yujun Ng, Alessandra Borlotti, Rafail Kotronias, and Giovanni Luigi De Maria for helping me run the very challenging OxAMI studies. I thank Roberto Scarsini and Ambra Masi for working with me on important projects which have since been published in high-ranking journals. I also

would like to thank Abhirup Banerjee and Matthew Burrage for providing me with immense academic and pastoral support and, more importantly, friendship throughout the past 4 years.

I am grateful to have received the Alison Brading Memorial Graduate Scholarship from Lady Margaret Hall, University of Oxford to fund my DPhil study. I also acknowledge support from NIHR BRC for funding my research projects. I sincerely thank all the volunteers and patients who participated in the research projects that have contributed to my thesis.

I thank Prof Saul Myerson and Prof Stefan Neubauer for supporting and supervising my clinical training in reporting of CMR scans throughout my time in OCMR. I am very grateful to Qiang Zhang to have been offered a chance a participate in his pioneering research outputs of late.

Last but not the least, I would like to thank my entire family including my loving wife and our beautiful children, who offered much needed mental and physical support and were kind enough to put up with my absence from family time on many evenings during the past four years. I am indebted to both my Sithappa and Sithi, to whom I dedicate this Thesis for raising me with so much love and making me who I am today, and my Maama and Maami for their kind understanding and immense help in supporting me and my family during my studies in Oxford.

"What is learnt is a handful of sand, while what is unknown is the size of the world"

"Never stop learning"

-Translated from Āthichūdi by Avvaiyar, Tamil poet, ~12th Century AD-

Declaration

The work presented in thesis is my own unless otherwise indicated. I have acknowledged assistance from colleagues and collaborators where relevant. It has not been submitted, either wholly or substantially, for another degree at this university, or for a degree at any other institution.

Word count: The Abstract and Chapters 1 to 7 contain ~30,000 words

Abstract

Acute myocardial injury, defined as an acute rise and fall in cardiac Troponin, is a common reason for hospital admission, and can be triggered by ischaemic and non-ischaemic pathologies. Accordingly, most patients admitted to hospital with clinically significant acute myocardial injury undergo an invasive coronary angiogram (ICA) to screen for coronary artery disease (CAD). However, there are clinically-important limitations with this approach and it is likely that cardiovascular magnetic resonance imaging (CMR), given its status as the gold standard imaging test in the assessment of the causes and the extent of myocardial disease, can add clinical value as a non-invasive approach, either alone or in conjunction with ICA. However, at present, CMR's use is mostly confined to stable outpatients. In this Thesis, I examine the role of acute CMR in four different cohorts of acutely ill hospitalised patients with acute myocardial injury.

Firstly, a significant proportion of patients admitted to hospital with acute myocardial injury and suspected Non-ST-segment Elevation Myocardial Infarction (NSTEMI) are found to have unobstructed coronary arteries, suggestive of either a non-ischaemic acute myocardial injury such as myocarditis or MI with non-obstructive coronary arteries (MINOCA). At present an early Cardiovascular magnetic resonance imaging (CMR) is recommended in patients with unobstructed coronary arteries within twenty-eight days of discharge from hospital to reach a clinical diagnosis, which has therapeutic and prognostic implications. On the other hand, some patients with confirmed MI on ICA are found to have stenosis in more than one coronary artery, which can render it difficult to identify the infarct related artery (IRA). Taken together, diagnosing non-ischaemic pathologies upfront may obviate the need for ICA whilst identifying the IRA can offer precise management of MI. In Chapter 3, I investigated if a *CMR-first strategy* in patients with acute myocardial injury has the potential to change management in patients waiting to have ICA for suspected NSTEMI. I found that a

such a strategy could have changed the clinical management in at least 31% of patients by reclassifying diagnosis in those with non-obstructed coronary arteries (17%) and in MI (7%) and offering a new IRA in MI (7%).

Secondly, acute myocardial injury was reported in approximately one fifth of hospitalised and unvaccinated patients with COVID-19 infection at the beginning of the current pandemic and it was associated with reduced survival. However, the cause of the myocardial injury remained unclear as these patients were not systematically evaluated with CMR at the time of the injury due to pandemic restrictions. Interestingly, CMR scans of unselected survivors of COVID-19, performed a few months after the acute illness, had reported myocardial inflammation and infarction in some patients, but the clinical implication to acutely-hospitalized patients with acute COVID-19 remained unclear. Chapter 4 investigated for the presence of myocardial abnormalities on CMR in unvaccinated, acutely ill and hospitalised COVID-19 patients with and without acute myocardial injury when compared to uninfected and asymptomatic controls from the community. I observed that acute COVID-19 induces mild myocardial oedema in some patients, but it returns to normal levels at six months after the acute illness.

Thirdly, some patients with acute myocardial injury due to with ST-segment elevation myocardial infarction (STEMI) present late, when the injury may already be established. Characterising of the extent and nature of acute myocardial injury in these patients (presenting twelve to forty-eight hours after the onset of chest pain) prior to ICA may of be of use when deciding whether to revascularise. Chapter 5 reports the investigation that involved performing CMR in patients with late-presenting STEMI just before and three days after revascularisation. I found no significant changes in ventricular function, area at risk and infarct size between the two scans except a reduction in the size of microvascular obstruction.

The study's findings suggest that it is feasible to safely conduct acute CMR scans in patients with late-presenting STEMI prior to ICA and that revascularisation appears to confer neither a positive or negative immediate impact on the magnitude of the acute myocardial injury.

Finally, the degree of acute myocardial injury in the infarcted myocardium in patients with revascularised STEMI has been shown to be strongly associated with long-term clinical outcomes. However, less is known about the prognostic relevance of the changes that are known to take place in the non-infarcted myocardium immediately after STEMI; acute injury to the remote non-infarcted myocardium is believed to represent an adverse inflammatory reaction secondary to a response to the MI from the innate immune system and it has been detected with CMR T1-mapping. In Chapter 6, I used CMR T1 mapping to detect the injuries in the entire heart including both the infarcted and the non-infarcted myocardium at two days after timely reperfused STEMI. I found that non-infarcted myocardial injury is an independent predictor of the risk of developing heart failure and related cardiac events at long-term, justifying further research into therapeutic modulation of myocardial inflammation post-STEMI. Moreover, I found that the T1 values in the infarcted and non-infarcted myocardium provided superior risk prediction than the conventional CMR indices of the infarcted myocardium (intramyocardial haemorrhage, area at risk, infarct size and microvascular obstruction) and of global left ventricular function (left ventricular ejection fraction). My findings indicate that non-contrast T1-mapping offers a more complete assessment of the pan-myocardial injury post-STEMI than the traditional contrast-based metrics of the infarcted myocardium and perhaps could be used as a biomarker in future clinical trials of patients with MI.

Overall, this Thesis presents fresh evidence to support the clinical application of acute CMR in acutely ill hospitalised patients with acute myocardial injury, as it can accurately diagnose

both non-ischaemic and ischaemic pathologies, enable avoidance of unnecessary invasive testing and guide treatment pathways. Moreover, it provides new and highly promising evidence that an acute CMR (in particular T1 mapping) can help identify patients at long-term risk of heart failure after a revascularised STEMI. Both of these findings lay the foundation to build clinical trials to test the clinical and cost-effectiveness of acute CMR in patients admitted to hospital with acute myocardial injury.

Publications

Manuscripts Contributing to DPhil Thesis

1. Acute Response in the Noninfarcted Myocardium Predicts Long-Term Major Adverse Cardiac Events After STEMI. **Shanmuganathan M**, Masi A, Burrage MK, et al... JACC Cardiovasc Imaging. 2023;16:46–59.
2. Acute changes in myocardial tissue characteristics during hospitalization in patients with COVID-19. **Shanmuganathan M**, Kotronias RA, Burrage MK, et al... Front Cardiovasc Med. 2023;10:1097974.

Abstracts / Presentations contributing to DPhil Thesis

1. Long-term prognosis after acute ST-segment elevation myocardial infarction is determined by characteristics in both non-infarcted and infarcted myocardium on cardiovascular magnetic resonance imaging. **Shanmuganathan M**, Masi A, Burrage MK, et al… Heart. 2021;107:A1–A1. [BSCMR 2021]
2. Hospitalized patients with Covid-19 and bacterial sepsis have similar T1 and T2 abnormalities on CMR. **Shanmuganathan M,** et al… [SCMR 2022 Scientific Sessions]
3. CMR first strategy in patients with suspected NSTEMI may help identify MINOCA and infarct related artery. **Shanmuganathan M**, Borlotti A, Scarsini R, et al. Eur Heart J - Cardiovasc Imaging. 2021;22:jeaa356.255. [ESC Cardiovascular Imaging Congress 2020]

Other publications related to DPhil studies

3. Coronary microvascular dysfunction assessed by pressure wire and CMR after STEMI predicts long-term outcomes; R Scarsini*, **M Shanmuganathan***, GL De Maria, A Borlotti, RA Kotronias, …JACC: Cardiovascular Imaging 14 (10), 1948-1959 15 2021[***Joint first authors**]
4. Angiography-derived index of microcirculatory resistance (IMRangio) as a novel pressure-wire-free tool to assess coronary microvascular dysfunction in acute coronary syndromes …R Scarsini*, **M Shanmuganathan***, RA Kotronias, D Terentes-Printzios, ...et al The International Journal of Cardiovascular Imaging 37 (6), 1801-1813 24 202 [* **Joint first authors**]
5. Myocardial Involvement After Hospitalization for COVID-19 Complicated by Troponin Elevation: A Prospective, Multicenter, Observational Study. J Artico, H Shiwani, JC Moon, m Gorecka, HP McCann, G Roditi, A Morrow, K Mangion, E Lukaschuk, **M Shanmuganathan M**… et al. Circulation. 2023 Jan 27;147(5):364-374.
6. Artificial Intelligence for Contrast-Free MRI: Scar Assessment in Myocardial Infarction Using Deep Learning–Based Virtual Native Enhancement; Q Zhang, MK Burrage, **M Shanmuganathan**, RA Gonzales, E Lukaschuk, ...et al Circulation 146 (20), 1492-1503 2 2022

Neuropeptide-Y Levels in ST-Segment–Elevation Myocardial Infarction: Relationship With Coronary Microvascular Function, Heart Failure, and Mortality; T Gibbs, N Tapoulal, **M Shanmuganathan**, MK Burrage, A Borlotti, ...et al Journal of the American Heart Association 11 (13), e024850 3 2022

7. Neutrophils incite and macrophages avert electrical storm after myocardial infarction J Grune, AJM Lewis, M Yamazoe, M Hulsmans, D Rohde, L Xiao, ...**M Shanmuganathan**,…et al;Nature cardiovascular research 1 (7), 649-664 6 2022

Rapid neutrophil mobilization by VCAM-1+ endothelial cell-derived extracellular vesicles; N Akbar, AT Braithwaite, EM Corr, GJ Koelwyn, C van Solingen, ...**M Shanmuganathan**…; Cardiovasc Res. 2023 Mar 17;119(1):236-251

8. Pressure-controlled intermittent coronary sinus occlusion improves the vasodilatory microvascular capacity and reduces myocardial injury in patients with STEMI; R Scarsini, D Terentes-Printzios, **M Shanmuganathan**, RA Kotronias, ...Catheterization and Cardiovascular Interventions 99 (2), 329-339 5 2022
9. Comparative and Integrated Analysis of Plasma Extracellular Vesicles Isolations Methods in Healthy Volunteers and Patients Following Myocardial Infarction; D Paget, A Checa, B Zohrer, **M Shanmuganathan,** R Dhaliwal, E Johnson, ...Journal of Extracellular Biology 1 (11), e66 2022
10. From anatomy to function and then back to anatomy: invasive assessment of myocardial ischemia in the catheterization laboratory based on anatomy-derived indices of coronary; GLDE Maria, S Wopperer, R Kotronias, **M Shanmuganathan,** R Scarsini, ... Minerva cardiology and angiology 69 (6), 626-640 2021 Minerva Cardiology and Angiology 2021
11. Pre-procedural ATI score (age-thrombus burden-index of microcirculatory resistance) predicts long-term clinical outcomes in patients with ST elevation myocardial infarction …C Montalto, RA Kotronias, F Marin, D Terentes-Printzios, ...**M Shanmuganathan**…et al International Journal of Cardiology 339, 1-6 2 2021
12. Toward replacing late gadolinium enhancement with artificial intelligence virtual native enhancement for gadolinium-free cardiovascular magnetic resonance tissue; Q Zhang, MK Burrage, E Lukaschuk, **M Shanmuganathan**, IA Popescu, .. et al. Circulation 144 (8), 589-599 27 2021

MOCOnet: robust motion correction of cardiovascular magnetic resonance T1 mapping using convolutional neural networks; RA Gonzales, Q Zhang, BW Papież, K Werys, E Lukaschuk, IA Popescu, **M Shanmuganathan**…et al Frontiers in Cardiovascular Medicine 8 2 2021

13. Long-term clinical outcomes in patients with an acute ST-segment-elevation myocardial infarction stratified by angiography-derived index of microcirculatory resistance; RA Kotronias, D Terentes-Printzios, **M Shanmuganathan**, F Marin, ..et al. Frontiers in cardiovascular medicine 8 17 2021
14. Medium-term effects of SARS-CoV-2 infection on multiple vital organs, exercise capacity, cognition, quality of life and mental health, post-hospital discharge; B Raman, MP Cassar, EM Tunnicliffe, N Filippini, L Griffanti, ... **M Shanmuganathan** …et al; EClinicalMedicine 31, 100683 397 2021

COVID-19 and cardiac considerations in the community; C A'Court, **M Shanmuganathan,** JC Leoni-Moreno; British Journal of General Practice 70 (700), 524-525 1 2020

15. Angiography-derived index of microcirculatory resistance as a novel, pressure-wire-free tool to assess coronary microcirculation in ST elevation myocardial infarction; GL De Maria, R Scarsini, **M Shanmuganathan**, RA Kotronias, ...et al, The international journal of cardiovascular imaging 36 (8), 1395-1406 48 2020

Pressure-bounded coronary flow reserve to assess the extent of microvascular dysfunction in patients with ST-elevation acute myocardial infarction. R Scarsini, GL De Maria, **M Shanmuganathan**, RA Kotronias, ...et al, Eurointervention: EuroIntervention. 2021 Apr 20;16(17):1434-1443.

Awards and Prizes during DPhil study

1. **Alison Brading Graduate Scholarship in Medical Sciences by Lady Margaret Hall, University of Oxford**

2. **University's Award for Excellence, RDM Cardiovascular Medicine, University of Oxford, 2019/2020 –** received for exceptional level of commitment, flexibility and adaptability towards AVIC and OxAMI studies

3. **Finalist in Rapid-fire oral presentation at the 16th British Society of CMR annual meeting 2021, London**
    a. *"Long-term prognosis after acute ST-segment elevation myocardial infarction is determined by characteristics in both non-infarcted and infarcted myocardium on cardiovascular magnetic resonance imaging"*

Table of Contents

Acknowledgements 2
Declaration 5
Abstract 6
Publications 10
Manuscripts Contributing to DPhil Thesis 10
Abstracts / Presentations contributing to DPhil Thesis 10
Other publications during my DPhil studies (2019-to-date) 10
Awards and Prizes during DPhil study 12
Abbreviations 17
1. Introduction to Thesis 19
1.1 Overview 20
1.2 Acute myocardial injury 23
1.2.1 Definition of acute myocardial injury 23
1.2.2 Pathophysiology of acute myocardial injury 23
1.2.3 Definition of Acute Myocardial Infarction 25
1.2.4 Importance of differentiating between types of acute myocardial injury 27
1.3 Invasive coronary angiography 31
1.4 Cardiovascular Magnetic Resonance Imaging 33
1.4.1 Physics foundations of MRI 33
1.4.2 CMR sequences 34
1.4.3 CMR in contemporary clinical practice ..... **Error! Bookmark not defined.**
1.4.4 CMR's current role in assessing acute myocardial injury 37
1.5 Knowledge gaps – clinical application of acute CMR in acute myocardial injury 40
1.5.1 Acute myocardial injury in suspected Non-ST-segment Elevation Myocardial Infarction prior to invasive coronary angiography 40
1.5.2 Acute myocardial injury in acute COVID-19 42
1.5.3 Acute myocardial injury in late presenting ST-segment Elevation Myocardial Infarction 43
1.5.4 Prognostic significance of acute changes in the non-infarcted myocardium in revascularised ST-segment Elevation Myocardial Infarction 44
1.6 Overview of Thesis 46
2. Methods 48
2.1 Ethical considerations 49

2.1.1 OxAMI study 49
2.2 Study Participants 50
2.2.1 Patients 50
2.2.2 Controls (asymptomatic volunteers) 52
2.3 Standard OxAMI Study Protocol 53
2.4 CMR methods 54
2.4.1 CMR imaging protocol 54
2.4.2 CMR sequences 54
2.4.3 CMR image analysis 57
2.5 Invasive coronary physiology 61
2.6 Blood sampling and ECGs 62
2.7 Follow up for the assessment of clinical outcomes 62
2.8 Statistical analysis 63
2.9 Summary 64
3. **Clinical Utility of Cardiovascular Magnetic Resonance Prior To Invasive Coronary Angiography In Suspected Non-ST Segment Elevation Myocardial Infarction** 65
3.1. Introduction 66
3.2. Methods 67
3.2.1. CMR scanning 68
3.2.2. CMR image analysis 68
3.2.3. Clinical management 69
3.2.4. Statistical analysis 70
3.3. Results 70
3.3.1. Study population – suspected NSTEMI 70
3.3.2. CMR findings pre-invasive coronary angiography (ICA) 70
3.3.3. Invasive coronary angiography (ICA) findings 76
3.3.4. Comparison of diagnoses made on CMR and ICA 76
3.3.4.1. ICA-NOCA vs CMR diagnoses 79
3.3.4.2. ICA-IRA vs CMR-IRA 79
3.4. Potential clinical utility of CMR pre-ICA 79
3.5. Discussion 81
3.5.1. Limitations 84
3.6. Conclusion 85
4. **Acute changes in myocardial tissue characteristics during early hospitalization in patients with COVID-19** 86

4.1 Introduction 87
4.2 Methods 87
4.3 Results 90
4.4 Discussion 98
4.4.1 Limitations 102
4.5 Conclusion 104
5. The Impact of Acute Revascularisation in Late-Presenting ST-Segment Elevation Myocardial Infarction: A Study of Acute Myocardial Injury Using Cardiovascular Magnetic Resonance 105
5.1 Introduction 106
5.2 Methods 107
5.2.1 Study population 107
5.2.2 CMR methods 107
5.2.3 CMR image analysis 108
5.2.4 Invasive coronary angiogram, angiographic analysis, and indices of microcirculatory function 109
5.2.5 Statistical analysis 109
5.3 Results 110
5.3.1 Angiographic findings 111
5.3.1.1 Pre-PCI findings 111
5.3.1.2 Post-PCI findings 111
5.4 CMR findings 114
5.4.1 Ventricular function, area at risk and infarct size at both time points 114
5.4.2 Microvascular injury (MVO and IMH) at both time points 114
5.4.3 Associations between clinical features and CMR findings 115
5.5 Discussion 122
5.5.1 Limitations 126
5.6 Conclusion 126
6. Acute Response in the Non-infarcted Myocardium Predicts Long-term Major Cardiovascular Events After ST-elevation Myocardial Infarction 127
6.1. Introduction 128
6.2. Methods 130
6.2.1. Study population and treatment 130
6.2.2. CMR imaging 130
6.2.3. Image analysis 131
6.2.3.1. Deriving T1 values in infarcted, non-infarcted and remote myocardium 132

6.2.3.2. Angiographic analysis 132
6.2.4. Major adverse cardiac events (MACE) 134
6.2.5. Statistical analysis 134
6.3. Results 136
6.3.1. Baseline clinical characteristics 136
6.3.2. Acute tissue characteristics of the infarcted myocardium 140
6.3.2.1. Acute tissue characteristics of the non-infarcted myocardium 140
6.3.2.2. Acute tissue characteristics of the remote zone *within* the non-infarcted myocardium 140
6.1.1. LV characteristics at 6-month follow-up 142
6.1.1.1. Predictive power of acute T1 indices for short-term (6-month) outcomes 143
6.1.2. Long-term MACE and Cox regression analysis 144
6.1.2.1. Univariate Cox regression analysis of long-term MACE 144
6.1.2.2. Multivariate Cox regression analysis of MACE 146
6.1.2.3. Discrimination and risk reclassification for MACE using novel T1 indices 150
6.4. Discussion 153
6.4.1. Limitations 158
6.5. Conclusion 161
7. Conclusions and Future Directions 163
List of Tables 166
List of Figures 167
References 170

Abbreviations

AMI	Acute Myocardial Infarction
AVIC	Acute Vascular Imaging Centre
cTn	Cardiac Troponin
CAD	Coronary Artery Disease
CFR	Coronary Flow Reserve
CMP	Cardiomyopathy / Cardiomyopathies
CMR	Cardiovascular Magnetic Resonance Imaging
DCM	Dilated Cardiomyopathy
ECG	Electrocardiogram
ECV	Extracellular Volume
EDV	End-Diastolic Volume
EF	Ejection Fraction
ESV	End-Systolic Volume
FOV	Field of View
FFR	Fractional Flow Reserve
GBCA	Gadolinium-Based Contrast Agent
HLA	Horizontal Long Axis
ICA	Invasive Coronary Angiography
IHD	Ischaemic Heart Disease
IMH	Intramyocardial Haemorrhage
IMR	Index of Microcirculatory Resistance
IRA	Infarct Related Artery
IQR	Interquartile Range
IV	Intravenous
LGE	Late Gadolinium Enhancement
LV	Left Ventricle/Ventricular
LVOT	Left Ventricular Outflow Tract
MINOCA	Myocardial Infarction with non-obstructive coronary arteries

MOLLI	Modified Look-Locker Inversion Recovery
MVD	Multivessel disease
MVO	Microvascular obstruction
Mz	Longitudinal Magnetization
NSTEMI	Non ST-segment Elevation Myocardial Infarction
NT-proBNP	N-Terminal pro B-type Natriuretic Peptide
OCMR	Oxford Centre for Clinical Magnetic Resonance Research
OUH	Oxford University Hospitals NHS Foundation Trust
OXAMI	Oxford Acute Myocardial Infarction Study
PCI	Percutaneous Coronary Intervention
PPCI	Primary Percutaneous Coronary Intervention
RF	Radiofrequency
SAX	Short Axis
SCAD	Spontaneous Coronary Artery Dissection
ShMOLLI	Shortened Modified Look-Locker Inversion Recovery
SSFP	Steady-State Free Precession
STEMI	ST-segment Elevation Myocardial Infarction
SV	Stroke Volume
TD	Trigger Delay
TE	Echo Time
TI	Inversion Time
TR	Repetition Time
T1	1st time constant (Longitudinal, Spin-Lattice Relaxation) in Bloch equation
T2	2nd time constant (Transverse, Spin-Spin Relaxation) in Bloch equation
T2w	T2 weighted
URL	Upper Reference Limit

1. Introduction to Thesis

1.1 Overview

Acute myocardial injury is a common cause of hospital admissions and is associated with significant morbidity, mortality and socio-economic ramifications (1). Whilst there are many causes of acute myocardial injury, the most common is acute myocardial infarction (AMI) (2). Besides clinical history, electrocardiography (ECG), cardiac troponin levels and echocardiography, invasive coronary angiography (ICA) is frequently undertaken during the patient's hospital admission to make a diagnosis and plan the treatment (3). ICA allows the detection of coronary artery abnormalities and enables revascularisation of any coronary stenosis in the same setting. However, a significant proportion of clinical presentations remain undifferentiated even after performing ICA and require further investigations to tease out the causes of acute myocardial injury. The non-ischaemic causes include stress-cardiomyopathy, myocarditis, and systemic illness (such as sepsis and COVID-19), amongst others (4). Even if the ICA is not conclusive, the aetiology of the acute myocardial injury may still be ischaemic (i.e. missed diagnosis during ICA or MI with non-obstructive coronary arteries [MINOCA]) (4). Making an early and accurate diagnosis of the aetiology without the use of ICA is highly desirable and has the potential to avoid ICA in patients with non-ischaemic myocardial injury, improve clinical management, outcomes and clinical cost-effectiveness. Avoidance of ICA, in particular, when not needed, is highly desirable, as it is associated with procedural risks, longer in-hospital bed use and higher healthcare costs (5).

Patients with confirmed acute MI may often have multivessel coronary artery disease (MVD), which can render the identification of the culprit stenosis during an ICA difficult (6). It would therefore be desirable to be informed of the exact location in the heart of the MI prior to having the ICA. Thus, there remains an ongoing demand for better non-invasive

diagnostic tools and clinical pathways to help offer patient-specific precision medicine for hospitalised patients with acute myocardial injury (5,7,8).

Moreover, even after a clinical diagnosis of acute myocardial infarction is made with an ICA and appropriate therapies have been administered in the acute setting, there remains a need to accurately risk-stratify the patients. At present, echocardiogram is used to quantify left ventricular systolic function using ejection fraction (LVEF) and to guide pharmacotherapy, driving restrictions, return to work and the need for future follow-up. However, the measurement of LVEF on echocardiography suffers from high inter and intra-observer variability and sub-optimal image quality in patients with difficult acoustic windows (9). Furthermore, echocardiography fails to characterise the extent and the nature of myocardial tissue injury, which have been shown to possess a stronger association with clinical outcomes than LVEF (10), and thereby limiting its clinical effectiveness as a risk-stratifying tool.

Multi-parametric cardiovascular magnetic resonance imaging (CMR) is widely considered to be the gold-standard non-invasive imaging modality for both quantification of cardiac volumes and function (11), and characterisation of myocardial tissue (12). CMR has the potential to delineate the aetiology of acute myocardial injury and can help avoid ICA in patients with non-ischaemic pathologies. CMR can locate the acutely infarcted area in patients with acute MI, and this has the potential to guide clinical care during an ICA in patients with atherosclerosis in multiple coronary arteries (and thereby allowing a clinician to treat the culprit artery).

However, at present, the use of CMR is limited mainly to stable patients with sub-acute or chronic illness, and not patients with acute myocardial injury whilst they are in hospital (13). This may, in part, be due to the paucity of evidence for CMR's safety, clinical utility and

cost-effectiveness in acutely ill patients, especially in settings involving those with suspected acute MI prior to undergoing ICA.

CMR can also quantify the degree of acute myocardial injury after acute MI. This has the potential to help guide management of special cohorts of patients, such as those who present with late ST-segment elevation MI (STEMI). On the other hand, there is mounting evidence that CMR's tissue characterisation is superior (when compared to clinical characteristics, blood biomarkers and conventional echocardiography) in predicting the risk of future cardiovascular events, such as heart failure, arrhythmia and cardiac death (10,14). Specifically, infarct tissue characteristics, such as a large infarct size and the presence of microvascular obstruction and intramyocardial haemorrhage, are associated with adverse outcomes (10,14). However, such evidence has not led to the wide adoption of CMR post-acute MI in clinical practice for various reasons, including higher financial cost, long scanning time (~45 minutes), shortage of scanning slots for hospitalized patients, and contra-indications to CMR scanning, including that related to the administration of gadolinium-based contrast agents (GBCA). Accordingly, over the past few years, significant technical development has been made toward faster, contrast-free (and thus needle-free) and therefore, potentially cheaper, CMR scanning which can produce similar diagnostic readouts (15–18).

However, the prognostic relevance of such non-contrast CMR imaging is yet to be tested in the post-STEMI population. Moreover, though pathological changes have been observed after MI in the remote zone of the non-infarcted myocardium on CMR (19), their relevance to long-term prognosis has not been established.

The remainder of this chapter reviews the literature and identifies gaps, especially pertaining to CMR's role for diagnostic and prognostic purposes, in acute myocardial injury in hospitalised patients.

1.2 Acute myocardial injury

1.2.1 Definition of acute myocardial injury

The universal definition of myocardial injury is the presence of elevated cardiac troponin (cTn) values with at least one value above the 99th percentile of the upper reference limit (URL) (3). The myocardial injury is considered to be acute if there is a rise and/or fall in the cTn values.

Acute myocardial injury can arise from ischaemic and non-ischaemic pathologies. The commonest cause of ischaemic myocardial injury is acute MI, whilst non-ischaemic pathologies include acute myocarditis, stress-induced cardiomyopathy, drug cardiotoxicity or or toxin cardiomyopathy, cardiac arrhythmias, acute heart failure, as well as secondary to systematic illnesses, such as sepsis (1).

1.2.2 Pathophysiology of acute myocardial injury

A rise and fall in the serum levels of cardiac Troponin (cTn) is the hallmark of acute myocardial injury. The Tn complex is made up of 3 proteins – TnI, TnT and TnC, and regulates skeletal and cardiac contraction. The cardiac isoforms of TnI and TnT are the established biomarkers cardiomyocyte injury. In healthy humans, there is a constant release of cTn by living cardiomyocytes as well as via necrosis or apoptosis, as part of normal cellular renewal, which leads to a baseline concentration of cTn in the peripheral blood stream (20). This baseline cTn concentration varies with the isoform studied (cTnI being the most commonly used test in clinical practice), sex and age (males and older subjects have higher levels) (20).

Injured cardiomyocytes release significant amounts of the intra-cellular cTnI into the blood stream, leading to raised measured concentrations of cTnI. This can result from various

causes (***Figure 1.1***) but can broadly be categorised into ischaemic or non-ischaemic aetiologies (1). In both cases, there may be cellular stretching, injury and oedema, apoptosis and necrosis, with severity of acute myocardial injury being the worst in the latter (20).

Ischaemic acute myocardial injury may be the result of acute MI (there are 5 subtypes, as discussed later), acute heart failure, pulmonary embolism, catecholamine excess with acute intracranial pathologies (e.g. subarachnoid haemorrhage), tachyarrhythmias or after excessive physical exertion.

Non-ischaemic acute myocardial injury may be the result of myocardial inflammation (myocarditis, endocarditis, sepsis) due to environmental triggers or abnormal immune response, Takotsubo syndrome (also referred to as stress cardiomyopathy), cardiomyopathies with an acute flare (e.g. sarcoidosis, arrhythmogenic cardiomyopathy and sometimes hypertrophic cardiomyopathy), drug or substance toxicity. Chest trauma or procedures involving the heart can also cause myocardial injury via mechanical cell destruction and local inflammation.

It is worth noting that patients can present with acute myocardial injury from a combination of ischaemic and non-ischaemic pathophysiologies. Ischaemic acute myocardial injury, especially those with acute MI, can produce a very pronounced secondary myocardial inflammation, and, thus, the ensuing myocardial dysfunction during the acute illness can be attributed to both ischaemic and non-ischaemic mechanisms (21). Equally, even conditions traditionally considered to be non-ischaemic can induce a degree of ischaemia (e.g. catecholamine surge following intracranial bleed and Takotsubo syndrome) (20). Similarly, multiple mechanisms have been proposed for acute myocardial injury that takes place in sepsis: these include type 2 MI due to demand and supply mismatch, microbe-induced

myocardial inflammation, endotoxin and cytokine related injury, free-radical generation and microvascular dysfunction (20).

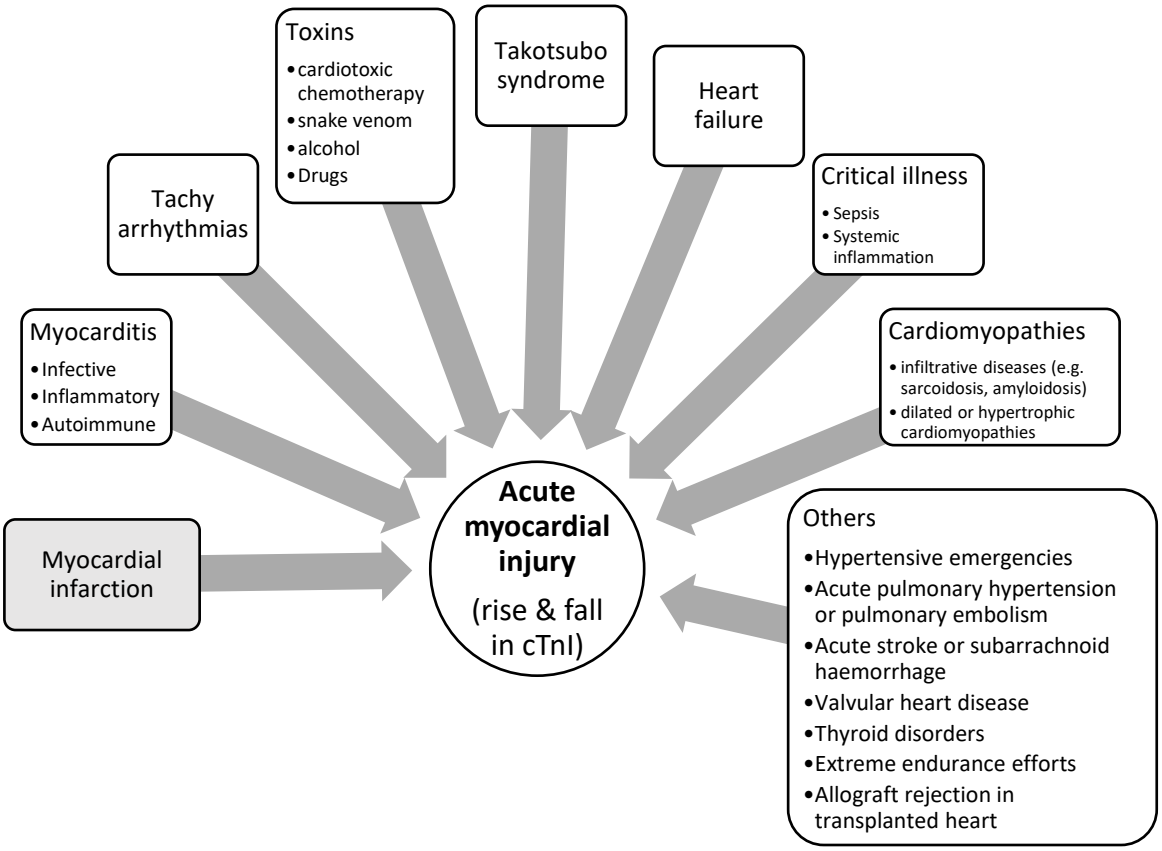


Figure 1.1 Causes of acute myocardial injury. Differentiating between myocardial infarction and non-ischaemic causes is crucial to the timely and precise management of patients with acute myocardial injury.

1.2.3 Definition of Acute Myocardial Infarction

Acute MI is diagnosed when the acute myocardial injury, with an associated rise and fall in cTn level, is present alongside clinical evidence of myocardial ischaemia. Myocardial ischaemia is confirmed when at least one of following is present: symptoms of myocardial ischaemia, new ischaemic ECG changes, development of pathological Q waves, imaging

evidence of loss of viable myocardium or new regional wall motion abnormality in a pattern consistent with an ischaemic aetiology, or the identification of coronary thrombus on angiography (3).

In terms of pathophysiology, acute MI is further categorised into five main types (3). The two commonest are: Types 1 and 2. Type 1 MI is caused by the rupture or an erosion of an atherosclerotic plaque in a coronary artery. Type 2 MI is due to an imbalance between demand and supply of myocardial oxygen in the presence of stable coronary atherosclerosis or due to vasospasm / coronary microvascular dysfunction or non-atherosclerotic coronary artery dissection or just due to oxygen supply-demand imbalance alone (3). (**Figure 1.2**).

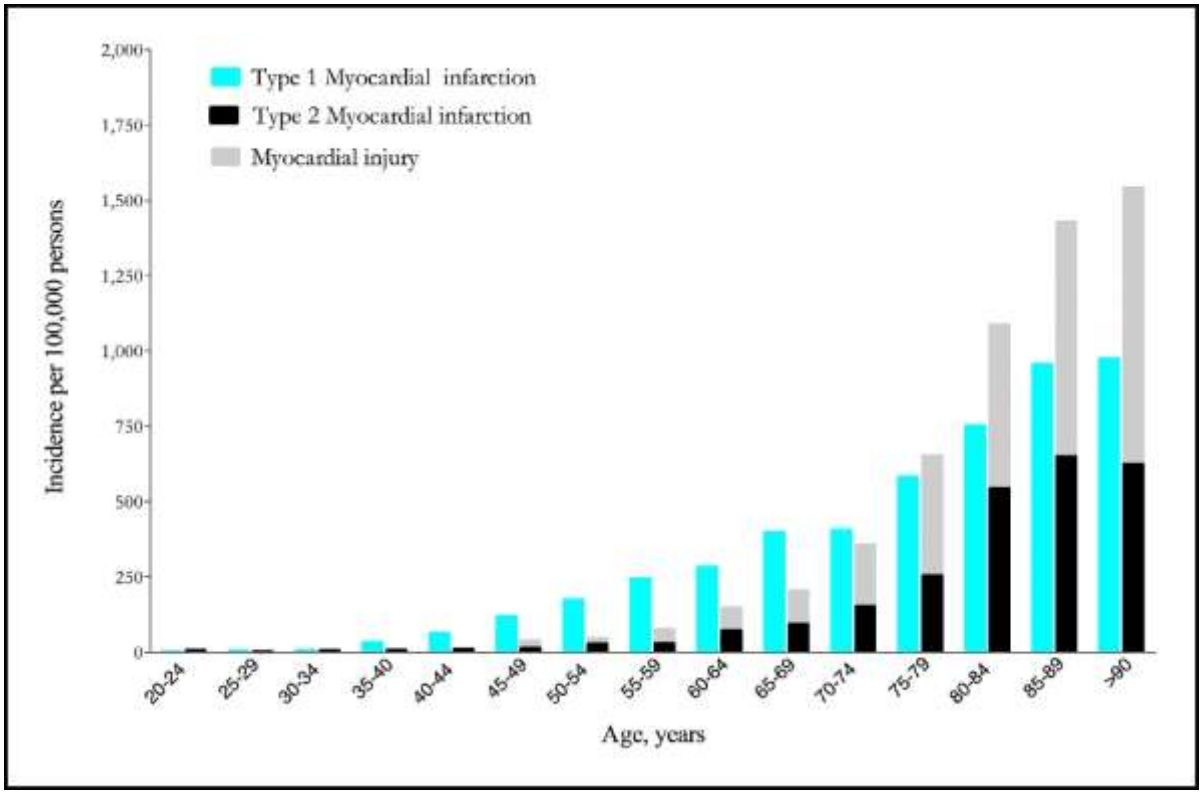


Figure 1.2 Incidence of Type 1 and Type 2 AMI and non-ischaemic acute myocardial injury in hospitalized patients with cardiac symptoms and rise in high-sensitive troponin in Lothian, Scotland. Source: Shah et al AJC 2015 (2), reproduced with permission (under Creative Comms)

Type 1 MI can also be sub-classified further into two forms, based on the abnormalities on ECG: ST-segment elevation MI (STEMI) and non-ST-segment elevation MI (NSTEMI), with both having distinctly different clinical management pathways. Type 3 MI is diagnosed when

a patient dies after having demonstrated evidence of myocardial ischaemia (e.g. chest pain or new ischaemic ECG changes or ventricular fibrillation) but before blood samples for cTn levels could be obtained. Type 4 MI is attributed to ischaemic complications during percutaneous coronary intervention and stent thrombosis and stenosis in the post-procedural period. Type 5 MI is diagnosed when a patient is found to have new MI after coronary artery bypass grafting (CABG).

This thesis focusses on acute myocardial injury due to Type 1 and Type 2 MI, and non-ischaemic causes. MI can present with or without ST-segment elevation on electrocardiogram (ECG). STEMI is widely considered to be a result of near or complete thrombotic occlusion of at least one coronary artery, and is treated as an emergency around the world; options include immediate pharmaco-thrombolysis or, as it is done in the UK, primary percutaneous coronary intervention (PPCI). Almost all cases of suspected NSTEMI are hospitalised, and approximately 70% undergo invasive coronary angiogram (ICA) within a few days. They may receive a PCI if a culprit coronary stenosis is found. Surgical revascularisation (CABG) may be offered in patients with significant multi-vessel disease not suitable for PCI.

1.2.4 Importance of differentiating between types of acute myocardial injury

Most non-ischaemic acute myocardial injury is treated supportively and, where applicable, by managing the precipitating conditions. Rarer conditions, such as giant cell or eosinophilic myocarditis or cardiac allograft rejection, require specific immunosuppressive therapies.

Clinical differentiation of the causes of acute myocardial injury based only on clinical history, ECG appearances and cTn dynamics can be challenging, and often requires ICA or computed tomography coronary angiography (CTCA) to exclude a Type 1 MI, and subsequent non-invasive imaging to help diagnose the cause. In patients with non-occlusive coronary artery disease (CAD), differentiating between Type 2 MI and non-ischaemic forms of acute myocardial injury can be very challenging (

Figure 1.3). MI can also take place in the setting of non-obstructed or normal coronary arteries (known as MINOCA), and adds further complexity to the diagnostic and treatment pathways. The uncertainty can lead to mis-diagnosis and inappropriate treatment, and has significant health and socio-economic implications (1,22). MVD is common in MI and the determination of the culprit or infarct related artery (IRA) can be challenging. The correct identification of IRA allows appropriate guideline-directed revascularisation strategies; for instance in STEMI trial evidence support the prompt reperfusion of the IRA with staged but urgent intervention to lesions with >50% luminal stenoses in the other coronary arteries; thereby achieving 'complete' revascularisation (23,24). The evidence for complete revascularisation in NSTEMI is less robust (24), meaning that it is important to accurately determine the IRA in patients with MVD before any decision on revascularisation is made in the acute setting.

The current coronavirus disease of 2019 (COVID-19) pandemic, caused by the severe acute respiratory syndrome coronavirus 2 (SARS-CoV-2), has led to significant number of hospitalisations and deaths across the globe, mainly due to its pulmonary involvement, hypoxia and systemic inflammation (25,26). However, early studies of hospitalized patients with COVID-19 reported high prevalence of acute myocardial injury (measured by Troponin rise) and its association with high in-hospital mortality (27–29). This raised several questions, including the need understand the cause of the acute myocardial injury (30). Clinical concerns regarding the apparent increased prevalence of myocarditis or myocardial infarction had to be balanced against the suggestion that acute myocardial injury was simply a marker of severe hypoxia and systemic inflammation secondary to an acute and severe respiratory illness (31). Due to pandemic restrictions and the need for infection control, systematic investigations (whether invasive or non-invasive) of hospitalized patients involving the coronary arteries and myocardial tissue proved difficult to conduct. This led to significant

clinical uncertainty and heterogeneity in medical treatment across the globe. Further concerns were raised when research studies on survivors of COVID-19 recovering in the community during the early phases of the pandemic suggested a significantly high prevalence of myocardial tissue abnormalities including myocardial infarction and myocarditis (30,32,33) whilst some studies reported no significant abnormalities (34).

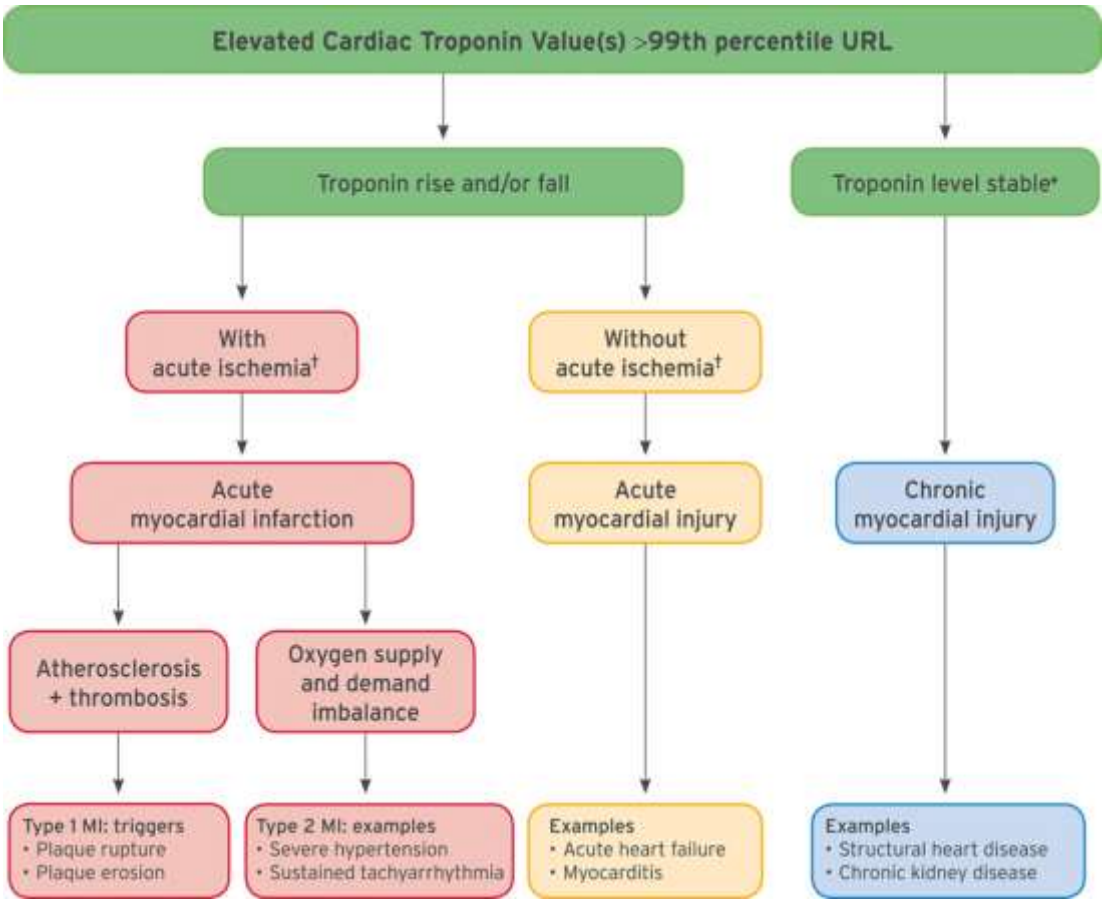


Figure 1.3 A model for interpreting myocardial injury. Ischaemic thresholds vary substantially in relation to the magnitude of the stressor and the extent of underlying cardiac disease. MI indicates myocardial infarction; URL, upper reference limit. *Source: Thygesen et al; Fourth Universal Definition of Myocardial Infarction (2018). Reproduced with permission (under Creative Commons CC-BY)*

Overall, irrespective of the cause, the diagnosis of acute myocardial injury is correlated with poor outcomes (35). Therefore, accurate differentiation of the causes of acute myocardial injury in a timely manner is highly desirable, so that appropriate therapies can be delivered at the earliest opportunity. At present, invasive coronary angiography is the most commonly-used specialist investigation to help delineate an ischaemic cause of acute myocardial injury.

1.3 Invasive coronary angiography

Most patients with acute myocardial injury undergo ICA to help determine the cause and guide treatment. It is commonly performed via the radial artery in the patient's wrist or via the femoral artery in the groin. Under local anaesthetic, a needle is used to enter the artery, followed by the introduction of a sheath over a fine tipped guide wire. Custom-made catheters over a longer guide-wire are then passed through the sheath to engage with the coronary arteries under fluoroscopic guidance. Iodine-based contrast is then injected under fluoroscopy images of the coronary arterial lumen to detect luminal stenosis, thrombus or related pathologies, such as coronary dissection. Occasionally, intravascular imaging using various ultrasound techniques is performed to characterise the nature of the coronary endothelium, to help differentiate between normal coronary arteries, stable and unstable atherosclerosis (36).

Modern practice of ICA is considered to be safe, and is often the quickest way to establish the diagnosis of Type 1 AMI, enabling the prompt revascularisation of occluded coronary arteries. However, there are two main issues: firstly, depending on the patient profile, ICA carries up to a 2% risk of major complications, including bleeding, blood vessel damage, cardiac arrhythmias, stroke, myocardial infarction and contrast-induced nephropathy, and an approximately 0.08% risk of death (37); secondly, it is expensive, with tariffs of £1848-£7516 for a hospitalised patient in UK (figures from 2021) (38). Furthermore, a substantial portion of patients with CAD have multivessel disease, and, therefore, the identification of the culprit artery can sometimes be difficult (6). Moreover, up to 13% of suspected cases of MINOCA; in such cases, clinical guidelines recommend intravascular imaging, to exclude subtle plaque erosion or rupture, which adds to procedural time, radiation exposure and contrast load (39). It is in this setting that the European Society of Cardiology guidelines

recommend CMR to help characterise the myocardial tissue in order to differentiate the causes of acute myocardial injury (40,41).

1.4 Cardiovascular Magnetic Resonance Imaging

CMR is widely considered to be the gold-standard imaging modality for assessing cardiac structure, function, and myocardial tissue characterisation (11). CMR is special type of Magnetic Resonance Imaging (MRI) that allows imaging of the beating heart (unlike all other relatively static organs in the body).

1.4.1 Physics foundations of MRI

MRI offers radiation-free non-invasive imaging of the body's tissues. MRI exploits the intrinsic magnetic resonance properties of the nuclei in the atoms of the body (42). All nuclei and the sub-atomic particles are characterised by a quantum mechanical property called spin. MRI relies on molecules with non-zero spin, in particular the nuclei of Hydrogen, as the most abundant atom in the body.

As per the laws of electromagnetic induction, nuclei with a charge and spinning motion create a magnetic field and a magnetic moment (axis of rotation). In their natural state, the magnetic moments of the hydrogen atoms are randomly aligned. This magnetic moment has the propensity to align to an applied external magnetic field (referred to as B_0) in a MRI scanner thereby creating a net magnetising vector (NMV) in the same direction as B_0. The NMV is very small; only about 1 in 1,000,000 spins is aligned with B0 in conditions of clinical scanners typically working at 1.5-3 Tesla. The crucial mechanism behind MRI imaging is that the individual spins precess under the influence of magnetic field. The precessional frequency (ω_0) is expressed in the Larmor equation as $\omega_0 = \gamma B_0$, where the gyro-magnetic ratio (γ) is a constant. At 3T, which is the approximate magnetic strength of the scanner used for the projects in this Thesis, the nominal precession frequency is 127.71 megahertz (MHz).

An MR signal generation starts from applying a radio frequency (RF) pulse that is equal to the precessional (Larmor) frequency; this causes the nuclei to resonate and thus gain energy thus the term resonance in MRI and CMR. The resulting precession of the coherent NMV induces magnetic and electric waves, which can be detected by appropriately constructed receivers (coils) and amplified for image reconstruction.

It is crucial to understand that the energy for any spin pool at any time is exchanged at the Larmour frequency resonance. Thus altering the magnetic field about the B_0 by small amounts, using so-called gradient coils, allows spatial encoding by affecting frequency of excitations and readouts. The MR scanner's system computer can then map individual frequencies and phases into spatial information that can be presented to human observers.

Beside the number of actual nuclei, coils and system amplifiers, MR signals depend on intrinsic MR properties of the body's tissues. The most basic ones are the T1 longitudinal magnetisation *recovery* time, and T2 transverse magnetisation *decay* time. The T1 and T2 times vary amongst body's tissues; mainly correlated with the water content; e.g. fat tissue contains a lot of densely arranged heavy molecules and has far shorter T1 and T2 than other body tissues, with blood or pericardial effusion at long end of the tissue relaxation times. For instance, in a 1.5T scanner, T1 time of fat and water are 250ms and 4000ms whilst T2 times are 70ms and 2000ms respectively.

1.4.2 CMR sequences

Contemporary CMR provides multi-parametric assessment of the heart by adjusting various scan parameters to amplify dependencies on T1, T2 and other tissue properties (43). Depending on the need, MRI operators can obtain various T1 or T2 weighted images depending on complex choices between manifold technical settings such as TR (repetition time), TE (echo time) flip angles, etc., subject to a specific sequence type selection and any

preparations, such as inversion or saturation. Most commonly cine imaging allows visualisation of wall motion throughout the cardiac phases., quantification of volumes and function (by calculating ejection fraction, strain) of the beating heart. Beside anatomic presentation, T1 and T2 weighted imaging, performed with or without injection of exogenous contrast agents, allows the detection of focal pathological changes such myocardial oedema myocardial fibrosis (12) (**Figure 1.4**).

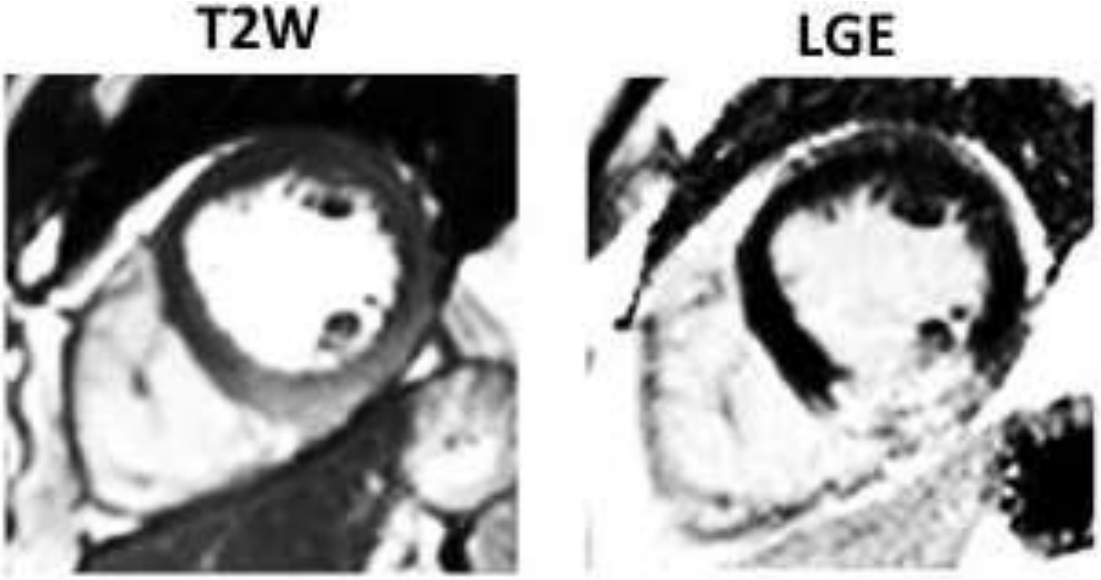


Figure 1.4 T2 weighted (T2W) and T1-weighted Late Gadolinium Enhancement (LGE) demonstrate myocardial oedema and necrosis in a patient with transmural inferior ST-segment Elevation Myocardial Infarction (STEMI). *Adapted from Dall'Armellina, E., Piechnik, S.K., Ferreira, V.M. et al. J Cardiovas Mag Reson 2012 (44). Reproduced with permission under Creative Commons CC-BY)*

Weighting towards other MR properties allows for further tissue contrast, e.g. relevant for this work, T2* weighted imaging for myocardial iron accumulation, including in areas of intramyocardial haemorrhage (IMH). Early imaging after GBCA injection (EGE) allows the detection of intracardiac thrombus. Late Gadolinium Enhancement (LGE) imaging (typically 10 -15 minutes after GBCA injection) enables the detection of myocardial scarring; which can be ischaemic (infarct) or non-ischaemic in origin. LGE also allows visualisation of

microvascular obstruction (MVO). Recent developments allow T1, T2 and T2* data to be depicted as 'maps', which provide pixel-wise visualisation and direct quantification of myocardial tissue characteristics (45,46) (**Figure 1.5**). Basic tissue composition can be assessed using combination of native and post-contrast T1 maps to generate extra cellular volume (ECV) fraction (with the use of blood haematocrit value).

In summary, myocardial oedema can be detected on pre-contrast T1 and T2 maps and T2w imaging (47) whilst myocardial fibrosis and infarction can be diagnosed with the use of T1 maps (pre and/or post contrast) and LGE imaging (12).

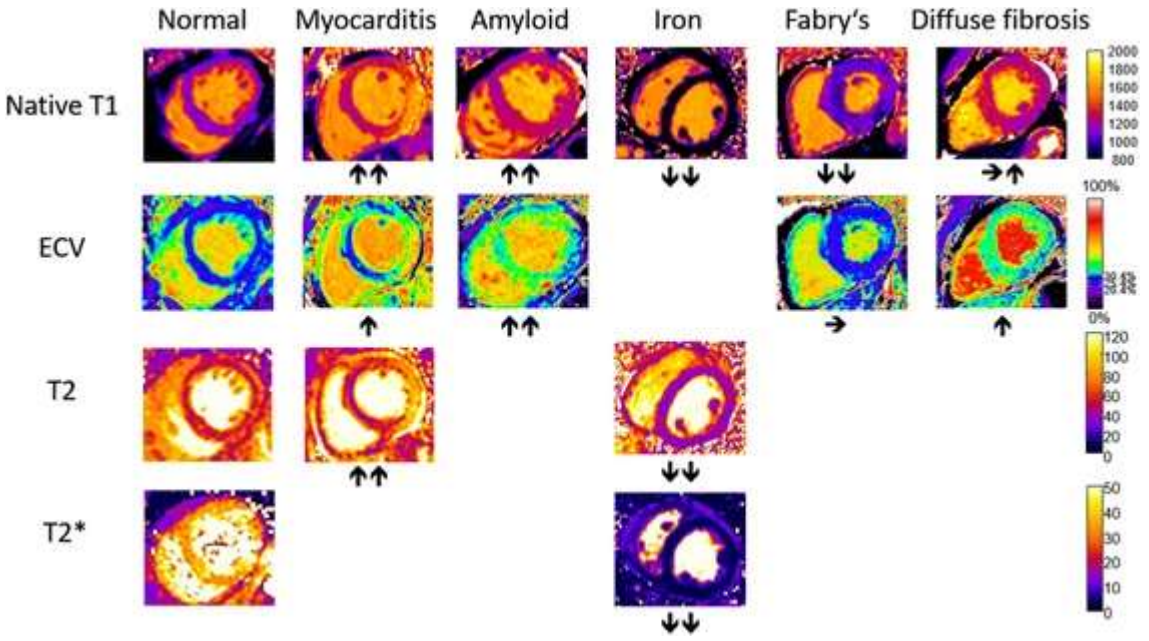


Figure 1.5 Typical appearance of T1, T2, T2*, and ECV maps in healthy subjects and in patients with myocardial disease. Arrows denote relative change in respective parametric maps**.** *Source: Messroghli et al 2017 (45); Clinical recommendations for cardiovascular magnetic resonance mapping of T1, T2, T2* and extracellular volume: A consensus statement by the Society for Cardiovascular Magnetic Resonance (SCMR) endorsed by the European Association for Cardiovascular Imaging (EACVI) reproduced with permission (under Creative Commons CC-BY)*

1.4.3 MR in contemporary clinical practice

Since its initial clinical adoption in the 1980s (48), the use of CMR has evolved rapidly, with 82 National Health Service (NHS) sites in UK offering CMR scanning at present (13). Overall, 114,967 scans were performed in 2018, which is equal to 1731 scans per million of UK's population and represented a 5 fold increase in usage over the previous 10 years (13). Although there are significant regional variations in the rates of use across four nations, UK's overall adoption of CMR is ~4 fold higher than that in the USA. However, at present, the majority of clinical CMR is performed in outpatient settings involving stable patients with chronic pathologies (13); regular but infrequent scanning slots are provided for stable hospitalized patients (also referred to as inpatients throughout this thesis), but usually after a period of stabilisation and observation in the hospital, and the waiting time for a scan is relatively long (approximately 3 [2-4] days) (13).

1.4.4 CMR's current role in assessing acute myocardial injury

Where available, CMR plays an integral part in the diagnostic work up in hospitalized patients with acute medical conditions. The most common indications include: resuscitated cardiac arrest, suspected myocarditis, and viability assessment prior to revascularisation following a recent acute MI.

Recent European and American guidelines make strong recommendations (Class 1B) for an 'early' CMR in patients with a diagnosis of MINOCA (**Figure 1.6**) (39,40). MINOCA, in its purest form, is confirmed (either with CMR or histopathology) acute MI in the presence of non-obstructive coronary arteries (with less than <50% stenosis on ICA) and in the absence of non-ischaemic causes of acute myocardial injury such as myocarditis (39,40). CMR's role in this case is to confirm the presence of an acute MI and, if not, to help identify non-

ischaemic causes of acute myocardial injury after the ICA has been performed. Classical non-ischaemic diagnoses that can be made based on CMR features include myocarditis, Takotsubo syndrome and other cardiomyopathies (**Figure 1.6**). Typically, such 'early CMR' is performed within the first 28 days after the patient's symptoms and before the resolution of the acute oedematous change in the injured myocardium.

Myocardial oedema is a common response to acute myocardial injury and is due to increased water content in the cellular and extracellular (interstium and blood vessels) compartments; the former occurs after a few minutes of cellular ischaemia whilst the latter is usually a result of prolonged ischaemia due to the disintegration of capillary membranes, cellular necrosis and the ensuing inflammation as well as hyperaemia (14,49). Pathologies such as Takotsubo syndrome or acute myocarditis, mediated through non-ischaemic mechanisms (e.g. catecholamine surge and pro-inflammation) can also induce myocardial oedema (50,51). The presence of acute myocardial oedema can be detected with CMR oedema imaging (T1 or T2 maps showing prolonged T1 and T1 relaxation times or T2w imaging showing regional or global hyperintensity) during the acute or sub-acute phase can help differentiate acute from chronic myocardial injury (47,52–54). Furthermore, in conjunction with wall motion assessment on cine imaging and fibrosis assessment using LGE imaging, oedema imaging can differentiate the types of acute myocardial injury (12). Myocardial oedema resolves in the first few weeks after acute myocardial injury in most cases (49,54,55); which explains the findings that early CMR scans (which included oedema imaging) after acute myocardial injury (in patients with unobstructed coronary arteries) offer high diagnostic utility as well as prognostic information (56,57). It is important to note that, whilst T1 and T2 based techniques can detect regional and global myocardial oedema, they cannot precisely quantify the water content in the different compartments within the myocardium (intracellular, interstial space and intravascular) (47).

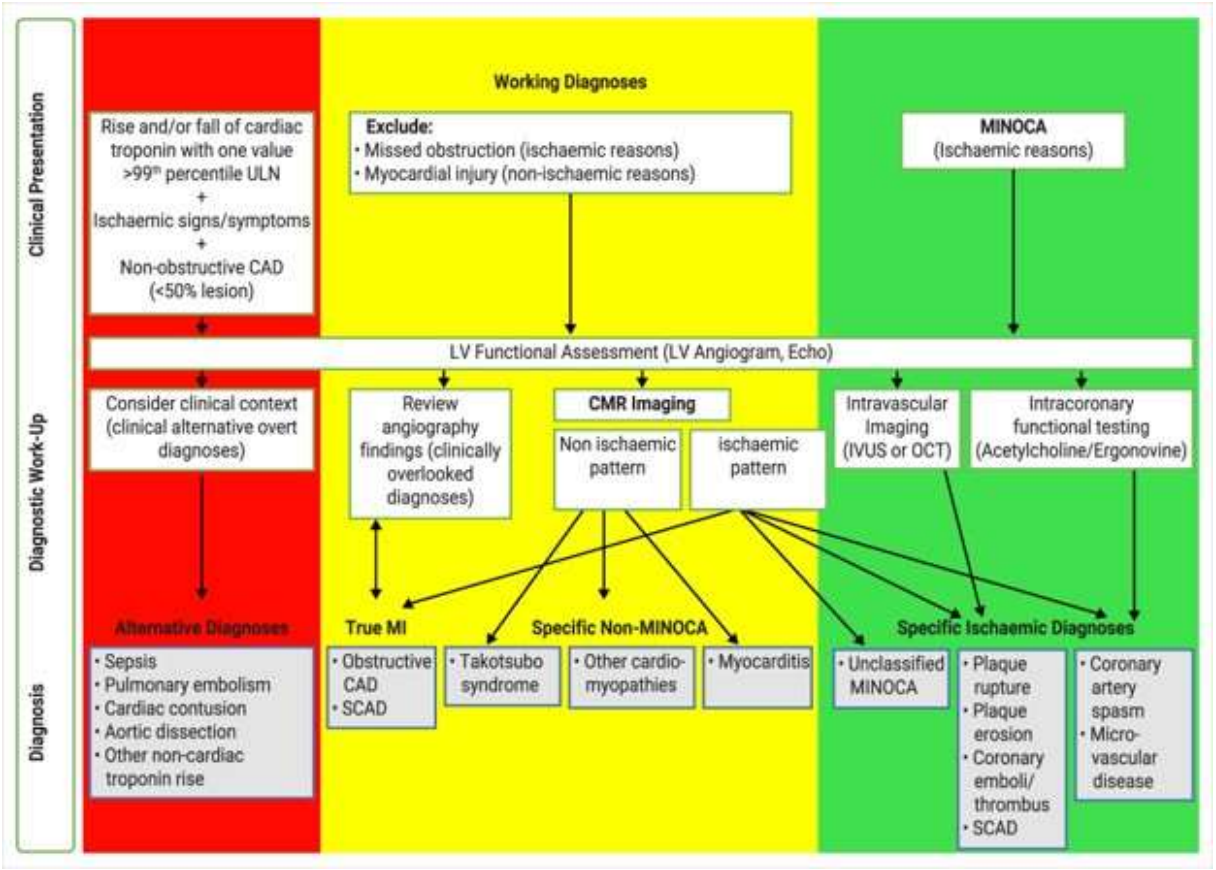


Figure 1.6 CMR's current role in the work-up of patients with MINOCA to identify non-ischaemic and ischaemic causes of acute myocardial injury. European Society of Cardiology (ESC) guideline. Source: Collet et al Eur Heart J 2021(40). ULN = Upper Limit of Normal, CAD = Coronary artery disease, MINOCA = Myocardial Infarction With Non Obstructive Coronary Arteries, IVUS = Intravascular Ultrasound, OCT = Optical Coherent Tomography, SCAD = Spontaneous Coronary Artery Dissection

1.5 Knowledge gaps – clinical application of acute CMR in acute myocardial injury

1.5.1 Acute myocardial injury in suspected Non-ST-segment Elevation Myocardial Infarction prior to invasive coronary angiography

As alluded to above, almost all the evidence for 'early CMR' in acute myocardial injury is in patients after the initial diagnostic work up that includes ICA, and only a handful of studies have examined its utility as a gatekeeper to ICA. In 2003, Kwong et al performed a CMR study of 161 patients with chest pain but inconclusive ECG with or without Troponin rise in the emergency department (58). Using cine and LGE imaging, they showed that CMR was more sensitive (84%) and specific (85%) than ECG, peak cTnI, and the clinical Thrombolysis in MI (TIMI) risk score in detecting an acute coronary syndrome (ACS), as verified on ICA. However, this work included patients without acute myocardial injury (without troponin rise), and the CMR protocol did not allow for the differentiation between acute and chronic myocardial infarction (no oedema-imaging). Cury et al performed a study in 2008 of 62 patients with chest pain, and used T2-weighted imaging, in addition to the sequences used by Kwong et al (59). They included only patients with normal cTn on the first blood test and normal ECG in the emergency department, and reported high specificity of 96% and positive predictive value (PPV) of 85% of CMR in predicting ACS (which includes unstable angina, NSTEMI and STEMI) during the rest of hospital stay, but only 3/62 patients had NSTEMI as confirmed with repeat cTn levels and ICA.

More recently, three studies have tested the role of acute CMR in patients with suspected NSTEMI, i.e. patients presenting with ischaemic symptoms and evidence of acute myocardial injury (acute rise in cTnI). Heitner et al's observational study of 114 patients with suspected

NSTEMI demonstrated that CMR (cine and LGE) diagnosed MI in 72% and non-ischaemic pathologies in 15% and showed normal findings in 14% of the patients. They went on to conclude that CMR had the potential to change management in up to 46% of the patients with the reclassification of diagnosis and identification of new IRA (6). Van Cauteren et al studied 51 patients with suspected NSTEMI and reported that a pre-ICA CMR (cine, T2 weighted imaging, LGE) had a 77% accuracy to detect obstructive CAD. The diagnostic accuracy improved to 86% after applying stress perfusion imaging in 19 patients (out of the 51 patients) who had normal/equivocal findings on the initial three CMR sequences. Finally, Smulders et al randomized patients with suspected NSTEMI to either CMR (n=60), Computed tomography (CT) coronary angiogram (n=70) or ICA (n=68); they found that a CMR-first strategy obviated the need for ICA in 13% of patients, and that the clinical outcomes of the three cohorts were similar at 1 year after recruitment (8). Amongst those that underwent CMR (n=60, cine, T2w, LGE and stress perfusion imaging), the diagnosis included MI in 77%, myocarditis in 2%, equivocal findings in 7% and normal findings in 13%. However, none of the studies included T1-mapping, which is an integral part of modern multi-parametric characterisation of myocardial tissue (12,45) has shown to be superior to T2 weighted imaging in detecting acute myocardial oedema in Takotsubo syndrome and aborted MI (52), myocarditis (53) and acute myocardial injury in NSTEMI (44). This knowledge gap is addressed in the results chapter 3 titled '*Clinical Utility of Cardiovascular Magnetic Resonance Prior To Invasive Coronary Angiography In Suspected Non-ST Segment Elevation Myocardial Infarction*'. In this chapter, I tested the hypothesis that a comprehensive multiparametric CMR, performed early and before ICA, utilising cine, T1-maps, T2-weighted and late-gadolinium imaging, will accurately identify non-ischaemic causes of myocardial injury and identify the culprit artery in confirmed myocardial infarction.

1.5.2 Acute myocardial injury in acute COVID-19

As discussed above, acute myocardial injury has been reported in acute COVID-19, and is associated with higher inpatient mortality (27). Although a handful of case reports and small studies described acute myocarditis (60,61), the pathophysiological origins of all acute myocardial injury were not systemically investigated during the acute illness with CMR, due to logistical difficulties during the pandemic that included infection control. A series of CMR studies of patients 1-6 months after acute COVID-19 showed a varied prevalence of myocardial tissue abnormalities (raised T1 and T2 signals, LGE abnormalities and pericardial abnormalities); however, it was unclear if these changes were attributable to acute COVID-19, as the patients did not have a baseline CMR scan prior to or during the acute illness (30,62,63). Furthermore, most studies lacked appropriate controls and data on cTnI during the acute illness, as they mostly included non-hospitalized patients. All of this highlighted the need for a systematic CMR examination of acute COVID-19 patients with and without Troponin rise, and comparison with matched COVID-19 negative and asymptomatic controls. I addressed this knowledge gap in this Thesis in the results chapter 4 titled '*Acute changes in myocardial tissue characteristics during hospitalization in patients with COVID-19'*. In this chapter, I tested the hypothesis that acute COVID-19 induces transient myocardial oedema in hospitalised patients, by using multi-parametric CMR including cine, T1-mapping, T2-weighted and late-gadolinium imaging.

1.5.3 Acute myocardial injury in late presenting ST-segment Elevation Myocardial Infarction

Patients presenting within 12 hours of chest pain onset and ST-segment elevation myocardial infarction (STEMI) are offered emergency percutaneous coronary intervention (PCI), also known as primary PCI (PPCI), as there is a high likelihood of an occlusive coronary thrombus and significant myocardial salvage with prompt reperfusion. However, there is much clinical uncertainty in how patients presenting late (i.e. >12 hours after the onset of chest pain) should be managed, not least by the possibility that the myocardium subtended by the occlusive coronary artery is likely to be irreversibly infarcted, but also by the concerns that reperfusion may worsen the myocardial injury and worsen the clinical situation (e.g. arrhythmias, myocardial wall rupture) (64). Thus, knowing the nature and extent of myocardial injury before deciding to perform ICA+/-PCI in late-presenting STEMI is of clinical value, and may enhance the provision of more personalised medical care in this setting. Even more importantly, this baseline assessment, when compared to a post-PCI assessment, may enable examination of the impact of revascularisation on the downstream, acutely infarcted myocardium. Given that CMR is the gold standard imaging to assess myocardial injury and tissue characteristics in acute myocardial infarction, this Thesis will examine its utility in the setting of late-presenting STEMI, where I conducted an early CMR before and after acute revascularisation. In this chapter, I examined the impact of acute revascularisation on the acutely infarcted myocardium in late-presenting STEMI, using multi-parametric CMR involving cine, T1-maps, T2*-weighted, T2-weighted and early and late-gadolinium imaging. The findings are presented in the results chapter 5 titled '*The Impact of Acute Revascularisation in Late-Presenting ST-Segment Elevation Myocardial Infarction: A Study of Acute Myocardial Injury Using Cardiac Magnetic Resonance'*.

1.5.4 Prognostic significance of acute changes in the non-infarcted myocardium in revascularised ST-segment Elevation Myocardial Infarction

A wide range of changes occur in the myocardial tissue immediately after STEMI and revascularisation. Amongst them are myocardial ischaemia, oedema, necrosis, microvascular injury (namely microvascular obstruction and intramyocardial haemorrhage), inflammation and fibrosis. These usually lead to regional wall motion abnormalities and decreased systolic function. These changes are dynamic in the first few days and weeks after the MI and the oedema resolves in most patients by 6 months (54). CMR has been used extensively to investigate these CMR abnormalities post-MI, and, individually, they have all been shown to be associated with long-term cardiovascular outcomes. However, infarct size, measured by LGE at 5±2 days after STEMI, is widely considered to be the best marker of clinical outcomes (14) (**Figure 1.7**).

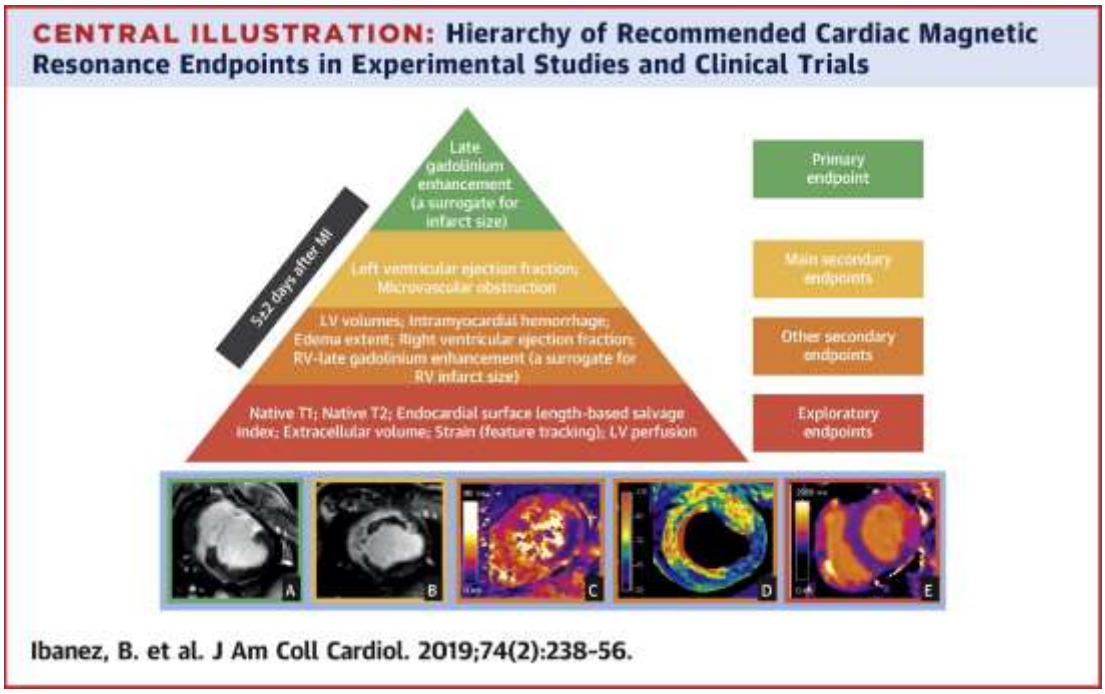


Figure 1.7 Recommended CMR endpoints in research involving patients post-STEMI.

Despite the wealth of data, CMR has not entered the clinical mainstream in the risk-stratification for patients post-STEMI. There may be several reasons for this, including: (1) CMR is not readily available in most hospitals for acutely ill patients; (2) contrast-enhanced CMR (necessary to obtain LGE images) requires administration of gadolinium-based contrast, relatively long-scanning time and sub-specialised facilities and personnel; and (3) the associated healthcare costs. Moreover, current recommendations place a strong emphasis on the prognostic relevance of the infarcted myocardial tissue characteristics (infarct size and MVO; see **Figure 1.7**), but not on changes that are known to take place in the rest of the heart (i.e. the non-infarcted myocardium). It has been known for some time that the zone of myocardium furthest away from the infarct (also known as the remote myocardium) undergoes inflammatory changes immediately after MI, and that this can be detected by T1-mapping (19,21,65,66). However, its prognostic implications have remained unclear.

If established as a superior prognostic marker, T1-mapping has the potential to address some of the barriers facing clinical uptake of CMR in the risk-stratification post-STEMI, as it obviates the need to administer of GBCA, and can therefore significantly shorten the scanning times and cost. This knowledge gap in literature will be addressed in the results chapter 6 titled "*Acute Response in the Non-infarcted Myocardium Predicts Long-Term Major Adverse Cardiac Events After STEMI*". In this chapter, I hypothesized that, in addition to changes in the infarcted myocardium, the non-infarcted myocardium may also demonstrate various grades of acute response immediately post-STEMI on CMR including T1-mapping, and that these changes may predict long-term major adverse cardiac events.

1.6 Overview of Thesis

The thesis presents a series of investigator-led prospective studies that help fill a number of knowledge gaps in the literature with regards to the utility of acute CMR in assessing acute myocardial injury in hospitalised patients.

Chapter 2 describes the methods used to achieve this.

Chapter 3 presents the findings of my research investigating the clinical utility of CMR as a gate-keeper to ICA in patients presenting with suspected NSTEMI. This is a manuscript in advanced form and will be shortly submitted to a medical journal for peer-review and publication:

> **Shanmuganathan M**, Nikolaidou C, Burrage MK et al, Clinical Utility of Cardiovascular Magnetic Resonance Prior To Invasive Coronary Angiography In Suspected Non-ST Segment Elevation Myocardial Infarction

Chapter 4 will present the findings of my research investigating the evidence of acute myocardial abnormalities in hospitalised COVID-19 patients with and without biochemical evidence of acute myocardial injury. The results of these investigations have been published as:

> **Shanmuganathan M**, Kotronias RA, Burrage MK, et al. Acute changes in myocardial tissue characteristics during hospitalization in patients with COVID-19. Front Cardiovasc Med. 2023;10:1097974.

Chapter 5 will present the findings of my research investigating the changes in the myocardial tissue characteristics before and after revascularisation in patients with late-presenting STEMI. This is a manuscript in advanced form and will be shortly submitted to a medical journal for peer-review and publication:

Shanmuganathan M, Borlotti AB, Burrage MK et al. The Impact of Acute Revascularisation in Late-Presenting ST-Segment Elevation Myocardial Infarction: A Study of Acute Myocardial Injury Using Cardiac Magnetic Resonance

Chapter 6 will present the findings of my research investigating the acute changes in the infarcted and non-infarcted myocardium at 2 days after timely revascularised STEMI and their predictive value of long-term clinical outcomes beyond conventional CMR indices of MI. The results of these investigations have been published as:

Shanmuganathan M, Masi A, Burrage MK, et al. Acute Response in the Noninfarcted Myocardium Predicts Long-Term Major Adverse Cardiac Events After STEMI. JACC Cardiovasc Imaging. 2023;16:46–59.

Chapter 7 offers a conclusion and future directions.

2. Methods

2.1 Ethical considerations

Patients with acute myocardial injury and control subjects who participated in the DPhil projects were recruited as part of the ongoing Oxford Acute Myocardial Infarction (OxAMI) study (67). It had received favourable opinion from the South-Central Oxford Research Ethics Committee (reference: 10/H0408/24) of the National Research Ethics Service (NRES) from the National Patient Safety Agency and Research Ethics Committees in England. The study was also approved by the Health Research Authority and Oxford University Hospitals NHS Foundation Trust (OUH). All patients gave written informed consent. All research activities were performed in accordance with institutional requirements and the principles of the Declaration of Helsinki (68). Consent forms were filed in a secured office. Patient identifiable electronic data was stored on a high-compliance server. Primary research data was first entered in an anonymised fashion case record forms (CRFs) and filed in a secured office, and subsequently entered on to dedicated research databases.

2.1.1 OxAMI study

The OxAMI study was set up in 2010 with the aim to investigate patients admitted to OUH with suspected acute myocardial injury. Since its inception, it has recruited over 1000 participants (including those enrolled for the research projects in this DPhil). The OxAMI study performs invasive and non-invasive investigations and aims to find biomarkers of disease and prognosis by correlating the investigative findings with short and long-term outcomes, obtained by serial follow-up of participants (67).

2.2 Study Participants

2.2.1 Patients

General Inclusion criteria:

1. Age - 18 to 90 years old
2. Evidence of myocardial injury (e.g. elevation of troponin or other cardiac biomarkers, ECG changes, wall motion abnormalities on cardiac imaging) and/or referred for coronary angiography with view to proceed to PCI, as indicated in either non-emergency or emergency settings.
3. In the case of non-emergency presentation, willing and able to give informed consent for participation in the study. In the case of emergency presentation, able to participate in verbal assenting procedure.

General Exclusion criteria:

1. Patients in whom safety or clinical concerns preclude participation.
2. Anaemia (Haemoglobin <90 grams per litre).
3. Pregnant or breast-feeding females.
4. Additional exclusion criteria for patients undergoing MRI:
    - claustrophobia which limits participants from remaining in the MRI scanner
    - patients who cannot lie flat on the scan table
    - patients with metallic implants (unless known to be MRI conditional) or any pacemakers or implantable defibrillators
    - patients with known allergy to medium of contrast (Gadolinium-based contrast)

The specific eligibility criteria for NSTEMI, COVID-19, late-presenting STEMI and STEMI cohorts are described below and in the methods section of the corresponding results chapters.

Patients with suspected Non-ST-segment Elevation Myocardial Infarction (NSTEMI)

Patients in hospital with suspected NSTEMI awaiting ICA were screened for eligibility. Patients who met inclusion and exclusion criteria and who gave written informed consent were recruited (Chapter 3).

Patients hospitalised for acute Coronavirus disease 2019 (COVID-19)

Patients in hospital for confirmed acute COVID-19 were screened for eligibility. Patients who met specific inclusion and exclusion criteria and who gave written informed consent were recruited (Chapter 4). The main exclusion criteria included past history of cardiac disease and COVID-19.

Patients with late-presenting ST-segment Elevation Myocardial Infarction (STEMI)

Patients presenting to hospital late (12-48 hours after chest pain) with STEMI were screened for eligibility. Patients who met inclusion criteria were approached, and verbal assent was taken before the first CMR scan was performed. All patients gave written informed consent before further participation in the study (Chapter 5).

Patients with timely reperfused ST-segment Elevation Myocardial Infarction

Patients brought to hospital via the primary PCI (PPCI) pathway with STEMI were screened for eligibility. They were enrolled using emergency assent during the PPCI, but subsequently gave written informed consent prior to their discharge from hospital (Chapter 6).

2.2.2 Controls (asymptomatic volunteers)

Asymptomatic control subjects were recruited from the community after they responded to electronic advertising (on the websites of the OUH and OxAMI study). They provided written informed consent after reading a patient information leaflet that was sent in advance of their visit to our site.

Specific eligibility criteria for Controls

Inclusion criteria

1. Age - 18-90 years old
2. Asymptomatic of cardiac diseases
3. Able to provide informed consent

Exclusion criteria

1. Past history of cardiac disease
2. Past history of COVID-19
3. Contra-indication for CMR (similar to those listed above)

2.3 Standard OxAMI Study Protocol

1. Clinically indicated invasive coronary angiography +/- research invasive coronary haemodynamics
2. Blood sampling (and storage of serum and plasma in freezers at -80 degrees Celsius) and electrocardiograms (ECGs) during index hospital admission and at 6 months
3. Clinical data collection including vital signs, blood test results, ECGs, demographics, past medical history, list of medications, discharge diagnosis
4. CMR scans (at least one) during index hospital admission and at 6 months
5. Follow-up for monitoring clinical outcomes at 6 months and then annually for 10 years with the use of:
    a. Patient questionnaire completed by research nurse or doctor (in-person at 6 months and via telephone interview then onwards)
    b. General Practioner's records in the community
    c. Hospital records

2.4 CMR methods

2.4.1 CMR imaging protocol

Scans were performed as per previously published methods on a 3T CMR scanner at the John Radcliffe Hospital, either the Magnetom TIM Trio (located in Oxford Centre for Clinical Magnetic Resonance and Research (OCMR)) or the Verio (located in Acute Vascular Imaging Centre (AVIC)), manufactured by Siemens Healthcare, Erlangen, Germany (44,54,69–71). The following typical protocol of CMR sequences was prescribed during all scans done for the purposes of this Thesis, unless specified otherwise in the methods section of the results chapters.

1. Anatomical scout
2. Pilots
3. Cine imaging (for cardiac anatomy, function, volumes and mass)
4. T1-mapping (pre and post contrast, using the ShMOLLI sequence (46))
5. T2 weighted (T2W) imaging
6. T2* mapping
7. Early gadolinium enhancement (EGE) imaging
8. Late gadolinium enhancement (LGE) imaging (Phase Sensitive Inversion Recovery (PSIR) sequence and or 'Single-Shot' sequence)

2.4.2 CMR sequences

After standard planning, balanced Steady State Free Precession (bSSFP) cine images were acquired. Typical imaging parameters were: Echo Time / Repetition Time (TE/TR) = 1.4/3.2 ms; flip angle = 50°; voxel size: 1.6 × 1.6 x 8 mm. Typical temporal resolution was 40 ms . Two to three-fold accelerated parallel imaging (GRAPPA) was used to

shorten the breath-hold. Cine images were acquired in 3 long-axis planes (vertical, horizontal and 3-chamber) as well as in short-axis plane offering full coverage of both ventricles from the atrioventricular groove to the apex. The short-axis stack was usually acquired after early gadolinium enhancement imaging. Retrospective gating was used for most patients who were in sinus rhythm. Prospective gating was used in patients with significant irregular heart rhythms.

ShMOLLI T1 maps were generated using the Siemens prototype sequence (work-in-progress WIP package 561, or above) from 5-7 SSFP images with variable inversion preparation time (46). Typical acquisition parameters were: TE/TR = 1.07/2.14 ms, flip angle = 35°, Field of View (FOV) = 340×255 mm, matrix size = 192×144, 107 phase encoding steps, actual experimental voxel size = 1.8 × 1.8 × 8 mm, interpolated reconstructed voxel size = 0.9 × 0.9 × 8 mm, GRAPPA = 2, 24 reference lines, cardiac delay time TD = 500 ms and 206 ms acquisition time for single image, phase partial Fourier 6/8. Quality assessment of T1 maps was performed by inspecting parametric goodness-of-fit (R^2) maps at time of acquisition and during image analysis; inspection of the raw T1-weighted images was also undertaken as needed (52). R^2 maps provide a means to identify areas of potentially compromised T1 accuracy and re-acquire maps of insufficient quality (46).

Bright-blood T2-weighted imaging (T2W) was acquired using a T2-prep-SSFP single shot sequence with surface coil correction. Typical imaging parameters were: TE/TR = 1/4.1 msec; effective TE = 60 msec; flip angle = 90°; FOV 300 x 400mm. voxel size: 2.1 × 1.6 × 8 mm. In order to reduce off-resonance artefacts, shimming and centre frequency adjustments were performed before T2W-imaging and T1-mapping.

T2* weighted images (and maps) were obtained using a gradient echo (GRE) sequence (70). Typical imaging parameters were: TE 22.14ms (5 echo numbers were 2.46, 7.38, 12.30,

17.22 and 22.14 ms). FOV = 340 × 225 mm, bandwidth 5260 Hz/Px, voxel size = 1.8 × 1.8 × 3.0 mm and Flip angle 20°.

After the acquisition of the aforementioned sequences, 0.1-0.13 mmol/kg of a GBCA (Gadoterate meglumine, Dotarem, Guerbet; or Gadodiamide, Omniscan, GE Healthcare, when this agent was in use in the earlier years) was administered. [0.03mmol/kg was given to acquire rest perfusion imaging as part of OxAMI protocol before a top-up of 0.1mmol/kg was given to acquire EGE and LGE imaging; see below].

EGE imaging was performed 1-2 minutes after GBCA injection using singe-shot GRE imaging. Typical imaging parameters were: TE 1.04, Flip angle 31°, FOV 360 x 400 mm and voxel 1.5x0.7x8mm. The inversion time (TI) was set long at 450ms. Approximately 9-10 short-axis slices (of 8mm thickness) were acquired offering full heart coverage.

LGE imaging was performed with a T1-weighted GRE-phase sensitive-inversion recovery (GRE-PSIR) sequence. Typical imaging parameters were: TE/TR=2.5 ms/5 ms, voxel size 1.8 ×1.4× 8 mm, flip angle 40°. An appropriate inversion time is obtained from T1 scout images and was used for optimal nulling of normal myocardium. Single-Shot inversion recovery GRE LGE imaging was obtained in patients with irregular heart beat or sub-optimal breath-hold. Typical parameters were: TE = 1.2ms, Flip angle 38°, voxel size 3.6 x 1.7 x 8mm. It allowed acquisition of short axis slices covering the entire left ventricle and the three long-axis images in a single breath-hold. Images in the three long-axis planes were also acquired.

Post contrast ShMOLLI T1 maps were obtained using the same slice position and sequence parameters as those used for native T1-mapping, typically at least 10 minutes after the administration of GBCA.

Complete coverage of the left ventricle was obtained with all short-axis imaging. All images requiring breathold were typically done in end-expiration.

2.4.3 CMR image analysis

CMR images were analysed by CMR experts including me and at least two other CMR experts (Dr Ambra Masi, Dr Alessandra Borlotti, Dr Matthew Burrage and Dr Chrysovalantou Nikolaidou) in the department with >3-year experience using the cvi42 software (Circle Cardiovascular Imaging Inc., Calgary, Canada) and MC-ROI, a dedicated in-house software (Myocardial Region-Of Interest, programmed in interactive Data Language (IDL), version 8.7, L3Harris Geospatial, Broomfield, Colorado, USA).

Biventricular indices

Left and right ventricular volumes and systolic function and left ventricular (LV) mass were obtained analysing the short-axis stack of cine imaging. Epicardial and endocardial contours were manually drawn in end-diastole (ED) and end-systole (ES). Papillary muscles were excluded from the calculation of LV mass but included in the derivation of ventricular volumes. Ejection fraction (EF in %) was obtained by dividing stroke volume by the end-diastolic volume, where stroke volume was the difference between end-diastolic and end-systolic volumes. LV mass was calculated as the difference between the endocardial and endocardial volumes in end-diastole, and multiplied by the specific density of myocardium (1.05g/ml).

Myocardial oedema

Area-at-risk in acute myocardial infarction using T1 maps: Firstly, quality control was performed by investigating the native T1 maps, raw T1-weighted images, and R^2 maps for any evidence of suboptimal data quality, such as those resulting from off-resonance artefacts,

partial volume effects, patient movement or low signal to noise ratio. Apical slices affected by partial volume effects and basal slices where the LV outflow tract is visible were excluded from the study.

On each short axis slice of ShMOLLI T1 map, after contouring the epicardium and endocardium, a region of interest (ROI) was placed in the remote myocardium, defined as a segment with normal thickness, wall motion (on cine imaging) and without scarring on LGE (at 180 degrees away from the infarction, where possible). For patients with MI, myocardial T1 >2SD higher than the mean T1 value of the remote ROI is considered to be in the area-at-risk (AAR), and was automatically delineated. The AAR % was derived by dividing the volume of myocardium with T1 >2SD above the mean T1 of the remote ROI by the myocardial volume and multiplying by 100 in line with the literature (69,72). However, it is appreciated that intensity and extent of myocardial oedema is dynamic in the first few days after MI, in a bi-modal pattern, and thus the latest expert consensus (published after my DPhil started) no longer recommends oedema based CMR imaging to delineate the AAR (14). I have acknowledged this issue in the results chapters 5 and 6 (involving patients with STEMI).

Myocardial oedema on T2w images: Myocardial oedema was quantified using T2w imaging for the COVID-19 study described in results chapter 4. On each short axis slice of T2w images, after contouring the epicardium and endocardium, a region of interest (ROI) is placed in adjacent skeletal muscle (47). The ratio of signal intensity (SI) of T2 between myocardium and skeletal muscle in each T2w short axis slice was obtained. A global T2SI ratio was then computed by averaging the T2SI ratios from all the short axis slices.

Infarct Size (IS)

On each short axis slice of LGE, after contouring the epicardium and endocardium, an ROI was placed in the remote myocardium (as described earlier). Myocardium with an SI >5 SD higher than the mean SI in the remote ROI was automatically delineated as infarction as previously published (70,73,74) with manual correction, if needed, by the CMR expert. The infarct size % was derived by dividing the LGE volume by diastolic myocardial volume and multiplied by 100. In patients with an old MI (defined as areas of LGE with no evidence of oedema on T1 mapping or T2 prepared imaging), the mass of the old infarct was excluded. The apical slice was not used due to partial volume effects. Areas with microvascular obstruction and intramyocardial haemorrhage (see below) were included in the infarct size.

It is acknoweldeged that there is a growing debate as to if the '5SD' technique is the most accurate method to quantify IS when compared to other methods. Such methods include the use of different SDs (e.g. 4 or 5), authomatic thresholding, the full-width at half-maximum technique and manual dileneation of the infarcted area with or without correction for pixels with interemediate signal intesnsity, which usually occur on the borders of the infarct (14,75). However, due to the use of a commonly used technique ('5SD'), which has been widely published. with added manual correction (for artefacts, reduced image quality especially in single-shote LGE imaging and microvascular obstruction for instance) and the active inclusion of intermediate signal intensities, all performed by imaging experts, the IS quantification in this DPhil study should be considered reliable and reproducible.

Microvascular Obstruction (MVO)

MVO on the CMR images is defined as the presence of a hypo-intense core inside an area of late gadolinium enhancement on LGE imaging. On short axis slice LGE images, MVO was manually delineated. The MVO % was derived by dividing the MVO volume by diastolic myocardial volume on LGE imaging and multiplied by 100%.

Intramyocardial Haemorrhage (IMH)

IMH on T2* imaging

IMH is defined on T2* maps as a hypo-intense area within the oedematous zone having a mean T2* value of at least 2SD below the T2* value at the periphery of the oedematous zone and, on average, measuring <20 ms (70,76). An additional check of the same area is performed on the raw T2* images using the R^2 mono exponential truncation method curve fitting (R^2 of >0.990 was considered as a good fit in line the published literature(77)).

IMH on T2W when T2* is not available or was not of good quality:

IMH on T2-weighted CMR images is defined as a hypo-intense area within the infarcted myocardium (as seen on LGE) having a mean SI 2SD below the mean SI of a region of interest placed at the periphery of the oedematous region (78).

ECV quantification

Extracellular volume (ECV) was calculated using the equation (79):

$$ECV = (1 - \text{haematocrit}) \times \frac{\Delta R1\ myocardium}{\Delta R1\ blood}$$

Haematocrit was obtained from laboratory blood testing performed just before the CMR scan. Blood T1 was obtained by placing a region of interest in the LV blood pool (with care to avoid papillary muscle). R1 values were obtained by inverting the T1 values obtained for myocardium and blood pool, respectively. ΔR1 (change in R1) was derived as the difference between the R1 values on pre-contrast and post-contrast T1 maps.

Global ECV was computed by averaging the ECV from all available short axis slices.

2.5 Invasive coronary physiology

When possible, Index of Microcirculatory Resistance (IMR), Coronary Flow Reserve (CFR) were obtained during invasive coronary angiography by the operating cardiologist. A standard pressure and temperature-monitoring guidewire (Abbott, Santa Clara, California) was advanced in the distal segment of the culprit vessel at completion of PPCI. Coronary flow was estimated using thermodilution to derive the mean transit time. Maximal hyperaemia was induced with adenosine intravenous infusion (140 μg/kg/min). IMR was defined as the mean distal pressure multiplied by the mean transit time at hyperaemia (71). CFR was defined as the ratio between the two transit times (80).

The Thrombolysis in Myocardial Infarction (TIMI) Flow was derived on invasive coronary angiograms using the recommendation from The TIMI Study Group 1985 (81) as stated below:

TIMI Grade	**Contrast-filled blood flow in the coronary artery**
0	no perfusion
1	penetration of the contrast material but without perfusion of the entire distal coronary bed
2	partial perfusion with slow flow (when compared with flow proximal to the obstruction or in another coronary artery)
3	complete perfusion

Angiographic thrombus score was graded from 0 to 5 after the passage of the guidewire, as previously described (82); Grade 0: no thrombus, Grade 1: Possible thrombus, Grade 2: the thrombus' greatest dimension is less than half of the vessel diameter, Grade 3: greatest dimension >1/2 to <2 vessel diameters, Grade 4: greatest dimension >2 vessel diameters, Grade 5: total vessel occlusion due to thrombus. Myocardial blush grade at the end of the procedure was evaluated according to van't Hof et al (83) .

2.6 Blood sampling and ECGs

Blood samples were drawn from study participants as per the established protocol in the OxAMI study to measure cardiac biomarkers, including Troponin-I and N-terminal pro–B-type natriuretic peptide (NT-proBNP) at various time points. Blood samples of up to 40ml were taken from patients with STEMI during the angiography and 3 time points (12 hours, 24 hours and 48 hours) during their hospital stay. A further sample was taken at 6 months follow up. The blood was centrifuged as per set protocols, and the serum and plasma were aliquoted and stored in -80^0C freezers for batch processing for biomarkers.

Serial ECGs were obtained on patient admission to hospital and at 6 months.

2.7 Follow up for the assessment of clinical outcomes

Study participants were followed up at 6 months with health questionnaire, ECG, blood test and a CMR scan. Subsequently, health outcomes were assessed by way of annual phone call and/or accessing electronic patient records and/or contacting their primary care provider. Patient reported clinical outcomes were always verified with medical records.

2.8 Statistical analysis

Statistical analyses were performed using SPSS (version 25, IBM Corp), Stata (version 16, StataCorp LLC), and R statistical software (version 4.0.5, RStudio, Inc, version 1.3); the SurvIDINRI package was used on R Studio for the calculation of C-statistic, Brier score, Net-Reclassification Index (NRI) and Integrated Discrimination Index (IDI). All statistical tests were 2-tailed, with values of $P < 0.05$ considered significant.

Normality of data was determined using Kolmogorov-Smirnov test. Normally-distributed data are presented as mean ± standard deviation (SD), and nonparametric data as median with interquartile range (IQR). Statistical comparisons for paired and unpaired samples were performed using Student's t-test, Wilcoxon signed rank test, the Mann-Whitney U test or the Kruskal-Wallis test, as appropriate. Categorical data and frequencies were compared with chi-square or Fisher's test or McNemar's test, as appropriate. Correlation between variables was assessed using Pearson's product-moment correlation coefficient (r) or Spearman's rank correlation coefficient (ρ), as appropriate.

Survival analysis and endpoint comparison between groups were performed using the Cox regression analysis for the calculation of hazard ratio with 95% confidence interval. Kaplan-Meier curves with log-rank test were constructed. Models of Cox regression multivariate analysis were created to explore the incremental predictive value of different variables. The goodness-of-fit, predictive performance, discrimination, and risk classification of models with T1 indices were produced with the help of Dr Rafail Kotronias and tested with: 1) concordance statistic (C-statistic); 2) Brier score; 3) NRI and 4) IDI for censored data.

2.9 Summary

The methods described above provide the backbone for the work conducted in this Thesis. Each individual Chapter will provide further details and clarification of the specific techniques and methods used.

3. Clinical Utility of Cardiovascular Magnetic Resonance Prior To Invasive Coronary Angiography In Suspected Non-ST Segment Elevation Myocardial Infarction

3.1. Introduction

Non ST-segment elevation myocardial infarction (NSTEMI) is highly prevalent and accounts for the majority of all acute myocardial infarctions (84–86). Typical presentations include chest pain or other cardiac symptoms, with evidence of acute myocardial injury (acute rise and fall in cardiac Troponin-I (cTnI) concentrations), which may be accompanied by changes on electrocardiography (ECG). The majority of patients with suspected NSTEMI are referred for early ICA in accordance with standard clinical care pathways (73).

However, ICA performed in this setting may demonstrate non-obstructed coronary arteries (NOCA), which are often due to non-ischaemic pathologies (e.g. myocarditis or Takotsubo cardiomyopathy), or true myocardial infarction with non-obstructed coronary arteries (MINOCA) (56,57,87,88). Causes of MINOCA include re-canalized coronary atherosclerotic plaques, spontaneous coronary artery dissection (SCAD), coronary thrombo-embolism, coronary vasospasm or coronary microvascular dysfunction. (4,89) Further, up to 70% of patients presenting with NSTEMI show multi-vessel coronary artery disease (MVD) on ICA (90), which makes identification of the infarct related artery (IRA) challenging, particularly when ECG findings are ambiguous. Inaccurate diagnosis of an MI (versus non-ischaemic causes) and incorrect determination of the IRA in MI are a frequent clinical challenge in NSTEMI, and may lead to suboptimal clinical outcomes.

Cardiovascular magnetic resonance imaging (CMR) is the imaging gold-standard for cardiac structure, function and myocardial tissue characterisation (91) and has the ability to distinguish MI from non-ischaemic causes of acute myocardial injury, and accurately determine the territory of acute infarction and its extent. Late gadolinium enhancement (LGE) imaging on CMR can accurately distinguish between ischaemic and non-ischaemic patterns of myocardial necrosis and scarring, while T1- and T2-based techniques can detect

acute myocardial oedema (47). The latest guideline from European Society of Cardiology recommend CMR *after* ICA in patients with acute myocardial injury and NOCA, as it can determine the cause of the acute myocardial injury and enable appropriate therapy and offer prognostic information. (40,56)

Given the procedural risks associated with ICA, (40) early identification of non-ischaemic causes of suspected NSTEMI is clinically attractive proposition as it may obviate the need for ICA in selected cases, or provide important information that may improve the interpretation of ICA findings and the need for adjunctive techniques such as intra-coronary imaging or pressure/flow studies. Furthermore, pre-ICA identification of the IRA in patients with MVD can help guide revascularisation. Thus, in this prospective study of patients presenting with suspected NSTEMI, we aimed to establish how comprehensive CMR performed *before* ICA would contribute to the precise diagnosis of acute myocardial injury, as well as identifying the correct IRA in cases with confirmed acute MI.

3.2. Methods

Consecutive patients admitted to Oxford University Hospitals with a clinical diagnosis of suspected NSTEMI and scheduled for inpatient ICA were prospectively enrolled in the Oxford Acute Myocardial Infarction (OxAMI) Study (92). Suspected NSTEMI was defined as the presence of new chest discomfort or an equivalent symptom with an acute rise in cTnI with or without acute ECG changes. Patients recruited to this study had already been reviewed by a member of the clinical cardiology team, and were started on dual antiplatelet therapy and anticoagulation, as part of standard clinical care for suspected NSTEMI (93). Exclusion criteria to the study included patients with ongoing chest pain, haemodynamic instability, estimated glomerular filtration rate (eGFR) <30, claustrophobia, a contra-indication to MR environment or to gadolinium contrast administration. The study protocol

was approved by the local ethics committee (REC:10/H0408/24) and all patients gave written informed consent.

3.2.1. CMR scanning

All patients in the study underwent CMR before ICA. Scans were performed on 3T MR systems (either MAGNETOM Tim Trio or MAGNETOM Verio, Siemens Healthcare, Erlangen, Germany). CMR protocol included cine steady-state free precessions (SSFP) imaging, short-axis T1-maps (Shortened Modified Look-Locker Inversion recovery; ShMOLLI) (46), bright blood T2-weighted imaging, and early and late gadolinium enhancement (LGE) imaging, all offering full left ventricular (LV) short-axis coverage from base to apex. LGE images were obtained 10–15 min after administration of a total of 0.13 mmol/kg of a gadolinium-based contrast agent (Gadoterate meglumine, Dotarem, Guerbet, Villepinte, France or Gadodiamide, Omniscan™, GE Healthcare, Amersham, UK).

3.2.2. CMR image analysis

CMR images were analysed by three CMR experts using the cvi42 software (Circle Cardiovascular Imaging Inc., Calgary, Canada) and MC-ROI, a dedicated in-house software (programmed in IDL, version 8.7, L3Harris Geospatial, Broomfield, Colorado, USA). Visual inspection for regional wall motion abnormalities, oedema and myocardial scar were performed on cine, T1-maps, T2w and LGE imaging. Volumetric analysis of biventricular function was performed using short axis stack of cine imaging. Myocardial T1 values higher than the normal range for our scanner (1124-1244ms) were highlighted using overlay masks in MC-ROI. Quality of T1, T2 and LGE images were graded on a four-point scale (Good, Acceptable, Poor and Uninterpretable) by three of the CMR experts. CMR analysis was blinded to the ICA findings to derive an independent CMR diagnosis, in line with current CMR guidelines (47,94). In cases of disagreement between the CMR analysts, consensus was

reached with input from a fourth CMR expert. The diagnosis of acute MI required the presence of ischaemic pattern of LGE with associated oedema (on T1/T2 imaging), with or without regional wall motion abnormality (RWMA). Aborted MI was diagnosed in the presence of a RWMA, with or without evidence of acute myocardial oedema, but in the absence of LGE. Both acute and aborted MI are referred to as MI from hereon. The determination of the IRA used the American Heart Association (AHA) 17 segment model of the left ventricle (95). Acute myocarditis was diagnosed using the modified Lake-Louise criteria (47). Takotsubo cardiomyopathy was diagnosed on the basis of classical regional wall motion abnormalities (e.g. apical hypokinesia and ballooning) with associated myocardial oedema and in the absence of ischaemic LGE. When a CMR scan showed normal cardiac anatomy, biventricular volumes, systolic function, T1, T2, EGE and LGE, this was reported as having no abnormalities (nonspecific fibrosis at the left and right ventricular insertion points were not considered to be abnormal in this context or related to the acute presentation).

3.2.3. Clinical management

The clinical team members providing care for the patients were blinded to the CMR findings, and performed investigations and treatment according to current clinical practice. Multivessel disease (MVD) was defined as coronary artery lesions with >50% luminal stenosis on ICA in ≥2 coronary arteries. NOCA was diagnosed by the clinical care team when the ICA did not detect obstructive CAD or spontaneous coronary artery dissection (SCAD). CMR results were provided, only upon request by the clinicians, to aid the clinical management in patients with NOCA after the ICA had been performed.

3.2.4. Statistical analysis

Normality of data was determined using Kolmogorov-Smirnov test. Normally-distributed data are presented as mean±SD; nonparametric data as median with interquartile ranges (IQRs). Statistical comparisons were performed using student's t-test, Mann-Whitney U test, Chi-square or Fisher's test or One-way ANOVA, as appropriate.

3.3. Results

3.3.1. Study population – suspected NSTEMI

A total of 100 patients (mean age: 62±11 years) were recruited and underwent CMR prior to ICA (**Table 3.1**). All patients were admitted with cardiac symptoms (95% with chest pain, with the other 5% having equivalent cardiac symptoms) and evidence of acute myocardial injury based on elevated cTnI (median rise of 23, IQR 6-94, fold above the upper limit of normal (ULN)). ECG changes of ischaemia were present in 41% of the patients. All patients were clinically-managed as suspected NSTEMI, had received dual anti-platelet therapy and anticoagulation, and were booked to have an ICA at the time of study recruitment.

3.3.2. CMR findings pre-invasive coronary angiography

The CMR scans were performed early at 33 [20-48] hours after admission to hospital and 4 [2-6] hours before ICA. The complete CMR protocol (cine, T1 maps, T2w, EGE and LGE) was performed on 88% (88/100) patients. Of the remaining 12% (12/100) patients, 7 had cine and LGE imaging alongside one of T1 maps or T2W imaging, whilst 2 had cine and LGE imaging only due to inability to tolerate a long duration of scan. The remaining 3 patients did not have LGE imaging, including 1 patient who did not have any interpretable images available, all due to claustrophobia (**Figure 3.1**). T1, T2 and LGE images were of interpretable quality in 97, 84 and 87 percent of the cases respectively.

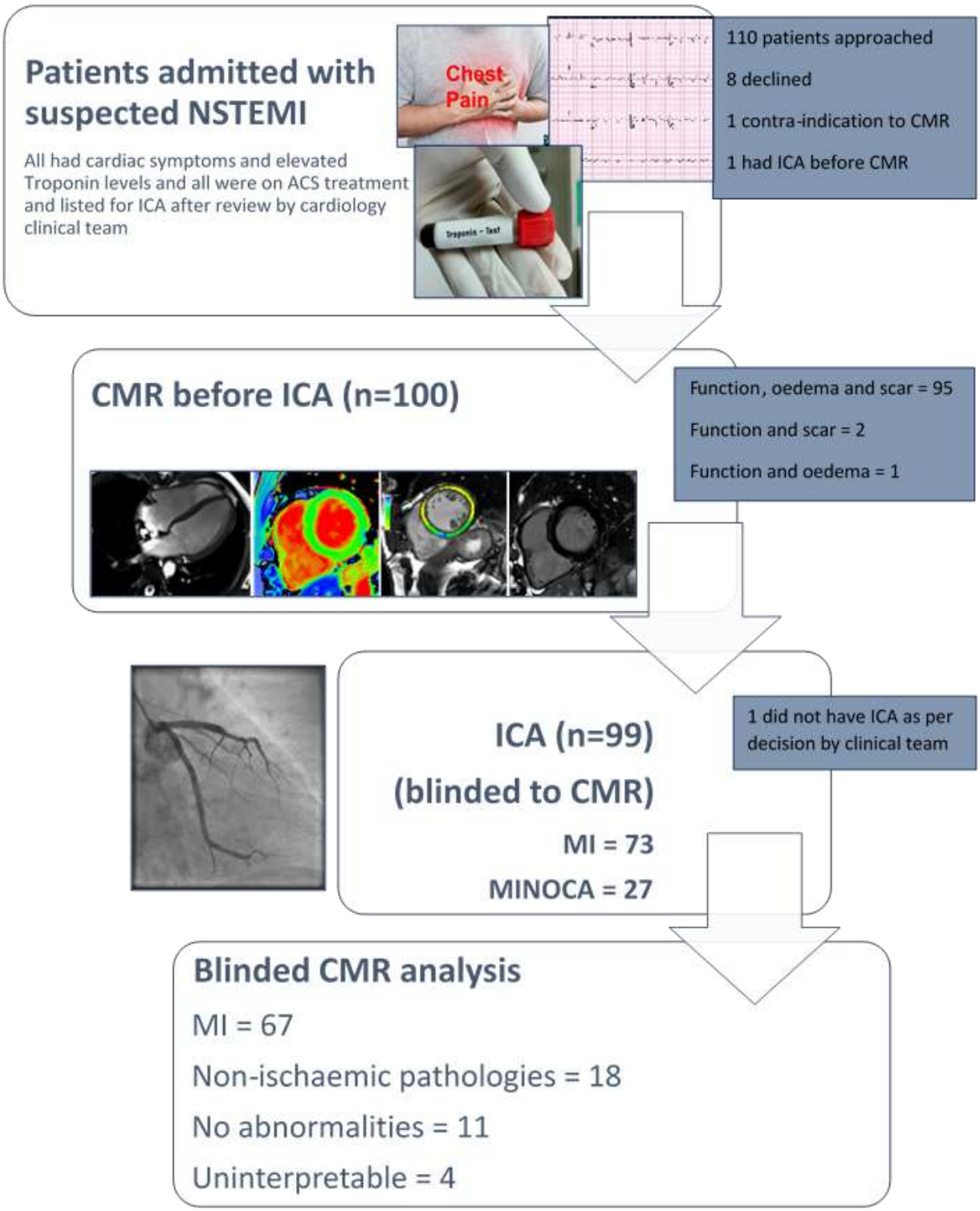


Figure 3.1 Study flow chart. NSTEMI = Non-ST-segment Elevation Myocardial Infarction. ACS = Acute Coronary Syndrome. ICA = Invasive Coronary Angiogram. MI = Myocardial Infarction. MINOCA = MI with non-obstructive coronary arteries (suspected). CMR = Cardiovascular Magnetic Resonance imaging

Table 3.1 Characteristics for All Patients and Patients Stratified by diagnosis made on Cardiovascular Magnetic Resonance performed before Invasive Coronary Angiogram

		Findings on CMR performed before ICA			
	Full cohort N=100	*Myocardial infarction N=67*	*Non-ischaemic pathologies N=18*	*No abnormalities N=11*	*P*
Demographics					
Age (years)	63±11	63±12	63±10	57±11	0.303
Male sex; (%)	70	81	44	64	0.008
BMI (kg/m^2)	29±5	29±5	27±4	27±5	0.189
Hypertension, (%)	45 (45)	35 (45)	9 (50)	4 (36)	0.774
High cholesterol %	26 (26)	17 (25)	6 (33)	3 (27)	0.794
Diabetes, %	12 (12)	9 (13)	3 (17)	0 (0)	0.385
Known CAD, %	15 (15)	11 (16)	3 (17)	1 (9)	0.403
CVA, %	3 (3)	3 (5)	0 (0)	0 (0)	0.512
Smoking history, %	51 (51)	36 (55)	8 (44)	7 (64)	0.584
CAD Family history, %	26 (26)	19 (28)	3 (17)	4 (44)	0.754
Acute admission					
Chest pain, %	95 (95)	65 (97)	15 (82)	11 (100)	0.046
Ischaemic ECG, %	41 (41)	48	24	46	0.218
C-TnI rise ^	31(7-106)	51 (12-155)	19 (5-77)	8 (2-10)	0.003
SBP (mmHg)	141±25	140±26	137±24	151±12	0.333
Heart rate (bpm)	74±18	74±16	78±25	71±16	0.583
Haemoglobin (g/L)	144	144±12	140±15	152±10	0.080
Creatinine (µmol/L)	82±18	82±17	80±20	82±12	0.948

Table 3.1 description: Average values are presented as mean±SD or median [IQR] where appropriate. Proportional data are presented as percentage for each column. P values are for comparisons amongst the three sub-groups. CAD = Coronary Artery Disease and refers to any abnormality in the coronary arteries including atherosclerosis and spontaneous coronary artery dissection. BMI = Body Mass Index. IRA = Infarct related artery. CVA = Cerebrovascular Accident. CTnI = Cardiac Troponin-I. SBP = Systolic Blood Pressure. mmHg = millimetre mercury. µmol/L = micromole / Litre. MI = Myocardial Infarction. LAD = Left Anterior Descending Artery. ^ CTnI rise = fold rise above the upper limit of normal range. # One patient did not have ICA after CMR but was diagnosed with MI by the clinical team as he had an ICA in the past which had demonstrated significant coronary artery disease. Data from the four patients with uninterpretable CMR images are not included.

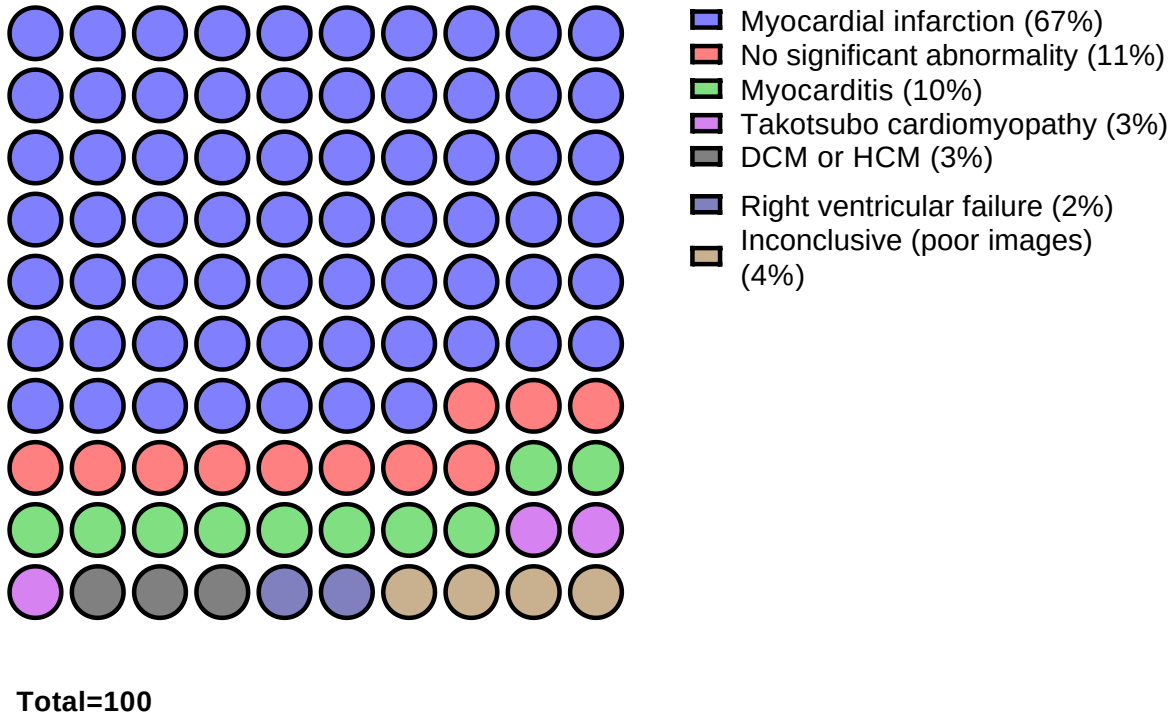


Figure 3.2 Break down (dot-plot) of diagnoses made on Cardiovascular Magnetic Resonance Imaging performed prior to the Invasive Coronary Angiogram. DCM = dilated cardiomyopathy, HCM = hypertrophic cardiomyopathy

CMR confirmed acute MI in 67% (67/100) of patients and non-ischaemic pathologies in 18% (18/100) and no significant abnormalities in 11% (11/100) whilst 4% (4/100) of the CMR scans was inconclusive, due to poor image quality (n=3) and a patient not completing the scan (n=1) (**Figure 3.2**).

The non-ischaemic diagnoses made on CMR included takotsubo cardiomyopathy (n=3), hypertrophic or dilated cardiomyopathy (n=3), myocarditis (n=10) and isolated RV failure in 2 patients. CMR did not detect any abnormalities in 11 patients (**Figure 3.2**).

Patients with a CMR diagnosis of confirmed MI (referred to as CMR-MI hereon) were predominantly males, when compared to patients with non-ischaemic aetiologies and normal findings (81% vs 33% vs 64%; p =0.008), and had a higher fold Troponin rise (51 [12-155] vs 19 [5-77] vs 8[2-10]; p = 0.003). The most significant difference in Troponin rise, based on post-hoc testing, was between the patients with MI and patients with normal findings (p = 0.006). All other baseline clinical characteristics were similar. LV ejection faction was lower in patients with CMR-MI and non-ischaemic pathologies, compared to those with no significant CMR abnormalities (51±8% and 50±12% vs 61±5%; p = 0.005) (**Table 3.2**).

Table 3.2 ICA and CMR findings

		Findings on CMR performed before ICA			
	Full cohort N=100	*Myocardial infarction N=67*	*Non-ischaemic pathologies N=18*	*No abnormalities N=11*	*P*
ICA findings					
MI diagnosed on ICA (%)	73 (73)[#]	61 (91)	7 (39)	4 (36)	<0.001
LAD is IRA (%)	31 (31)	27 (40)	4 (22)	0 (0)	<0.001
Revascularisation (%)	62 (62)	50 (75)	7 (39)	4 (36)	0.003
Multivessel CAD (%)	50 (50)	36 (54)	9 (50)	4 (36)	0.563
Multivessel revascularisation (%)	18 (18)	14 (21)	3 (17)	1 (9)	0.429
CMR findings					
Time since symptoms (hours)	57[26-70]	47[25-71]	43[38-83]	58[37-68]	0.601
Time since hospitalisation	33[20-48]	29[20-48]	37[24-48]	37[22-58]	0.475
Time before ICA	4[2-6]	3[2-6]	4[3-6]	7[2-22]	0.322
LVEDVi (ml/m^2)	77[67-88]	77[67-87]	78[65-89]	72[58-83]	0.296
LVESVi (ml/m^2)	36[29-41]	36[29-43]	39[35-42]	25[21-32]	0.005
LVEF (%)	52±10	51±9	50±12	61±5	0.004
LV mass index	49±14	53±14	49±13	46±9	0.124
RVEF (%)	55±8	55±8	52±13	58±4	0.156

Table 3.2 description and Abbreviations as per Table 1. LVEDVi – Left Ventricular End Diastolic Volume indexed to body surface area. LVESVi - Left Ventricular End Systolic Volume indexed to body surface area. LVEF – Left Ventricular Systolic Function. RVEF – Right Ventricular Ejection Fraction. #1 patient had MI diagnosed based on a previous but recent ICA. P values are for comparisons amongst the three sub-groups.

3.3.3. Invasive coronary angiography findings

Based on the ICA features, the clinical care team found a potential culprit coronary artery, and diagnosed MI in 73% (73/100) of the patients (one did not undergo ICA after CMR, but the clinical care team diagnosed MI based on a previous but recently performed ICA). These patients are referred to as ICA-MI from hereon. Of these, 85% received revascularisation (PCI; n=56 and CABG; n=6) whilst the remaining 15% received medical therapy alone (n=11).

MVD was present in 58% (42/73) of the patients with ICA-MI; LAD was involved in 21, LCX in 6 and RCA in 9, whilst 6 patients had disease in more than one non-culprit arteries. Multivessel revascularisation was performed in 57% of patients with MVD (PCI; n=18 and CABG; n=6). Of the 18 who had PCI to non-culprit arteries, 8 were to LAD, whilst LCX and RCA had PCI in 4 patients each and 1 patient had 2 non-culprit arteries.

NOCA was found in 27% (27/100) patients. These patients are referred to as ICA-NOCA hereon. 5/27 were diagnosed with Takotsubo syndrome after the ICA whilst 1 each were diagnosed as heart failure and hypertrophic cardiomyopathy. The remainder (n=20) had a smaller Troponin rise when compared to those with ICA-MI (9[6-24] vs 43[8-140] fold; p=0.019) and were discharged on dual antiplatelet therapy with a working diagnosis of MINOCA.

3.3.4. Comparison of diagnoses made on CMR and ICA

Overall, the diagnosis made by CMR and by ICA in the two broad categories of MI and NOCA were concordant in 79% (79/100) patients (MI = 61 or NOCA = 18). See **Table 3.3** and **Figure 3.3**.

Table 3.3 Reclassification of clinical diagnosis with ICA using CMR

		CMR diagnosis				Total
		MI	Non-ischaemic causes	No significant abnormalities	Inconclusive	
Clinical diagnosis based on ICA	MI	61	7	4	1	73
	NOCA	6	11	7	3	27
Total		67	18	11	4	100

Table 3.3; CMR provided a diagnosis in 85 patients which led to a reclassification of diagnosis in 24 patients. The diagnosis made by CMR and by ICA in the two broad categories of MI and NOCA were concordant in 79 patients (79%). CMR did not find any abnormalities in 11 patients, of whom 4 were found to have obstructive coronary artery disease and were treated as having had a MI. Non-ischaemic causes include myocarditis, dilated or hypertrophic cardiomyopathies, Takotsubo cardiomyopathy and right ventricular failure. NOCA = Non-obstructive Coronary Arteries.

In the patients with a presumed diagnosis of MI based on angiographic findings (ICA-MI; n = 73), CMR confirmed the presence of MI in only 84% (61/73); in the remaining 16% (12/73) of patients with ICA-MI, CMR demonstrated non-ischaemic causes in 58% (7/12), did not detect any MI or other abnormality in 33% (4/12) despite good image quality, and was inconclusive in 1 case due to poor image quality; see **Figure 3.3**.

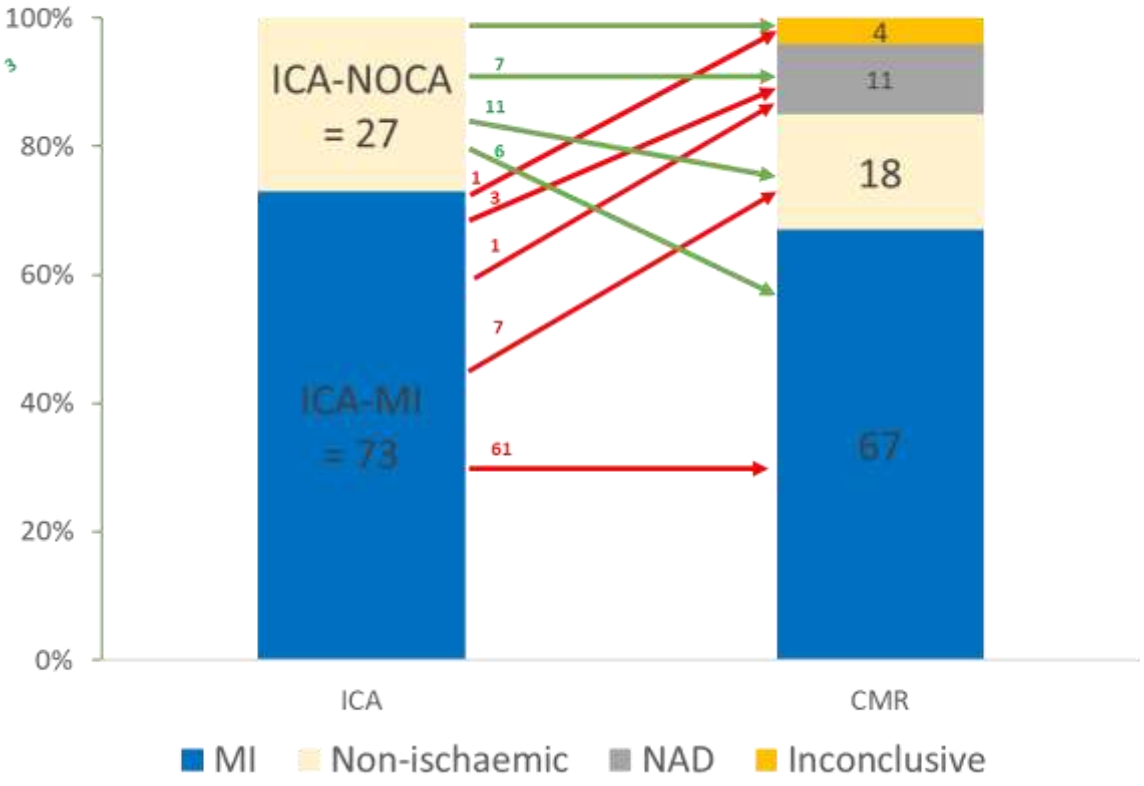


Figure 3.3 CMR diagnosis in patients treated for ICA-MI (n=73) and ICA-NOCA (n=27). Non-ischaemic causes include myocarditis, dilated cardiomyopathy, hypertrophic cardiomyopathy, Takotsubo cardiomyopathy and right ventricular failure. NAD = No significant abnormality detected.

3.3.4.1. ICA-NOCA vs CMR diagnoses

In patients with ICA-NOCA (n = 27), CMR confirmed the presence of a MI in 22% (6/27) (*true* MINOCA), a non-ischaemic cause in 41% (11/27), whilst it did not detect any significant abnormality in 26% (7/27). The remaining three scans (11%) were non-diagnostic due to incomplete scan or poor image quality.

The three subgroups within the ICA-NOCA cohort (MINOCA, non-ischaemic and normal) were of similar age (65±7 vs 65±10 vs 56±12; p=0.174) and had similar burden of chest pain at presentation (83 vs 85 vs 100%; p=0.248) and ischaemic ECG abnormalities (p=0.135) and level of Troponin (p=0.208).

3.3.4.2. ICA-IRA vs CMR-IRA

Amongst patients diagnosed with MI on both ICA and CMR (n=61), there was diagnostic concordance in 54 patients (89%). It identified a different IRA in 7 patients (11%). All 7 patients had MVD of whom 3 patients had PCI; amongst these the ICA-CMR IRA mismatches were RCA-LAD, RCA-LAD and LAD-RCA. Amongst the 4 who did not have PCI, the IRA was not determined on ICA but was identified as LAD in 3 and RCA and in the other on CMR; 2 of these patients had CABG and the other 2 were medically managed. See **Table 3.3**

3.4. Potential clinical utility of CMR pre-ICA

Overall, CMR pre-ICA had the potential to change diagnosis and management in 31% of patients by reclassifying the diagnosis in ICA-NOCA (n=17; 17%), change identification of the IRA in patients diagnosed with both ICA-MI and CMR-MI (n=7; 7%) and detect non-ischaemic pathologies (n=7; 7%) of patients diagnosed with presumed MI on ICA. See **Figure 3. 4**.

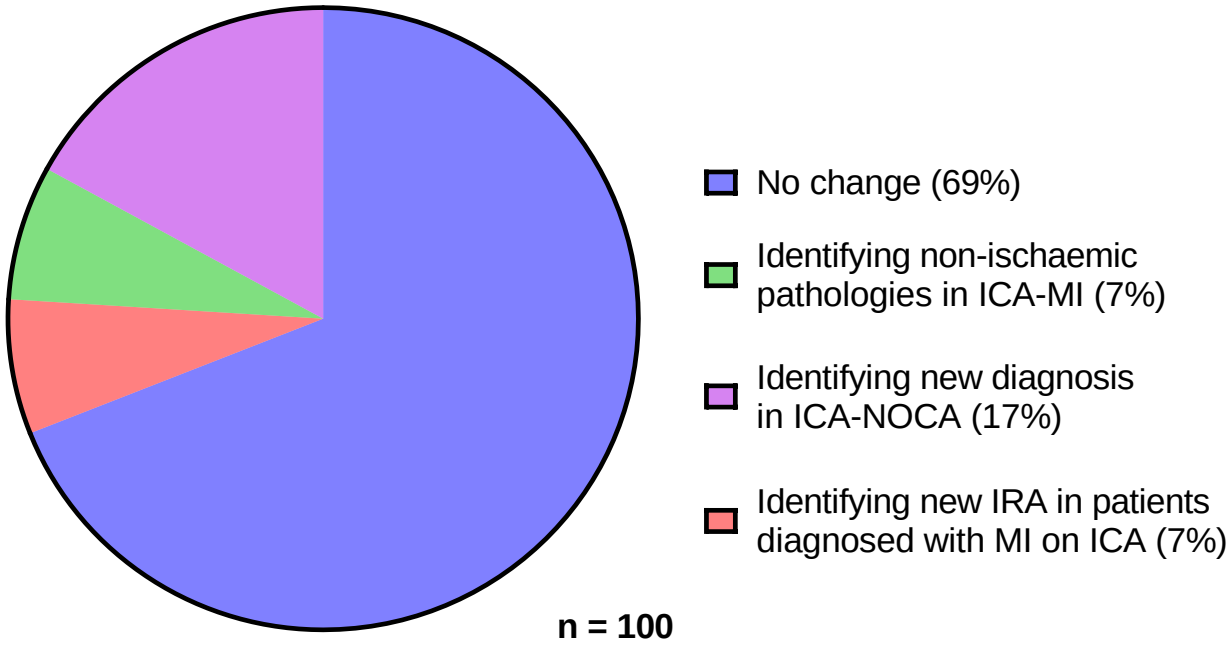


Figure 3. 4 Change in clinical management of patients with CMR prior to ICA. Such a strategy has the potential to change clinical management in 31% of the patients

	CMR-ICA agreement on IRA			Total
	Agreement	Discrepancy	Undetermined by both	
MI on both CMR and ICA	53 (87%)	7 (11%)	2 (3%)	61

Table 3.4 Agreement on IRA when both CMR and ICA diagnosed MI

3.5. Discussion

This study of CMR prior to ICA in patients with suspected NSTEMI found that:

1) CMR provided a diagnosis in 85% and showed normal findings in 11%.
    a. Amongst patients diagnosed with ICA-MI (n=73), CMR agreed with the diagnosis in 84% but showed non-ischaemic pathologies in 8% and no significant abnormalities in 5%.
    b. Amongst patients with ICA-NOCA (n=27), CMR detected MINOCA in 22%, non-ischaemic aetiologies in 41% and no significant abnormalities in 26%.
2) CMR-first strategy has the potential to change management in at least 31% of patients by reclassifying diagnosis in NOCA (17%) and in MI (7%) and offering a new IRA in MI (7%) to guide revascularisation and clinical decision-making.

In current clinical practice, a working diagnosis of MINOCA is made when a patient with acute myocardial injury is found to have NOCA on ICA (4). However not all in this group have MI and thus intracoronary imaging and vasoreactivity testing are recommended in all cases of NOCA to confidently exclude MI due to acute plaque rupture or coronary artery dissection or vasospasm. However, these investigations are not universally employed owing to procedural complexity, time, risks and financial implications and can still miss embolic MIs (4,96). Thus, contemporary guidelines recommend a CMR in patients with acute myocardial injury and NOCA (40). However, the role of acute CMR imaging as a gate-keeper to ICA in patients with acute myocardial injury and suspected NSTEMI is less well established which has led researchers to investigate this further (3 studies). (6,8,97) One of these studies relied only on cine imaging (for wall motion and ventricular function) and late gadolinium enhancement (LGE) imaging (for scar assessment) whilst the other two also employed T2 weighted imaging (for myocardial oedema) and stress perfusion imaging (for

detection of ischaemia) in addition. None of them employed non-contrast T1-mapping, as we have done in our study; T1-mapping can help establish the presence of oedema (52) and acute myocardial injury in NSTEMI better than T2 weighted imaging (54). Heitner et al's study of 114 patients with suspected NSTEMI showed that CMR (cine and LGE) diagnosed non-ischaemic pathologies in 15% of patients and showed normal findings in 14% and had the potential to change management in up to 46% of the patients (6). Van Cauteren et al study of 51 patients reported that a pre-ICA CMR (cine, T2w, LGE) had a 77% accuracy to detect obstructive CAD. The diagnostic accuracy improved to 86% after applying stress perfusion imaging in 19 patients (out of the 51 patients) who had normal/equivocal findings on the initial three CMR sequences. Lastly, Smulders et al randomized patients with suspected NSTEMI to either CMR (n=60) or CT coronary angiogram (n=70) or ICA (n=68) and found that CMR-first strategy obviated the need for ICA in 13% of patients and that the clinical outcomes of the three cohorts were similar at 1 year after recruitment (8). Amongst those that underwent CMR (n=60, cine, T2w, LGE and stress perfusion imaging), the diagnosis included MI in 77%, myocarditis in 2%, equivocal findings in 7% and normal findings in 13%. Allowing for differences in the clinical characteristics of the patients and in clinical practice amongst the centres, the findings reported in the three papers are strikingly congruent with ours as we diagnosed MI in 67% and non-ischaemic pathologies in 18% and normal findings in 11% (see Table 3).

A comprehensive CMR can diagnose acute and chronic MIs with high degree of precision (98). It can also help detect aborted MI even in the absence of scar by detecting regional wall motion abnormalities and myocardial oedema in the distribution of a single coronary artery territory.(99) Moreover, the same sequences can accurately diagnose non-ischaemic myocardial injury, where the LGE, if present, will spare the sub-endocardium. In our study, 11% of patients did not have any significant abnormalities on CMR. These patients had much

lower C-TnI rise than the cohorts with ischaemic and non-ischaemic diagnosis (5 fold vs 43 and 10-fold respectively, p=0.004, Table 1). 7 of the 11 patients (64%) with normal CMR findings also had NOCA on ICA and therefore it is possible that their symptoms and rise in C-TnI-I are unlikely to be due to a primary cardiac pathology. However, the remaining 4 patients (36%) were found to have obstructive CAD on ICA. The lack of evidence of RWMA or myocardial oedema or infarction in these 4 patients indicate that their presentation was likely to be due to mild myocardial ischaemia leading to mild elevation of high-sensitive C-TnI levels which may not be within the sensitivity of multi-parametric CMR. It is also known that CMR is not sensitive enough to detect mild injury to the thin right ventricular myocardium or very small myocardial infarction of either ventricles associated with a small C-TnI rise as previously described (100). Therefore, whilst a patient with a normal CMR has a high chance (64% in our study) of NOCA, an assessment of their coronary arteries will still have to be performed to exclude obstructive CAD.

In our study CMR yielded a diagnosis in 63% of patients with NOCA on ICA (n=27); MINOCA in 22% and non-ischaemic aetiologies (myocarditis, takotsubo cardiomyopathy, other cardiomyopathy) in 41% whilst 26% of the scans did not detect any significant abnormality and 11% were inconclusive. The diagnostic yield is slightly lower than many of the previously published literature with diagnostic rates of up to 80% (57,100); however this might be due to the fact that the patients in our study with NOCA and normal CMR (26%) had a very mild rise in Troponin rise (5 fold vs 10 fold in non-ischaemic pathologies vs 43 fold in MI). Such Troponin rise could represent a false positive result and would usually not result in a referral to CMR after ICA demonstration of NOCA.

We believe that a CMR-first strategy is both safe and clinically feasible as shown in our study and those by other groups (6,8). When used as a gatekeeper to ICA in acute myocardial injury, it has the potential to save healthcare costs as ICA is associated with a long hospital

stay and procedural complications. Our findings should inform large multi-centre randomised control trials of a CMR-first strategy vs ICA-first strategy vs a hybrid (CMR & ICA) strategy in determining the causes of acute myocardial injury in patients suspected to have NSTEMI. The recent advances in contrast-free CMR for tissue characterisation (101) and coronary imaging (Coronary CMR Angiogram) (102) may further this approach with the claimed threefold faster and cheaper imaging solutions and may help CMR to become a first-line non-invasive test for patients with acute myocardial injury. Other options to replace ICA as a first-line diagnostic test include a hybrid non-invasive imaging strategy using high-resolution computed tomography cardiac angiogram (CTCA) and CMR in all comers before proceeding to ICA; this approach might offer incremental diagnostical power in cases where either testing fails to detect the cause of acute myocardial injury. Any of these strategies will require the availability of scanners, fast imaging protocols and prompt reporting of scans to aid wide-spread adoption. If proved, they have the potential to offer precision medicine and improve patient experience by reducing unnecessary invasive procedures and the associated risks.

3.5.1. Limitations

Our study was performed in a single institution and thus multi-centre studies are needed to confirm the reproducibility our findings. Our scanner did not have a validated T2 mapping sequence, which is now an integral part of contemporary multiparametric CMR imaging to detect myocardial oedema; however, we did use both T1 mapping and T2w imaging which are well established methods in detecting oedema (52). Our definition of match between ICA and CMR in identifying the IRA was limited to the three main coronary arteries and is based on the standard 17 segment model assuming normal coronary anatomy. Mismatch was minimised where possible, when the IRA on ICA was either the intermediate ramus or the branches of the three main arteries. Comprehensive evaluation with intracoronary imaging

was not performed in the majority of the cases which could have improved ICA's performance in diagnosing MI and true NOCA alike.

3.6. Conclusion

In this single-centre prospectively conducted cohort study of patients with suspected NSTEMI, a CMR pre-ICA has the potential to change the management in at least 31% of patients by diagnosing non-ischaemic pathologies (24%) and by reclassifying the IRA in MI (7%). Based on this work, larger multi-centre studies are justified to test the clinical and cost-effectiveness of this hybrid approach.

4. Acute changes in myocardial tissue characteristics during early hospitalization in patients with COVID-19

4.1 Introduction

Early studies of COVID-19 survivors at 3-6 months post-infection found a high prevalence (26-78%) of cardiac abnormalities when evaluated using cardiovascular magnetic resonance imaging (CMR), mainly reporting high myocardial T1 and T2 signals (103–105). However, a case-control study found no excess in CMR abnormalities at 6 months after mild COVID-19 (106). These discrepancies may be multi-factorial, including heterogeneity in the severity of COVID-19, prevalence of past cardiac disease, scan timing and protocols (T1 and T2 assessments did not offer full heart coverage in most published studies). Additionally, there was also a lack of systemic testing for biochemical evidence of acute myocardial injury (Troponin rise) at the time of acute illness, and lack of control groups (104). Importantly, it is unclear if the myocardial T1 and T2 abnormalities found during convalescence were present during the acute COVID-19 illness. Elevated T1 and T2 indicate elevated myocardial water content, and has been observed in patients with other acute non-cardiac systemic illnesses (107); these may not necessarily indicate histopathologic myocarditis, but may reflect acute myocardial oedema. Thus, in this prospective study, I investigated the cardiac findings during the acute and recovering phases of COVID-19 using CMR, in patients without a history of cardiac disease, and compared them to controls without COVID-19 but with matching cardiovascular risk factors.

4.2 Methods

Two cohorts of participants (total n=42) were prospectively recruited near the start of the COVID-19 pandemic, between May 2020 and May 2021: (1) patients hospitalized for acute COVID-19 (n=23) and (2) outpatient controls without COVID-19 but with cardiovascular risk factors and no cardiac symptoms (n=19). Ethical approval was obtained (REC:10/H0408/24); all participants gave written informed consent. The acute COVID-19

cohort included patients admitted with hypoxia requiring oxygen and/or steroid therapy. COVID-19-negative controls were prospectively recruited from the community to match the clinical characteristics (age, sex and cardiovascular risk factors) in the acute COVID-19 cohort. Exclusion criteria included documented history of pre-existing cardiac disease or cardiac symptoms (verified by electronic patient records), previous COVID-19 and/or vaccination (verified on history and with dedicated antibody testing) and hemodynamic or respiratory instability (i.e. escalating oxygen support) at the point of scanning. Cardiac Troponin levels (cTnI) were measured before the CMR scan. Normal Troponin level in Oxford University Hospitals is <34ng/L. Patients with a clinical diagnosis of acute myocardial infarction (MI) or a clinical indication for CMR were excluded; this was done to investigate the incidental cardiac findings on CMR during acute COVID-19. COVID-19 severity was graded on the World Health Organization (WHO) four-point scale on chest imaging (108). All patients were recruited after they became clinically and haemodynamically stable, and underwent blood sampling and CMR, per this study's prospective research protocol. Safety precautions, including the wearing of full personal protection equipment (PPE) by researchers, were implemented in line with hospital-wide guidance at the time of the study (See **Figure 4.1**).

The CMR (3-Tesla) methods included whole-heart slice-matched cine, native T1-mapping (ShMOLLI), bright-blood T2-weighted imaging (T2 signal intensity ratio of myocardial vs skeletal muscle; T2SI), late gadolinium enhancement (LGE) imaging, and extracellular volume (ECV) quantification (46,109–111). Acute COVID-19 patients were invited for a 6-months follow-up CMR and blood tests. Image analysis was performed on CVI_{42} (Circle Cardiovascular Imaging Inc, Canada) by three experts. Abnormally high myocardial T1 and T2SI were defined as T1>1244ms (>2SD above mean in healthy volunteers; 1184±30ms) and T2SI>1.4 (>2SD above mean in healthy volunteers and rounded up; 1.2±0.1), respectively.

Statistical analysis was performed on SPSS v25 (SPSS Inc, USA). Categorical values are presented as frequencies and percentages. Continuous values are presented as mean±SD or median (IQR), where applicable. Between-group comparisons were performed using independent and paired t-tests, Wilcoxon signed-rank test, Kruskal-Wallis test, Fisher's exact test or McNemar's test, as appropriate.



Figure 4.1 Photo showing a patient admitted to John Radcliffe Hospital with acute COVID-19 infection being placed in the bore of the 3T scanner in Acute Vascular Imaging Centre (AVIC*)* for the purposes of this research study. *All the healthcare professionals involved in the research scan wore level 2 or 3 personal protection equipment (PPE) in line with their role in the care of the patient during the CMR scan and the local infection control policies of that time (this scan took place on 3rd August 2020)..*

4.3 Results

Acute COVID-19 patients and controls had similar baseline characteristics, although there was a trend towards higher proportion of smokers in the acute COVID-19 cohort (11% vs 40%, p=0.075). Patients with COVID-19 had higher temperature and heart rate and lower blood pressure and arterial oxygen saturation. They also had higher C-reactive protein levels and lower lymphocyte count and haematocrit and higher levels of D-dimer and NT-pro BNP (**Table 4. 1**). 65% of acute COVID-19 patients had ≥ WHO grade 2 disease severity on chest imaging; 22% had received non-invasive ventilation and 13% had a diagnosis of pulmonary embolism prior to the CMR scan. CTnI was elevated in 8 (35%) patients with acute COVID-19, which were considered by the clinical care team to be mild and part of their acute illness (median rise of 2.4-fold above the normal threshold), and thus these patients were not on treatment for acute coronary syndrome or myocarditis. None of the patients had any documented arrhythmia prior to recruitment.

Table 4. 1 Baseline characteristics and blood test results

	Control (n=19)	COVID-19 (n=23)	p-value
Age (years)	57±12	58±14	0.838
Male sex (%)	63	69	0.748
Ethnicity (White Caucasian %)	74	70	1
Past history of cardiac disease	0	0	1
Diabetes (%)	0	9	0.492
Hypertension (%)	16	35	0.291
Smoker (%)	11	40	0.075
Temperature (ºC)	37.13±0.5	37.96±0.71[#]	<0.001
Oxygen saturation (%)	97.37±1.8	90.13±4.61[#]	<0.001
Systolic blood pressure (mmHg)	136±16	103±23[#]	<0.001
Heart rate (bpm)	67±7	98±17[#]	<0.001
White blood cell count (10^9/L)	5.63±1.9	7.1±3.9[#]	0.143
Lymphocyte count (10^9/L)	1.59 (1.42-1.94)	0.69 (0.48-1.00)[#]	<0.001
Haematocrit	0.43±0.03	0.40±0.04	0.031
D-dimer (ng/ml)	227 (167-317)	1609 (769-2723)[#]	<0.001
C-reactive protein (mg/L)	1 (0.60-1.5)	120 (60-160)[#]	<0.001
Troponin-I (ng/ml)	1.99 (1.99-3)	9 (5-62)[#]	<0.001
Elevated Troponin (>34ng/ml) (%)	0	8 (35)	0.005
NT-pro-BNP (pg/ml) (normal <400pg/ml)	53 (25-77)	217 (70-365)[#]	0.001
COVID-19 severity score ≥2 on CT	N/A	65	N/A
Pulmonary embolism diagnosed (%)	N/A	13	
Treatment with steroids (%)	N/A	57	
Treatment with Remdesevir (%)	N/A	48	
Treatment with antibiotics (%)	N/A	74	
Non-invasive ventilation (%)	N/A	22	

Table 4.1 description: Baseline demographics, vital signs, blood test results ([#] worst values during hospitalization for the patient cohorts), treatment administered and CMR findings. Categorical values are presented as frequencies in percentage (%). Continuous values are presented as mean±SD or median (IQR) where applicable. CTnI levels reported as <2ng/ml in the laboratory assay are presented as 1.99ng/ml. NT-pro-BNP – N-Terminal prohormone of brain natriuretic peptide. CT- computed tomography.

Median time between admission for COVID-19 infection and CMR was 3 days [1-7]. On CMR imaging, controls and acute COVID-19 patients had similar left and right ventricular ejection fraction (LVEF 62±7 vs 65±6%; p=0.103, RVEF 60±6 vs 58±6%; p=0.373). They also had similar ECV (31±3 vs 31±4%; p=0.804) and frequency of LGE abnormalities (16 vs 14%; p=0.981). Non-ischaemic LGE, suggestive of myocarditis, was observed in two participants each from the control (11%) and acute COVID-19 (9%) cohorts. Myocardial infarction was present in one each from the two cohorts (**Table 4. 2**).

Compared to controls, patients with acute COVID-19 had significantly higher myocardial T1 (1183±22 vs 1217±41ms; p=0.002) and T2SI (1.13±0.09 vs 1.47±0.36; p<0.001) (**Figure 4.2**). Whilst all control subjects had normal T1 and T2SI, abnormally high T1 and T2SI was present in 26% and 50% of acute-COVID patients, respectively. Those with abnormally high T1 had significantly higher LVEF compared to patients with normal T1 (68±8 vs 62±5%; p=0.04), whilst there was no significant difference in the LVEF between patients with abnormally high and normal T2SI (65±7 vs 63±6%; p=0.519). There were no significant differences in the T1, T2SI or ECV between patients treated with and without corticosteroids (1220±42 vs 1213±41ms (p=0.703), 1.43±0.34 vs 1.53±0.40 (p=0.543) and 32±4 vs 30±4% (p=0.303) respectively).

The acute COVID-19 patients with mildly elevated CTnI had similar CMR findings compared to acute COVID-19 patients with normal CTnI levels; the T1 was 1217±28 vs 1205±45ms (p=0.357) and the T2SI was 1.51±0.33 vs 1.37±0.45 (p=0.274), respectively (**Figure 4.3).** Pathological LGE was seen in 2/8 patients with raised CTnI and 1/15 patients with normal CTnI levels, leading to further cardiology referrals, and coronary revascularization in one patient. The CMR findings did not change the clinical management of other patients.

Table 4. 2 CMR and blood test findings in controls, acute COVID-19 patients and at follow up

	Controls (n=19)	**Acute COVID-19 (n=23)**	***P* *(vs controls)***	**Follow up COVID-19 (n=12)**	***P* *(vs controls)***	***P* *(vs acute) (paired analysis)***
Time of CMR scan after admission (days)	N/A	3 (1-7)	N/A	166 (116-184)	N/A	N/A
Heart rate during scan (bpm)	67±7	72±15	0.077	65±11	0.571	0.199
LVEDV indexed to BSA (ml/m^2)	74±13	67±15	0.103	75±13	0.920	0.761
Left ventricular ejection fraction (%)	62±7	65±6	0.272	65±7	0.397	0.615
RVEDV indexed to BSA (ml/m^2)	77±15	69±15	0.118	72±14	0.356	0.975
Right ventricular ejection fraction (%)	60±6	58±6	0.373	61±6	0.490	0.085
Global LV myocardial T1 (ms)	1183±22	1217±41	**0.002**	1180±36	0.435	0.177
Global myocardial T2 Signal Intensity ratio (T2SI)	1.13±0.09	1.47±0.36	**<0.001**	1.24±0.09	**0.006**	0.127
Global myocardial extracellular volume (ECV) (%)	31±3	31±4	0.804	29±3	0.073	0.234
Presence of pathological LGE[§], n (%)	3 (16)	3 (14)	1	0 (0)	N/A[#]	N/A[#]
Presence of ischaemic LGE, n (%)	1 (5)	1 (5)	0.981	0 (0)	N/A[#]	N/A[#]
Presence of non-ischaemic LGE, n (%)	2 (11)	2 (9)		0 (0)	N/A[#]	N/A[#]
C-reactive protein (mg/L)	1 (0.60-1.5)	120 (60-160)	**<0.001**	1.4 (1-2.2)	0.104	**0.005**
Troponin-I (ng/ml) (normal <34ng/ml)	1.99 (1.99-3)	9 (5-62)	**<0.001**	4.1 (1.99-7.3)	0.085	**0.004**
NT-pro-BNP (pg/ml) (normal <400pg/ml)	53 (25-77)	217 (70-365)	**0.005**	83 (36-230)	0.346	**0.033**

Baseline CMR findings. Categorical values are presented as frequencies in percentage (%). Continuous values are presented as mean±SD or median (IQR) where applicable. LVEDV – Left Ventricular End Diastolic Volume. BSA – Body Surface Area. ECV – extracellular volume. Myocardial T2 signal intensity ratio (T2SI) was compared to skeletal muscle. LGE – late gadolinium enhancement. Other abbreviations as per **Table 4. 1**. § Presence of LGE in the ventricular insertion points was not considered pathological. The patterns of non-ischaemic LGE seen in each group: two control subjects had sub-epicardial LGE and two COVID-19 patients had mid-wall fibrosis.

Twelve acute COVID-19 patients returned for follow-up at around 6 months (median 166, IQR 116-184 days) after the acute CMR scan. At follow up, patients had normal inflammatory (CRP 1.4 (1-2.2) mg/L) and cardiac biomarkers (Troponin-I 4.1 (1.99-7.3 ng/L); NT-proBNP 83 (36-230)) pg/ml (all $p<0.05$ when compared to blood tests during the hospitalization) (**Table 4. 2**). All patients demonstrated normal myocardial T1 (1180±36ms) and T2SI (1.24±0.09) on the 6-months scan (**Table 4. 2, Figure 4.4**). There were no new LGE abnormalities at follow up.

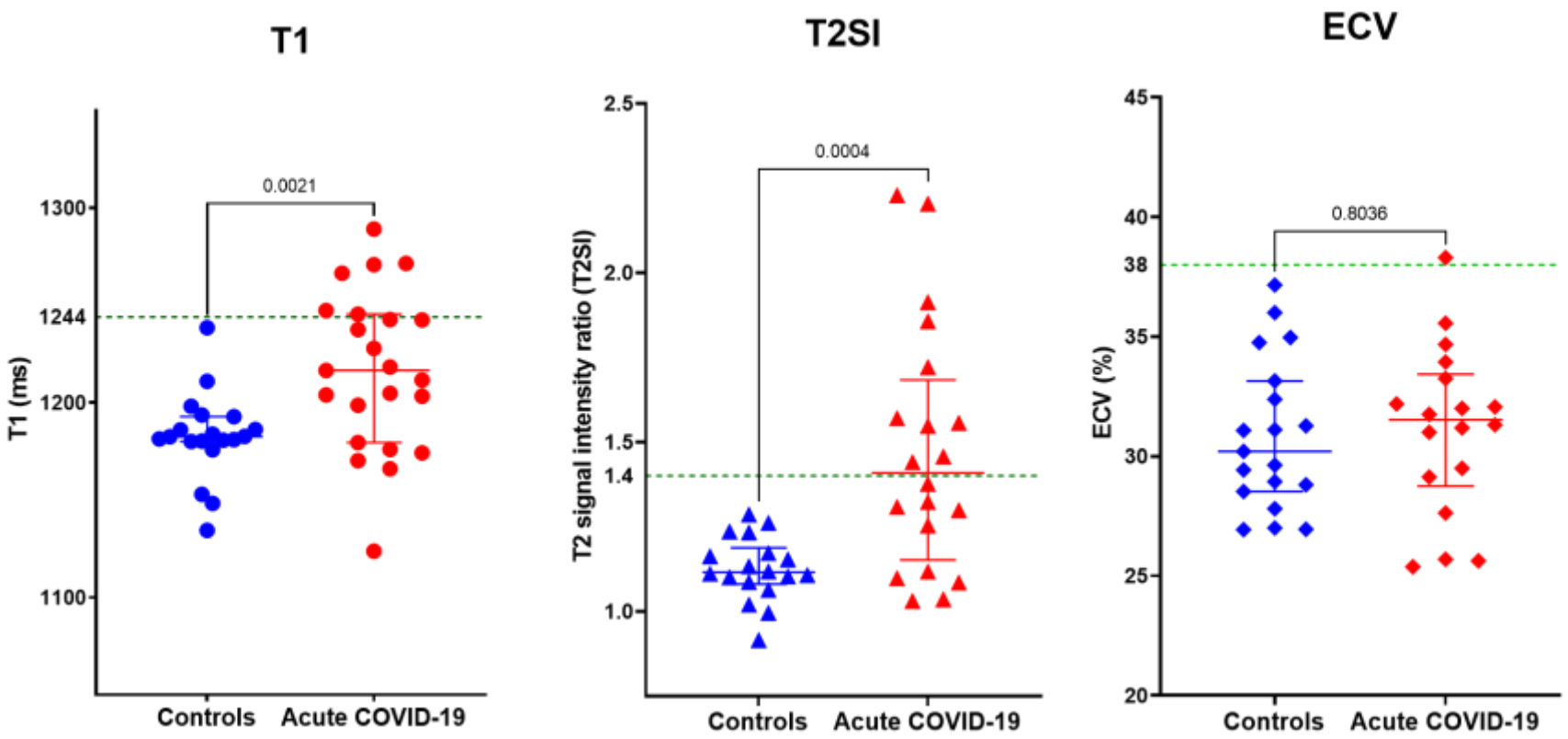


Figure 4.2 Myocardial tissue characteristics on CMR during acute COVID-19 in hospitalized patients compared to controls without COVID-19 from the community matched for cardiovascular risk factors. *Comparison of global myocardial T1, T2SI (T2 signal intensity) ratio and extracellular volume (ECV) fraction between outpatient controls without COVID-19 and patients with acute COVID-19 during their hospitalization. Green dotted line in the graphs denote the upper limit of normal ranges for T1, T2SI ratio and ECV in the 3T MR scanner used for this study.*

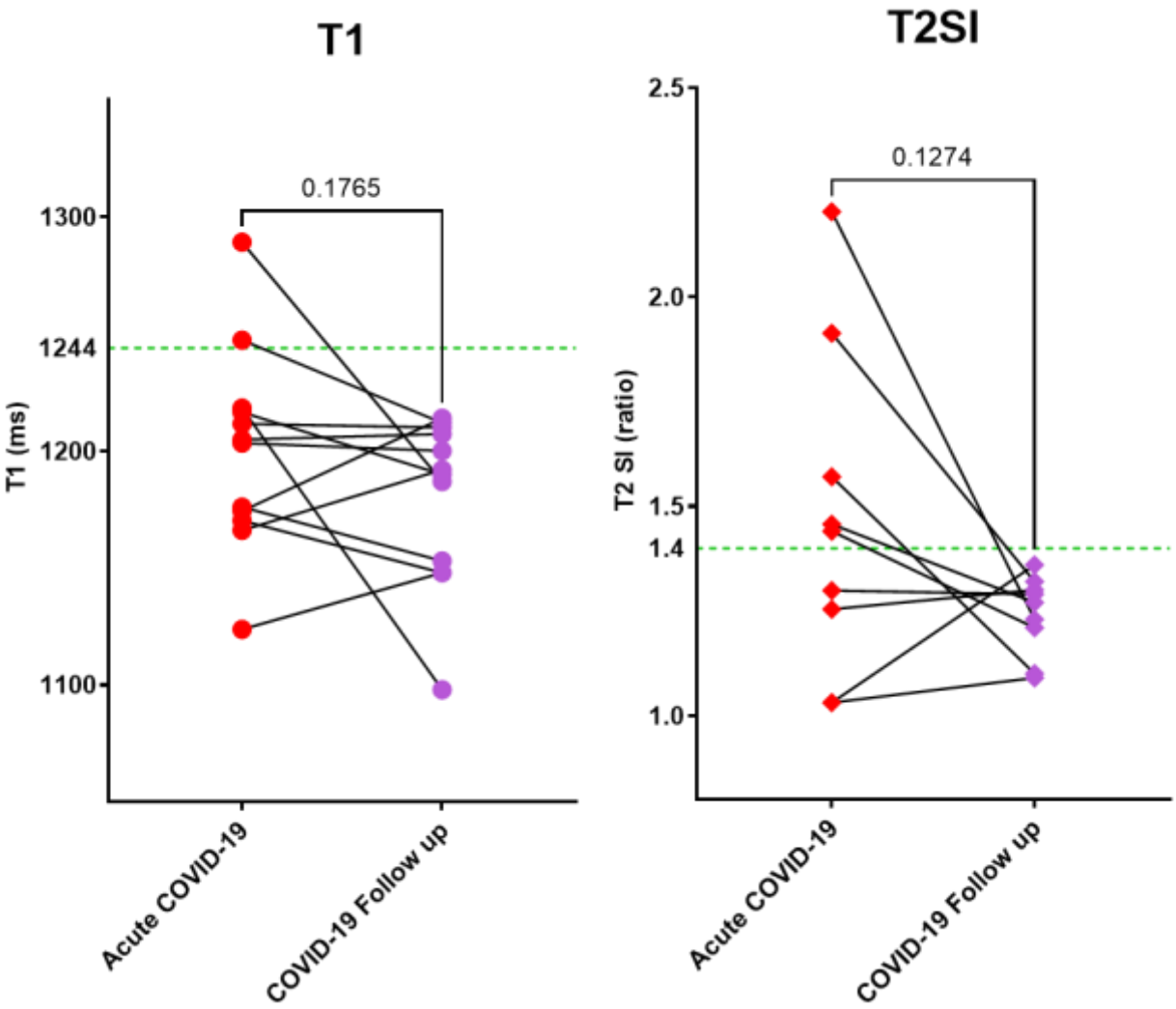


Figure 4.3 Myocardial oedema as measured by CMR T1 and T2SI during acute COVID-19 and at follow up (at 6 months). *Out of 23 patients scanned during acute COVID-19, 12 returned for follow up during the pandemic. All patients had normal T1 and T2SI ratio at follow up. Green dotted line in the graphs as per* ***Figure 4.2***

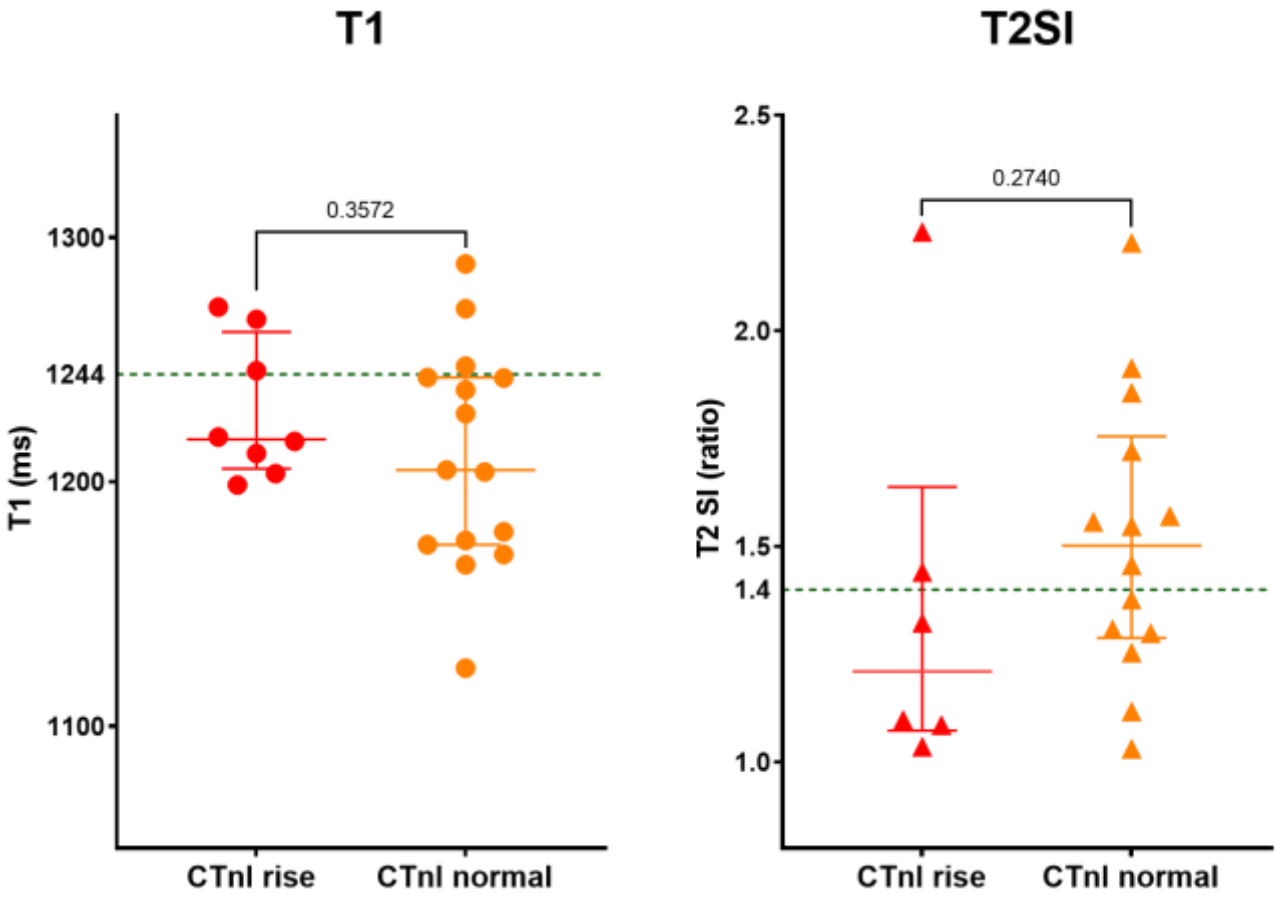


Figure 4.4 Myocardial tissue characteristics on CMR during acute COVID-19 in hospitalized patients with and without mild cardiac Troponin (CTnI) rise. *Green dotted line in the graphs as per **Figure 4.2**. Out of 23 patients, 8 had mildly elevated CTnI levels (on average 2.4-fold above normal range). Green dotted line in the graphs denote the upper limit of normal range for T1 and T2SI ratio in the 3T MR scanner used for this study.*

4.4 Discussion

For the first time, this study describes the acute cardiac findings using CMR in hospitalized patients with acute COVID-19, and compared them to matched controls and at 6-months. I found that acute COVID-19 was associated with significant myocardial oedema in some patients, as demonstrated by significantly elevated myocardial T1 and T2 signals compared to controls (**Figure 4.5**). Otherwise, both cohorts had normal biventricular systolic function, similar ECV fraction and frequency of LGE findings. Given the similar ECV fraction between acute COVID-19 patients and controls, I propose that the mechanism of raised T1 and T2 signals in acute COVID-19 may, in part, be attributed to the presence of intracellular oedema. Findings from the follow up CMR scans suggest that the acute myocardial oedema tend to normalize over time during the convalescent phase, with preserved biventricular function.

SARS-CoV2 has been reported to induce acute myocardial injury and heart failure, similar to other cardiotropic viruses (112,113). Earlier studies of COVID-19 survivors in the community reported significantly elevated myocardial T1 and T2 signals on CMR in convalescence; but the pathophysiologic origins of these imaging findings were unclear, especially in the absence of evidence for acute myocardial injury (troponin rise and fall) during the acute illness and the inclusion of patients with previous history of cardiac disease (32,104). T1 and T2 signals can be prolonged due to increased myocardial water content, regardless of injury to the cardiomyocytes or histopathological myocarditis. Such a change in water content can take place in either or both intracellular or extravascular (including coronary arteries) compartments and be attributed to physiological changes during stress (114,115). Therefore, it is possible that similar alterations may occur during a systemic

inflammatory condition such as acute COVID-19, leading to elevation in T1 and T2 values, which then regress to normal during convalescence.

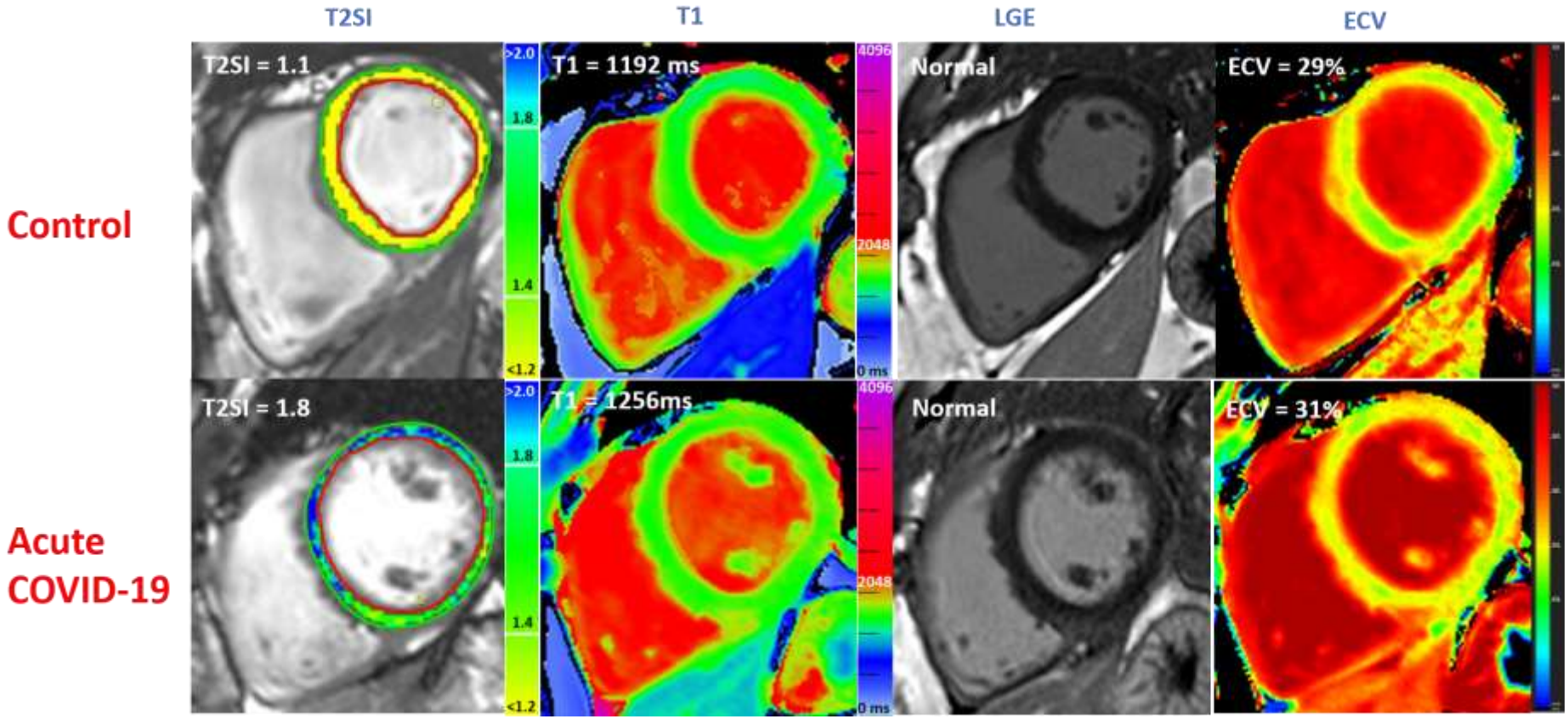


Figure 4.5 Multiparametric CMR imaging in 3T MRI scanner comparing acute COVID-19 patient during their hospitalization with matched control without COVID-19 from the community. *T2SI = T2 signal intensity ratio (myocardium : skeletal muscle). LGE = Late Gadolinium Enhancement. ECV = Extra cellular volume fraction. Normal values: T1<1244ms, T2<1.4. All values correspond to single slice have been shown.*

To my knowledge, the only study to-date to describe findings in acutely ill COVID-19 patients was performed by Chen et al (116): it was retrospective study of a young cohort (median age 23 years) of well COVID-19 patients (n=25) with suspected myocardial injury (Troponin rise (n=8) or ECG changes or cardiac symptoms) at ~6 days after symptoms onset, and who had a clinical indication for CMR. They observed higher T1, T2 and ECV fraction when compared to healthy controls. In contrast, given the association of older age with negative clinical outcomes (117), my prospective study recruited older (mean age 56 years) and sicker acute COVID-19 patients without a clinical indication for CMR, to investigate the clinical significance of incidental troponin rises in this unique setting. Furthermore, to reduce the effects of confounding factors, I excluded patients with a history of cardiac disease, and included a control group with similar cardiovascular risk factors, measured cardiac troponin levels acutely, investigated their associations with the imaging findings, and performed follow-up CMR imaging.

I observed that myocardial T1 and T2SI abnormalities in acute COVID-19 patients with mildly elevated cTnI levels were not different from acute COVID-19 patients who had normal cTnI levels. This is similar to the observation made by Chen et al (116). This suggests that myocardial oedema in COVID-19 can occur independently of troponin rise. Moreover, I found no differences in the frequency of LGE abnormalities between controls and acute-COVID patients (who were recruited on the basis of no documented history of cardiac disease). This suggests that the LGE abnormalities described in recent studies of patients during the recovering phase of COVID-19 could have been pre-existing, pre-dating the acute COVID-19 illness; thus longitudinal studies of healthy subjects who had CMR scans performed pre-pandemic are needed (104). Furthermore, whilst patients in this study with mild rise in cTnI exhibited similar CMR findings to those with normal cTnI, in clinical practice, the magnitude of cTnI and clinical context, especially the presence of past history of cardiovascular disease, need to be carefully evaluated. Moreover, I did

not detect any arrhythmias, a potential cause of cTnI rise, in this study's cohort during the hospital admission; but previous reports have documented arrhythmias during acute COVID-19 (118,119).

The findings from the follow-up of acute COVID-19 patients on their 6-months CMR suggest that the myocardial tissue abnormalities (T1, T2) improved (and normalized) in convalescence, in keeping with previous reports (120,121). The preservation of global biventricular systolic function during both the acute and recovery phases of COVID-19 in this study supports evidence from other reports that T1 and T2 abnormalities were not correlated with biochemical or imaging evidence of heart failure at the time of assessment during the recovery phase (103,104,122). Furthermore, the presence of higher LVEF in patients with abnormally high myocardial T1 raises the possibility that acute COVID-19 leads to a hyperdynamic state resulting in increased myocardial blood volume (plasma and red blood cells) which may have been detected as higher myocardial T1(115). Such a hyperdynamic state would be expected to return to baseline after the resolution of the acute illness resulting in normalization of T1.

4.4.1 Limitations

This study has some limitations. This is a small study that was confined to hospitalized acute COVID-19 patients and conducted before the launch of mass vaccination programmes; thus, the findings may not be applicable to those managed in the community or those who have had the COVID-19 vaccine. Due to pandemic restrictions and patient preferences, I was unable to complete follow-up assessments in all COVID-19 patients, which may have under-powered some of the results; such as the lack of statistical significance in the differences of T1 and T2SI between the acute and follow-up time points. The thinness of the RV free wall renders it almost impossible to accurately quantify its T1 and T2 characteristics; thus, important pathophysiological changes in the RV myocardium secondary to acute COVID-19, which can increase the RV afterload, cannot be ascertained here (123). The influences of the differences in pathophysiology (e.g. hypoxia) and treatment (e.g. oxygen therapy and steroids) in acute COVID-19 on myocardial T1 and T2 signals

were not explored in this study. On average, patients in my study were scanned at ~3 days into their hospitalisation with acute COVID-19; it is unclear if the infection may lead to different or more myocardial abnormalities at a later time point during the acute illness. Whilst 65% of the patients had moderate or severe grade of COVID-19 illness on chest imaging (**Table 4. 2**), I recruited relatively stable patients and thus my findings may not be generalizable to a sicker cohort. It is not yet clear if myocardial oedema associated with SARS-COV2 illness is unique or whether similar changes happen with other viral illnesses. Thus, this study's findings should be viewed as hypothesis-generating, and may inform future study designs with a larger sample of patients with the ability to compare between vaccinated and unvaccinated patients, as well other cohorts of patients with different viral illnesses.

4.5 Conclusion

In this prospectively conducted study of participants with no history of cardiac disease or COVID-19 vaccination, patients hospitalized for acute COVID-19 demonstrated acute myocardial oedema on CMR when compared to controls with similar cardiovascular risk factors, which normalised at 6-months; biventricular systolic function was normal and scar burden was low and otherwise similar between the two groups. Acute COVID-19 appears to induce acute myocardial oedema in some patients, which resolves in convalescence, without significant impact on biventricular structure and function in the acute and short-term.

5. The Impact of Acute Revascularisation in Late-Presenting ST-Segment Elevation Myocardial Infarction: A Study of Acute Myocardial Injury Using Cardiovascular Magnetic Resonance

5.1 Introduction

Late-presenting ST-segment Elevation Myocardial Infarction (STEMI) is defined as when patients present with ST-segment Elevation on ECG and chest pain that started 12 hours or earlier with biomarkers of acute myocardial injury. This cut-off is inferred from outcome studies with pharmaco-thrombolysis, which found no survival benefit in administering lytic therapies when the ischaemic time is greater than 12 hours (124). However, given that research in the modern era of primary percutaneous coronary intervention (PPCI) has produced conflicting results (125–128) and that there is much clinical variation amongst patients, current guidelines recommend clinical discretion in making a decision to undertake PPCI or urgent PCI in late-presenting STEMI (129,130). At present, the European Society of Cardiology provides a class IIB recommendation for primary PCI in asymptomatic patients arriving 12-48 hours after the onset of chest pain (130). This reflects the lack of mechanistic understanding and absence of biomarkers for stratification that are necessary to overcome the clinical heterogeneity amongst patients. Clinical factors to take into consideration would be the patient's recollection of time of symptom-onset and individual variations, including spontaneous recanalization or reperfusion. Furthermore, acute reperfusion has the potential to worsen microvascular injury, including microvascular obstruction (MVO) and intramyocardial haemorrhage (IMH), in the infarcted myocardium downstream (64).

CMR is considered the imaging gold standard for assessing cardiac structure, function and myocardial characterisation (12). In particular, CMR can detect the acute dynamic myocardial changes after STEMI, including myocardial oedema, infarct size (IS) and microvascular injury (MVO and IMH). IS, MVO and IMH are all important prognostic markers but the effect of revascularisation in late-presenting STEMI on them had not been studied until now (14,54,70,92,131–135) Therefore, in this study, CMR was performed in the acute setting to understand the myocardial changes before and after PCI, and the impact, if any, of revascularisation in late-presenting STEMI.

5.2 Methods

5.2.1 Study population

Consecutive patients arriving at the John Radcliffe Hospital and reporting chest pain at least 12 and no more than 48 hours earlier with new ST-segment elevation on ECG were invited to participate. Exclusion criteria included ongoing chest pain, haemodynamic instability, contra-indication for CMR and estimated glomerular filtration rate (eGFR) <30. Patients were recruited after verbal assent was obtained, in line with OxAMI study research protocol (approved by the South Central – Oxford C Research Ethics Committee; reference 10/H0408/24) as previously described (136,137). In brief, verbal assent was ascertained by an OxAMI investigator in the presence of an independent patient advocate, whilst the patient was in the emergency room or in the ward, awaiting ICA. All patients provided written informed consent after the ICA but prior to discharge from hospital.

5.2.2 CMR methods

CMR was performed using a 3.0-T magnetic resonance scanner (MAGNETOM TIM Verio, Siemens Healthcare, Erlangen, Germany). Patients were transported to the scanner under close clinical supervision by a cardiology doctor and nurse. The scan protocol included Steady-State Free Precession (SSFP) functional (cine) images, Shortened Modified Look-Locker Inversion recovery (ShMOLLI) (46,138) native T1-mapping for area at risk characterization (136), T2* mapping and T2-weighted (T2-prepared SSFP single shot sequence with coil signal intensity correction) for IMH assessment, early gadolinium enhancement (EGE) for identification of intracardiac thrombus, and late gadolinium enhancement (LGE) for infarct size and MVO quantification. LGE was performed with a ‘single-shot’ sequence and/or a T1-weighted segmented inversion recovery gradient echo-phase sensitive-inversion recovery (GRE PSIR).

LGE images were collected 10-15 min after the administration of contrast agent (0.1 mmol/kg, Dotarem, Guerbet, Villepinte, France).

5.2.3 CMR image analysis

Image analysis was performed by three operators (CMR experience >3 years) on cvi42 software (Circle Cardiovascular Imaging Inc., Calgary, Canada). LV and RV volumes and ejection fraction were assessed from cine images. In cases where short-axis cine images were unavailable, LVEF was derived with the biplanar method using 2-chamber (vertical long axis) and 4-chamber (horizontal long axis) cine images. AAR was derived from T1-mapping and defined as the percentage of myocardium with T1 values >2 SDs above the mean T1 value of a region of interest (ROI) in the remote myocardium. Myocardial area with elevated T1 (1250ms which is 2SD above the mean T1 in healthy subjects in 3T) was also computed. Presence of IMH was detected on T2w images (area of hypo-intensity within the hyper-intense/oedematous myocardium) and/or T2* maps (area with T2* value <20ms with an acceptable R^2 derived from the mono-exponential truncation method curve fitting; R^2 of >0.990 was considered as a good fit) (139). IS was derived from LGE as the volume of myocardium with a signal intensity >5 SDs higher than the mean signal intensity in a ROI in the remote myocardium. In patients with an old MI (defined as areas of LGE with no evidence of associated surrounding oedema on T2-weighted imaging or T1 mapping), the mass of the old infarct was excluded. MVO was defined as the hypointense area within the infarcted region on LGE imaging, and its size (grams) was quantified by manual delineation and also presented as percentage of total myocardial weight. Remote myocardial ROI was drawn 180^o away from the acutely infarcted segments where possible, with normal regional wall motion and no LGE. The area with LGE (including MVO) was always included in the AAR.

5.2.4 Invasive coronary angiogram, angiographic analysis, and indices of microcirculatory function

ICA was performed on a non-emergency basis, in line with clinical standards and the decision to perform PCI to the culprit and/or non-culprit coronary artery disease was left to the discretion of the consultant cardiologist performing the procedure. TIMI (Thrombolysis In Myocardial Infarction) flow in the culprit artery pre and post PCI (if applicable) was measured, as previously described (81). Index of microcirculatory resistance (IMR) and coronary flow reserve (CFR) were measured in the culprit artery, where clinically appropriate and possible, using standard pressure and temperature-monitoring guidewire (92). IMR>25U and CFR<2 were considered to indicate coronary microvascular dysfunction (80,92). Multi-vessel coronary artery disease was defined as the presence of >50% luminal narrowing in a non-culprit or bystander coronary artery. PCI was defined as any attempt to re-open the culprit artery and includes the use of a coronary wire, balloon or stent.

5.2.5 Statistical analysis

Statistical analyses were performed using SPSS (version 25, IBM Corp). Normality of data was determined using Kolmogorov-Smirnov test. Normally distributed data are presented as mean ± SD; nonparametric data as median [interquartile range]. Statistical comparisons for paired and unpaired samples were performed using Student's t-test, Wilcoxon signed rank test, or the Mann-Whitney U test, as appropriate. Categorical data and frequencies were compared with chi-square or Fisher's test for unpaired analysis and McNemar's test for paired analysis, as appropriate. Correlation between variables was assessed using Pearson's product-moment correlation coefficient (r) or Spearman's rank correlation coefficient (ρ) as appropriate. All statistical tests were 2-tailed, with values of $p < 0.05$ considered significant. During assessment of correlation between two continuous variables, $\underline{p}$ values between 0.05 and 0.1 were considered to represent a possible trend.

5.3 Results

Twenty-four patients (mean age 63±14 years; 83% male) were recruited between 2019 and 2021. The duration of chest pain from onset prior to the first CMR scan was 35±13 hours. All patients had been started on dual antiplatelet therapy prior to recruitment. The median peak troponin level was 21175 [6501-35719] ng/L, confirming acute myocardial infarctions (normal <34ng/L). ST elevation and pathological Q waves were each present in 91% of the patients. All patients had either or both ST segment elevation or Q waves. Average blood pressure, pulse rate and arterial oxygen saturation at presentation were in the normal range (134/80 mmHg, 87 beats per minute and 98% respectively) (***Table 5.* 1**). Pre-ICA CMR with at least cine and LGE imaging was obtained in 23/24 (96%) patients (1 patient did not tolerate the scan after the cine images were acquired). ICA was performed 2 [1-5] hours after the first CMR. Post-ICA CMR was performed 3.5±1.5 days after the ICA in 18 patients. (***Table 5.* 1**). Reasons for non-attendance for the 2nd scan included patient preference (n=4) and clinical deterioration (n=2). No adverse events took place during the CMR scans.

5.3.1 Angiographic findings

5.3.1.1 Pre-PCI findings

The left anterior descending artery (LAD) was the culprit artery in 54% of patients whilst the Left Circumflex artery (LCX -17%) and right coronary artery (RCA – 29%) constituted the remainder. Multivessel disease was present in 46% of cases. Culprit artery TIMI-flow grade was 0-1 in 71%.

5.3.1.2 Post-PCI findings

PCI to culprit artery was performed in two thirds of the patients (n=16); resulting in a TIMI flow grade of ≥2 in 10 patients at the end of the procedure. Post-PCI IMR and CFR were measured in the culprit arteries in 12 patients and were 27±10U and 1.59±0.24 respectively and were not significantly different between those with and without PCI (***Table 5. 1***). In patients who did not receive PCI (n=8), the TIMI flow grade was ≥2 in 25%.

Table 5. 1 Baseline characteristics, ICA and CMR findings

		All (n=24)	ICA + PCI (n=16)	ICA but no PCI (n=8)	P
Age		63±14	63±17	63±13	0.952
Male sex (%)		83	81	88	0.699
BMI (Kg/m2)		27±5	27±4	25±6	0.319
Diabetes (%)		2 (8)	1 (6)	1 (13)	0.602
Hypertension (%)		11 (46)	9 (56)	2 (25)	0.148
Hypercholesterolaemia (%)		9 (38)	8 (50)	1 (13)	0.074
Previous known MI (%)		1 (4)	1 (6)	0	N/A
CVA/TIA (%)		3 (13)	1 (6)	2 (25)	0.190
Smoker (%)		14 (59)	10 (64)	4 (50)	0.512
Troponin ng/L (normal <34)		21175 [6501-35719]	23199 [14000-35531]	14000 [4026-45,000]	0.630
ECG Q waves presence (%)		21 (91)	15 (94)	6 (86)	0.529
ECG ST elevation presence (%)		21 (91)	14 (88)	7 (100)	0.328
Systolic blood pressure (mmHg)		133±31	138±36	124±18	0.312
Heart rate (beats per minute)		85±15	84±17	87±12	0.713
SpO2 on room air (%)		97±1	97±1	98±2	0.165
First CMR findings before ICA					
Time after chest pain (hours)		34±13	36±13	31±11	0.422
LVEF (%)		41±9	42±9	40±9	0.656
RVEF (%)		53±10	53±11	53±9	0.990
Area at risk (% of myocardium)		50±15	52±17	47±12	0.488
Area with T1 >1250ms (%)		57±19	58±21	55±16	0.766
IMH presence (%)		11 (48%)	9 (60)	2 (40%)	0.617
MVO presence (%)		18 (78%)	14 (88%)	4 (57%)	0.142
MVO size (grams)		1.28 [0.22 -9.0]	2.04 [0.49-7.72]	1.09 [0-4.32]	0.341
MVO size (% of myocardium)		1.20 [0.20-7.56]	2.4 [0.54-9.2]	1.09 [0-6.39]	0.278
Infarct size (% of myocardium)		31±15	28±12	30±10	0.701
LV Thrombus (%)		5	6	0	N/A
RV myocardial infarction		0	0	0	N/A
ICA findings					
Time after CMR (hours)		2 [1-5]	2[1-6]	3 [1-5]	1.00
Culprit artery	LAD (%)	54	62	38	0.496
	LCX (%)	17	25	25	
	RCA (%)	29	38	38	
TIMI-0-1 flow pre-PCI (%)		71	69	75	0.583
TIMI-0-1 flow post-PCI (%)		46	31	75	N/A
Stent (total) length (mm)		30 [24-51]	30 [24-51]	N/A	N/A
Stent (largest) width (mm)		3.5 [3-4]	3.5 [3-4]	N/A	N/A
Multivessel disease (%)		46	38	63	0.247
IMR		27±10	29±11	21±5	0.244
CFR		1.59±0.24	1.62±0.12	1.50±0.46	0.479
Second CMR findings post-ICA					
Time after 1st CMR (days)		3.5±1.5	3.6±1.6	3.4±1.3	0.399
LVEF (%)		44±10	46±10	42±11	0.523
RVEF (%)		54±9	55±10	51±6	0.388

Area at risk (% of myocardium)	51±15	52±17	50±13	0.884
IMH presence (%)	33	42	17	0.289
MVO presence (%)	72	75	67	0.710
MVO size (grams)	0.69 [0.00-2.86]	0.69 [0.07-3.27]	0.77 [0.00-1.71]	0.820
MVO size (% of myocardium)	0.83 [0.00-3.18]	1.02 [0.07-3.22]	0.77 [0.00-2.27]	0.820
Infarct size (% of myocardium)	30±13	29±15	30±8	0.399
LV thrombus (%)	11	17	0	N/A

Table 5.1 Abbreviations: BMI – Body Mass Index, MI = Myocardial infarction, CVA= Cerebrovascular attack, TIA = Transient Ischaemic Attack, SpO2 = peripheral oxygen saturation, LAD = Left Anterior Descending artery, LCX = Left Circumflex artery, RCA = Right coronary artery. LVEF = Left ventricular ejection fraction, RVEF = Right ventricular ejection fraction, MVO = microvascular obstruction, IMH = intramyocardial haemorrhage, TIMI = Thrombolysis In Myocardial Infarction, IMR = Index of Microcirculatory Resistance, CFR = Coronary Flow Reserve. Ng/l = nanograms/Litre, mmHg = millimetres mercury, ms = milliseconds. The p values presented are derived from statistical comparisons of the two groups (ICA+PCI & ICA but no PCI) ns = Non-significant p value (>0.05). N/A = non applicable.

5.4 CMR findings

5.4.1 Ventricular function, area at risk and infarct size at both time points

LVEF pre-PCI was 41±9% and showed numerical, but statistically insignificant improvement after ICA to 44±10% (p=0.27) in all patients. RVEF was also similar at both time points (53±10 vs 54±9; p=0.75). (**Table 5. 1**, **Figure 5.1**).

The AAR was comparable pre and post-ICA at 50±15% and 51±15% (p=0.55) respectively (**Table 5. 1, Figure 5.2**). Similarly, the myocardial area with elevated T1 values (>1250ms) were not different at the two time points (**Table 5. 1**).

The acute infarct size was also similar at the two time points (31±15% vs 30±13%, p=0.97) (**Table 5. 1**, **Figure 5.3**).

The abovementioned observations were not different between the patients who had PCI and those who did not have PCI (**Table 5.2**, **Table 5.4**, **Table 5.5**). Amongst those who had a PCI, there was no significant differences in the CMR indices between those with and without successful restoration of coronary blood flow (defined as post-PCI TIMI flow 2-3); see **Table 5.3**.

LV thrombus was present in 2 patients who had PCI (one at both time points and another post-PCI only). LV thrombus was not observed in patients who did not undergo PCI.

5.4.2 Microvascular injury (MVO and IMH) at both time points

MVO was present in 18/23 patients (78%) on the first CMR scan; the size was 1.28% [0.20-7.56] (**Table 5. 1**). Of the patients with MVO on the first scan, 14 patients had a post-ICA CMR scan and MVO was present in all but one (n=13; 93%) and it was much smaller at 0.83% [0.00-3.18]; p = 0.005 (**Figure 5.4**, **Figure 5.5**). The MVO size pre- and post-ICA was not different between the patients who had PCI and those who did not (**Table 5.2**, **Table 5.4** & **Table 5.5**). The regression

in MVO size was numerically larger (but statistically insignificant) in patients who had a successful restoration of coronary blood flow (TIMI ≥2) post-PCI than those with TIMI ≤1) (**Table 5.3**). The magnitude of change in the MVO size appeared to correlate with the time interval between the two scans; with most marked changes taking place at 4-5 days after the first scan (**Figure 5.5**).

IMH was detected in 11/20 patients (46%) who had T2*/T2w imaging in the first CMR. Of the patients with IMH on the first scan, 9 patients had a post-ICA CMR scan and IMH was still detectable in 5 (56%). Of those who did not have IMH on the first scan, 8 had a post-ICA CMR scan of whom 1 patient was noted to have new IMH. The difference in the prevalence of IMH at the two points was not statistically significant on paired analysis in the whole cohort (p=0.5) and between the two sub-groups (PCI and no-PCI). Patients with IMH had much larger MVO than those without IMH on the pre-ICA scan (6.2[1.17-10.08] vs 0.22[0-0.93]; p=0.007). A similar observation was made on the second CMR scan as well (3.22[3.18-6.36] vs 0.14 [0-0.83]; p = 0.002).

There were no significant differences, at either time points, in the LVEF, AAR and IS between patients with and without MVO and patients with and without IMH.

5.4.3 Associations between clinical features and CMR findings

The duration of chest pain was negatively correlated with LVEF (r=-0.515; p=0.016,**Error! Reference source not found.**) and positively correlated with infarct size (r=0.459; p=0.037, **Error! Reference source not found.**) and trended towards a positive correlation with AAR (r= 0.408; p=0.067). The duration of chest pain was not correlated with the peak Troponin levels (r=0.378, p = 0.1). Peak troponin was however correlated with LVEF (r=-0.499; p=0.018), but not with AAR and IS. There was no statistically significant difference in the chest pain time, troponin,

LVEF, AAR and IS between patients with and without MVO, and between patients with and without IMH.

When compared to patients with Q waves on their ECGs at presentation, the two patients who did not have Q waves had numerically larger LVEF (41±9 vs 45±4) and smaller AAR (51±16 vs 38±3) and IS (28±11 vs 22±1). MVO size was numerically higher in the patients without Q waves (0.44 [0-3.22] vs 2.17 [1.16-3.18]). However, due to the small number of patients without Q waves (n=2), statistical significance was not achieved for any of these comparisons.

IMR correlated with MVO size (r=0.619; p=0.032) and patients with MVO had a higher IMR than those without MVO (30±9 vs 14±4; p=0.048) but the CFR was not significantly different (1.58±0.26 vs 1.67±0.09; p=0.652).

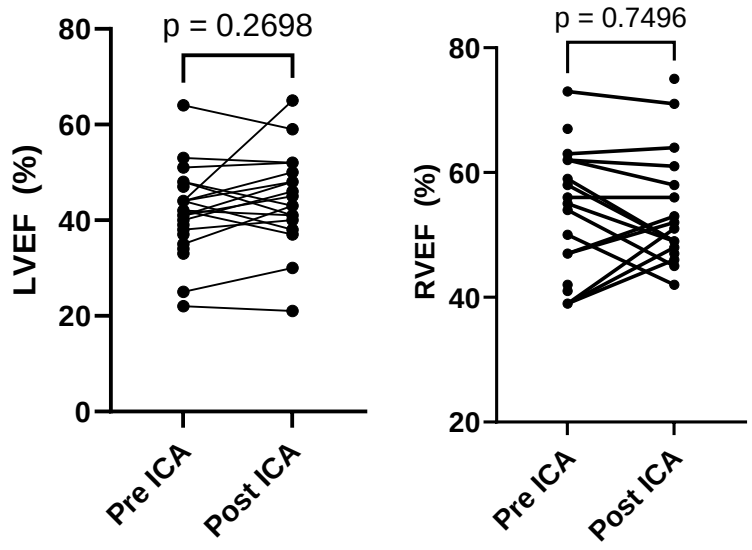


Figure 5.1 Left and right ventricular function pre and post ICA. *24 patients underwent CMR pre-ICA and 18 underwent CMR post-ICA. Of the 18 who underwent the second CMR, 16 had had a percutaneous coronary intervention (PCI) to the culprit artery. LVEF was quantified in all patients using Short axis or long axis (biplanar) cine images. RVEF was quantified only in patients with interpretable short axis cine images.*

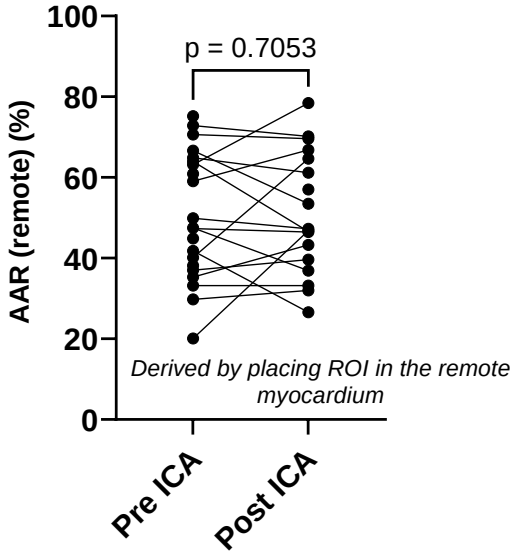


Figure 5.2 Area at risk pre and post ICA*. Abbreviations and explanations as per Figure 5.1*

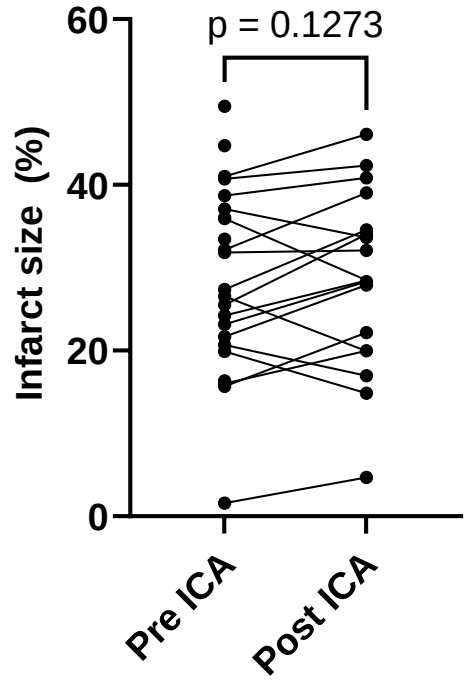


Figure 5.3 Infarct size pre and post ICA. *Abbreviations and explanations as per Figure 5.1*

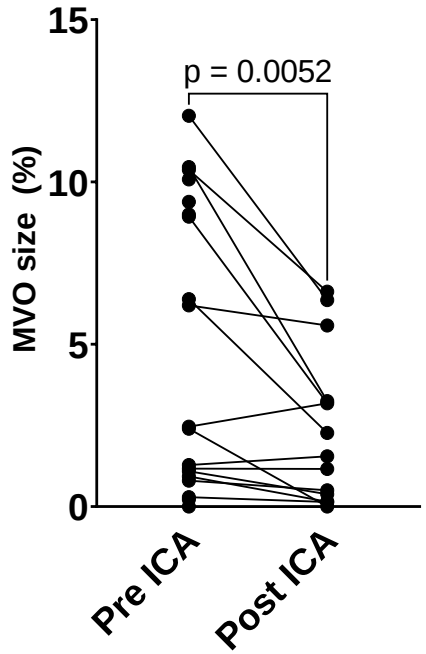
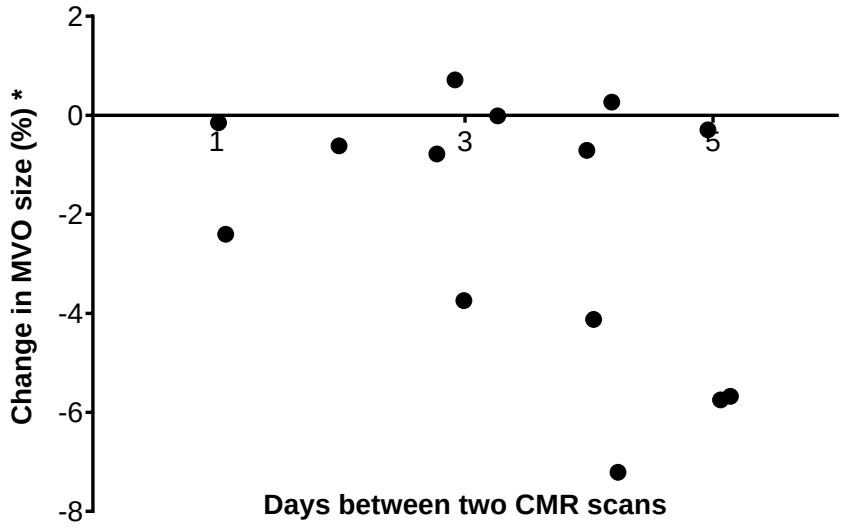


Figure 5.4 Microvascular obstruction (MVO) size (% of total myocardial mass) pre and post ICA. *Abbreviations and explanations as per Figure 5.1*



* Analysis restricted to patients with MVO on the first CMR scan (pre-ICA)

***Figure 5.5 Change in MVO size**, derived by subtracting MVO size on the pre-ICA CMR from the MVO size on the post-ICA CMR. Analysis was restricted to patients with MVO on the 1st CMR scan. Abbreviations and explanations as per Figure 5.1*

***Table 5.2 Absolute change in CMR indices after ICA+/-PCI in patients with paired scans**.*

Absolute change	All	PCI	No PCI	p-value
ΔLVEF%	0 [(-)1- 4]	3 [(-)5-6.50]	0 [(-)1-4]	0.553
ΔRVEF%	-1 [(-)8-6]	-1[(-)6-5]	-1[(-)9-6]	0.679
ΔAAR%	-0.4 [(-)3.7-8]	-1.8 [(-)11.9-7.9]	1.3 [(-)0.9-12.3]	0.335
ΔIS%	-0.3 [(-)5-8]	1.88[(-)3.58-4.08]	5.8 [5.08-6.86]	0.102
ΔMVO absolute size (grams)	-0.26 [(-)2.61-0.00]	-0.3[(-)2.5-0]	-0.4 [(-)2.6-0.0)	1.000

The absolute change (Δ) is derived by subtracting variables on pre-ICA CMR from post-ICA CMR. A negative figure indicates reduction in the size of the variable.

Table 5.3 Absolute change in CMR indices after PCI in patients with paired scans; stratified by post-PCI TIMI-flow.

Absolute change	All PCI	PCI resulting in post-PCI TIMI 2-3	PCI resulting in post-PCI TIMI 0-1	p-value
ΔLVEF%	3 [(-)5-6.50]	4.5[(-)3-7]	-1.5 [(-)5-4.5]	0.570
ΔRVEF%	-1[(-)6-5]	-2 [(-)6-1]	3.5[(-)6 -10.5]	0.610
ΔAAR%	-1.8 [(-)11.9-7.9]	-2.6[(-)14-0.6]	11.6 [(-)1.3-21]	0.073
ΔIS%	1.88[(-)3.58-4.08]	1.2[(-)4.2-4.08]	2.36[(-)1.06-4.68]	0.102
ΔMVO absolute size (grams)	-0.3[(-)2.5-0]	-0.45[(-)2.9-(-) 0.02]	-0.11[(-)0.16-0.12]	0.461

The absolute change (Δ) is derived by subtracting variables on pre-ICA CMR from post-ICA CMR. A negative figure indicates reduction in the size of the variable. Post-PCI TIMI 2-3 flow represents relatively successful revascularisation.

Table 5.4 Paired analysis of CMR characteristics in patients who had PCI to culprit artery

N= 12	Pre-PCI (n=12)	Post-PCI (n=12)	p-value (paired)
Time after 1st CMR (days)	N/A	3.6±1.6	N/A
LVEF (%)	43±10	46±10	0.275
RVEF (%)	54±11	55±10	0.931
AAR (%)	52±17	52±17	0.955
Area with T1 >1250ms (%)	57±22	52±25	0.323
IS (%)	28±12	27±11	0.548
MVO size (%)	2.4 [0.5-9.2]	1 [0.07-3.22]	0.037
MVO presence (%)	83%	75%	1^
IMH presence (%)	58%	42%	0.5

Table 5.5 Paired analysis of CMR characteristics in patients with no PCI to culprit artery

N = 6	Pre-ICA (n=6)	Post-ICA (n=6)	p-value (paired)
Time after 1st CMR (days)	N/A	3.4±1.3	N/A
LVEF (%)	42±10	42±11	0.010
RVEF (%)	52±9	51±6	0.354
AAR (%)	45±11	50±13	0.307
IS (%)	28±9	32±10	0.121
MVO size (%)	1.09 [0-6.39]	0.77 [0-2.27]	0.068
MVO presence (%)	67%	67%	1^
IMH presence (%)	40%	20%	1^

^ p=1.0000 on SPSS. Such paired comparisons of binomial outcomes were done with McNemar's test.

Paired compairsons of indices in Table 5.4 and Table 5.5 were performed on 12 and 6 patients respectively, in whome CMR was done at both time points.

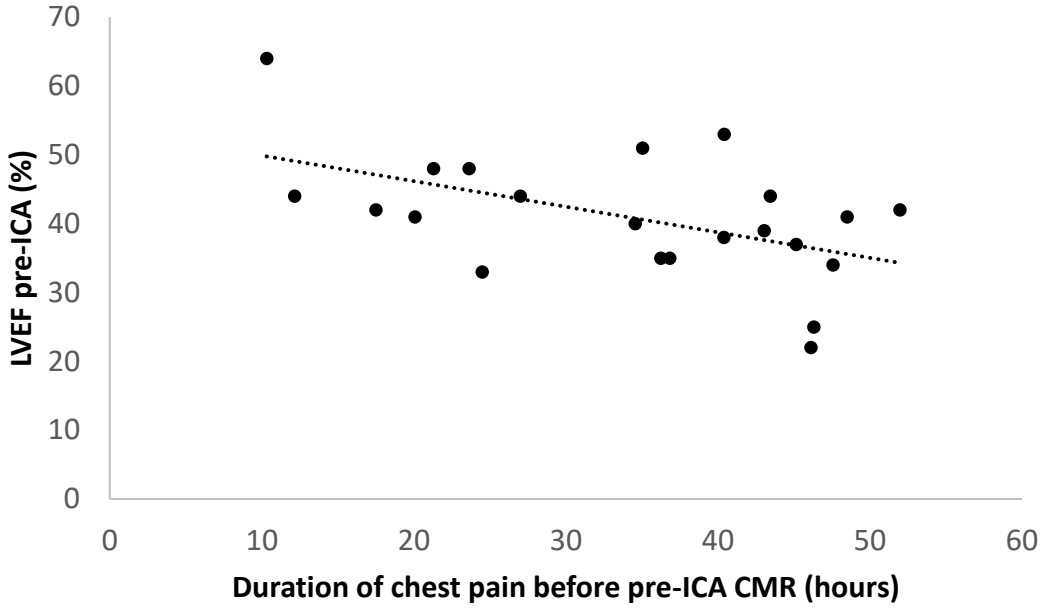


Figure 5.6 Correlation with chest pain duration and LVEF on CMR pre-ICA. (r=-0.515; p=0.014). Abbreviations and explanations as per Figure 5.*1*

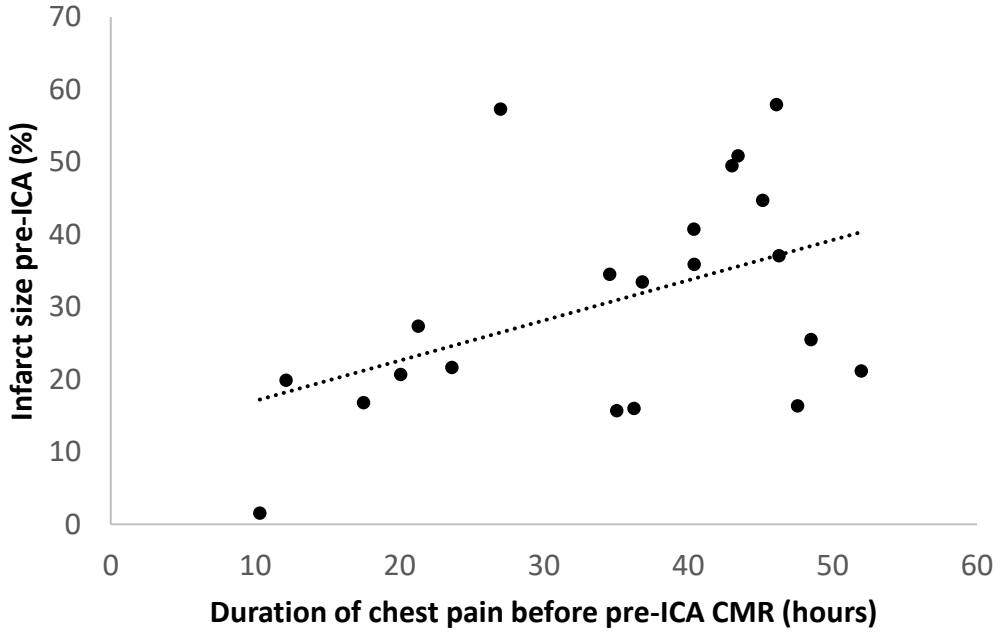


Figure 5.7 Correlation with chest pain duration and infarct size on CMR pre-ICA. (r=0.459; p = 0.037). Abbreviations and explanations as per Figure 5.1

5.5 Discussion

Our study shows, for the first time, the impact of revascularisation on myocardial tissue characteristics in stable patients presenting 12-48 hours after the onset of chest pain with evidence of STEMI, using CMR as the imaging gold standard. We found that the patients had moderately impaired left ventricular function (41%), large area at risk (50%) and infarct size (31%) and a high prevalence of coronary microvascular dysfunction (MVO and/or IMH in 78%). All of these remained unchanged post-ICA but the size of MVO became smaller (from 1.2% to 0.8%) (**Table 5. 1** and **Figure 5.8**). The frequency of IMH did not change. Furthermore, these findings did not differ between patients who received revascularisation and those who did not.

Multiple trials at the turn of the century demonstrated that primary PCI, performed within 12 hours of chest pain in STEMI, offers significantly better outcomes than fibrinolysis.(140) However there is much uncertainty in how a patient presenting over 12 hours after the chest pain should be managed. Studies of revascularisation in late presenting STEMI have failed to show significant clinical benefit (124–126,141); however some imaging studies of suggest that a significant amount of myocardium can be salvaged with early revascularisation(142). Using the notion that 'time is myocardium' in occlusive MI/STEMI, it is highly conceivable that prolonged ischaemia will render the at-risk myocardium irreversibly damaged and that reperfusion is unlikely to offer any salvage and observational. A further point of contention is whether mechanical reperfusion may worsen the coronary microvascular injury over and beyond what had taken place during the ischaemic period. This phenomenon is widely considered constitute a form of 'ischaemia-reperfusion injury'(143) and is regarded as a threat to the healing and the structural integrity of the injured myocardium. Although widely described in pre-clinical settings, a study in humans has proved difficult to conduct as it requires a non-invasive probing of the myocardium before and after revascularisation(64).

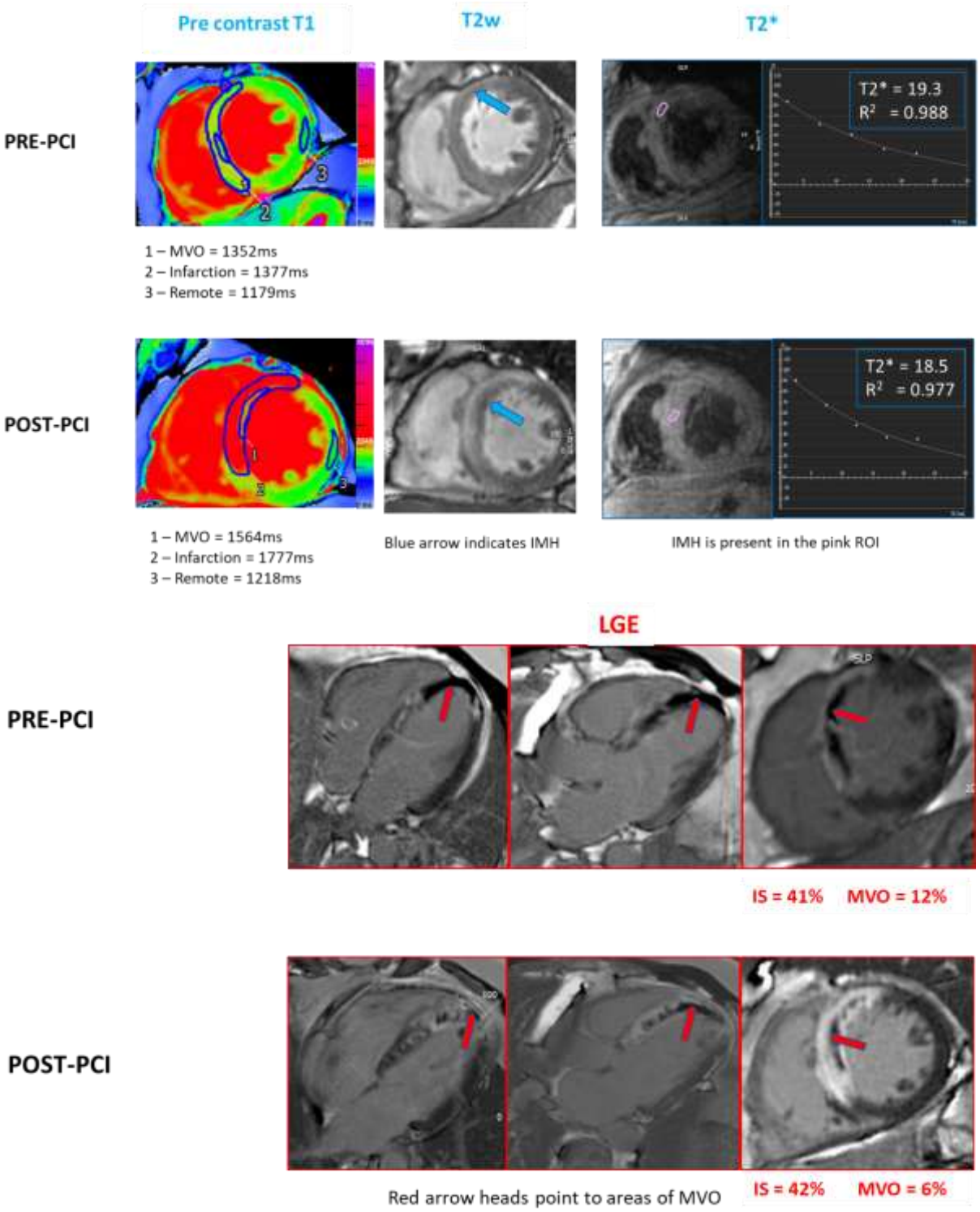


Figure 5.8 Multiparametric CMR in a patient with late presenting STEMI with images just before and 5 days after PCI. *In this example, pre-contrast T1 maps and T2w imaging show evidence of significant myocardial edema pre and post PCI. The degree of edema appears to have increased after PCI (T1 and T2 mapping and T2w imaging). The infarct size (LGE) did not change pre- and post-PCI. There was evidence of microvascular obstruction (red arrows on LGE imaging) which became smaller on the second CMR scan post-PCI on day 5. There is imaging evidence of intramyocardial haemorrhage (hypo intensity indicated by blue arrows on T2w imaging and the pink ROI on T2* mapping) at both time points.*

CMR has been used to interrogate the myocardium after revascularisation in patients who had presented late with STEMI and ongoing ischaemic symptoms to obtain useful insights. (142) Nepper-Christensen et al scanned 58 patients immediately and 3 months after PCI for late-presenting STEMI with ongoing ischaemic symptoms and observed that although the infarct size was large the PCI was associated with significant amount of myocardial salvage (on average, 58%) (142). Busk et al also made a similar observation in 2009 using nuclear perfusion imaging on 55 patients presenting after 12 hours of chest pain and STEMI (144). Both studies concluded that symptom duration had poor correlation with final myocardial infarct size and salvage. Equally, the lack of chest pain or presence of Q waves on ECG at the time of presentation does not amount to irreversible myocardial injury in all cases (145). These findings raise questions about the current clinical practice of determining the appropriateness of revascularisation purely on the duration of chest pain and ECG changes and emphasises the need for deeper phenotyping of such patients prior to clinical decision making (145).

Our study is the first to: 1) correlate clinical characteristics with myocardial tissue characteristics before revascularisation and 2) compare the changes in the myocardial tissue after revascularisation, in stable patients with late-presenting STEMI. In our cohort, the time between chest pain onset and pre-ICA CMR was only moderately correlated with the LVEF and infarct size (r =0.4 and 0.5 respectively; **Figure 5.6**, **Figure 5.7**) and 92% of the patients had pathological Q waves at presentation; confirming that they are unlikely to provide clinical utility in determining which patients will benefit from revascularisation. The only significant change between the two scans was the regression of the MVO size (**Figure 5.4**). Such a regression in the first few days and weeks after myocardial infarction has previously been demonstrated in a handful of reports(69,133,146) but this is the first time it has been demonstrated pre and post PCI in any myocardial infarction and provide fresh insights into coronary microvascular dysfunction

in non-revascularized MI. The long duration and large extent of ischaemia and the resultant cardiomyocyte oedema can cause capillary damage and occlusion and external compression of the capillaries respectively, leading to MVO. Interestingly, our observations suggest that reperfusion of an occluded coronary artery does not necessarily worsen the coronary microvascular dysfunction nor the infarct size. For instance, in those who received a PCI with successful restoration of flow (TIMI 2-3), the changes in MVO and IS were not significantly different when compared to those whose coronary blood flow post PCI was sub-optimal (TIMI 0-1) (***Table 5.3***). We also noted that of the patients with MVO had a higher post-PCI IMR (higher microvascular resistance) than those without MVO, similar to previous reports (92,147). However, it could be argued that the infarct size and the degree of coronary microvascular dysfunction were already maximal at the time of ICA in late-presenting STEMI and cannot worsen any further with or without reperfusion injury and that regression of MVO and IMR over the first few days after STEMI would occur anyway (69). Nevertheless our study's findings underline the propensity for late presenting STEMI to induce large volume of infarction and coronary microvascular dysfunction, which are both strong indicators of adverse long-term prognosis post-STEMI, including heart failure and mortality (92,131).

Equally, it must be acknowledged that about 9% of our patients (n=2) did not have evidence of coronary microvascular dysfunction (presence of IMH or MVO/high IMR/low CFR) and one patient had a very low volume of infarcted myocardium (1%). This highlights the heterogeneity amongst the late-presenters and some patients may have relatively more salvageable myocardium, and may benefit from early clinical phenotyping with CMR to guide the clinical decision is made to perform urgent revascularisation. As such, a CMR scan prior to ICA±PCI has the potential to characterise the myocardium and inform the clinician of the likelihood of a benefit from revascularisation. Importantly, by demonstrating the safety and feasibility to conduct acute CMR

scans in stable patients with late-presenting STEMI, our study sets the platform for future research to help decipher the cohort of patients who will benefit from revascularisation.

5.5.1 Limitations

Our study has some limitations. This small study recruited only patients without chest pain and haemodynamic instability in a single centre, so caution needs to be exercised applying our findings to all comers with late-presentation of STEMI. A larger prospective randomised control trial of current practice vs an acute CMR-guided revascularisation is needed. Such a trial should be designed to study the impact of revascularisation in stable late-presentation STEMI on 1) myocardial salvage and functional recovery of the ventricular function in the short-term (e.g. 6 months) and 2) clinical outcomes at longer-term.

5.6 Conclusion

Patients with late-presenting STEMI without ongoing chest pain have moderately reduced left ventricular function and large infarct size pre-ICA which remain unaffected by revascularisation. Microvascular injury (MVO and IMH) was highly prevalent and also not worsened by revascularisation. IMR was higher in patients with MVO. The size of MVO regressed over 4 days and does not appear to be worsened by revascularisation. All findings were similar between patients who had revascularisation and who did not; however further research is needed to investigate if pre-ICA CMR could help identify a sub-set of patients who will benefit from revascualarisation.

6. Acute Response in the Non-infarcted Myocardium Predicts Long-term Major Cardiovascular Events After ST-elevation Myocardial Infarction

6.1. Introduction

Survival rate after acute STEMI has dramatically improved in recent times through primary percutaneous coronary intervention (PPCI) and optimal medical therapy (148). However, some patients experience poor long-term cardiovascular outcomes such as heart failure, arrhythmias and cardiac death (148). Thus, early identification of predictors of such adverse outcomes is desirable in order to improve long-term prognosis after STEMI.

The degree of acute injury to the infarcted myocardium, such as infarct size (IS), microvascular obstruction (MVO) and intramyocardial haemorrhage (IMH), is a known independent predictor of both short- and long-term clinical outcomes post-STEMI (14). The non-infarcted myocardium includes the salvaged area-at-risk (AAR) and the remote zone farthest away from the infarction. Emerging translational and clinical evidence suggests that the non-infarcted remote myocardium may also exhibit acute inflammation and injury post-MI (21,65,66,149,150). These acute pathophysiologic changes are thought to be mediated by the innate immune response (21,65) and may lead to maladaptive matrix changes, resulting in adverse LV remodelling and poor long-term outcomes (150–152). Characterization of the non-infarcted myocardium immediately post-STEMI may therefore help to improve risk stratification and identify therapeutic targets for cardio-protection against heart failure.

Multi-parametric CMR is a powerful non-invasive tool to interrogate myocardial tissue after STEMI (14). Advanced CMR techniques such as T1-mapping is highly sensitive for detecting increased free water content in acute myocardial injury, particularly myocardial infarction (44,52). Elevated T1 values can delineate the AAR (72) and predict the final IS post-STEMI (74). Lowered T1 in the core of the infarct, thought to reflect MVO and/or IMH, is inversely associated with short-term negative remodelling of the LV and long-term adverse outcomes (153). In the non-infarcted remote myocardium, elevated T1 is associated with negative remodelling of the LV

and adverse outcomes in patients at 6-months after STEMI (66,150). Thus, changes in the non-infarcted myocardium may also carry important clinical significance; however, their long-term prognostic relevance is unclear.

In this study, I hypothesized that, in addition to changes in the infarcted myocardium, the non-infarcted myocardium may also demonstrate various grades of acute response immediately post-STEMI. I sought to detect these changes non-invasively using CMR and to determine whether these changes may predict long-term major adverse cardiac events (MACE).

6.2. Methods

6.2.1. Study population and treatment

Patients with STEMI brought to hospital for PPCI were prospectively enrolled. The study protocol was approved by the local ethics committee as described in methods. All participants provided written informed consent. Patients underwent blood sampling at regular intervals during the hospital stay and CMR typically prior to hospital discharge. They were invited for a follow-up CMR scan and blood sampling at 6 months post-discharge.

Patients were eligible if the onset of symptoms had been <12 hours before PPCI and if they had ST-segment elevation of at least 0.1 mV in >2 contiguous limb leads or at least 0.2 mV >2 contiguous precordial leads. Standard exclusion criteria included severe heart valve disease, known cardiomyopathy, hemodynamic instability lasting >12 hours after revascularization, contraindications to CMR and non-MI diagnoses of ST-elevation syndromes (e.g. Takotsubo cardiomyopathy and myocarditis). PPCI strategy and treatment decisions were left to the operator's discretion.

6.2.2. CMR imaging

Scans were performed on 3T CMR scanners (either MAGNETOM Tim Trio or MAGNETOM Verio, Siemens Healthcare, Erlangen, Germany) (74). Briefly, the CMR protocol included cine, native T1-mapping (Shortened Modified Look-Locker Inversion recovery; ShMOLLI) (46,138), T2*, T2-weighted imaging, early gadolinium enhancement (EGE) and late gadolinium enhancement (LGE) imaging. LGE images were obtained 10–15 min after administration of a total of 0.13 mmol/kg of a gadolinium-based contrast agent (Gadoterate meglumine, Dotarem, Guerbet, Villepinte, France or Gadodiamide, Omniscan™, GE Healthcare, Amersham, UK).

6.2.3. Image analysis

CMR images were analysed using the CVI42 and MC-ROI as described in Chapter 2 (74,154). IS was derived from LGE as the volume of myocardium with a signal intensity (SI) >5 standard deviations (SD) higher than the mean SI in the remote region of interest (ROI). In patients with an old MI (defined as areas of LGE with no evidence of associated surrounding oedema on T2-weighted imaging or T1 mapping), the mass of the old infarct was excluded. MVO was defined as a hypointense core inside an area of LGE and was manually delineated on short axis (SAX) slices. The presence of IMH was defined on T2-weighted imaging or on T2* maps (70,74). AAR was derived from T1-mapping (70) and defined as the myocardium with T1 >2SD above the mean T1 value of a remote myocardial ROI. Remote myocardial ROI was drawn 180^{o} away from the acutely infarcted segments when possible and with no LGE and normal wall motion. The area with LGE (including MVO) was always included in the AAR.

Good LV coverage with T1 maps was achieved for each patient (7±2 slices per patient), resulting in 1487 slices overall. Using MC-ROI software, Dr Ambra Massi divided each slice into 6 segments; of these 10.3% (918/8922) were excluded due to artefacts. Infarct, remote and non-infarct T1 were derived from T1-maps based on the concept detailed in **section 6.2.3.1 and Figure 6.1**. Infarcted and non-infarcted segments on T1-maps were defined by the presence or absence of LGE respectively on anatomically matching segments of delayed enhancement imaging. T1>1250ms was considered to be abnormal and represents acute myocardial injury as previously published (74), and is >2SD above normal range at the 3T scanners used in this study (T1=1184±30ms).

6.2.3.1. Deriving T1 values in infarcted, non-infarcted and remote myocardium

T1-maps and LGE images were obtained at the same slice position in the scanner and compared side-by side to identify the non-infarcted and infarcted myocardial segments on each T1-map. Infarct T1 was derived by averaging the T1 values in all the pixels corresponding to regions with myocardial infarction (including MVO if present). Similarly, the mean non-infarct T1 was calculated by averaging the values all T1 pixels in the entire non-infarcted region. Remote T1 was obtained by drawing a myocardial ROI 180^{o} away from the acutely infarcted segments when possible in regions with no LGE and normal wall motion. See **Figure 6.1**.

6.2.3.2. Angiographic analysis

TIMI flow pre and post PPCI and myocardial blush grade were derived as described previously (92).

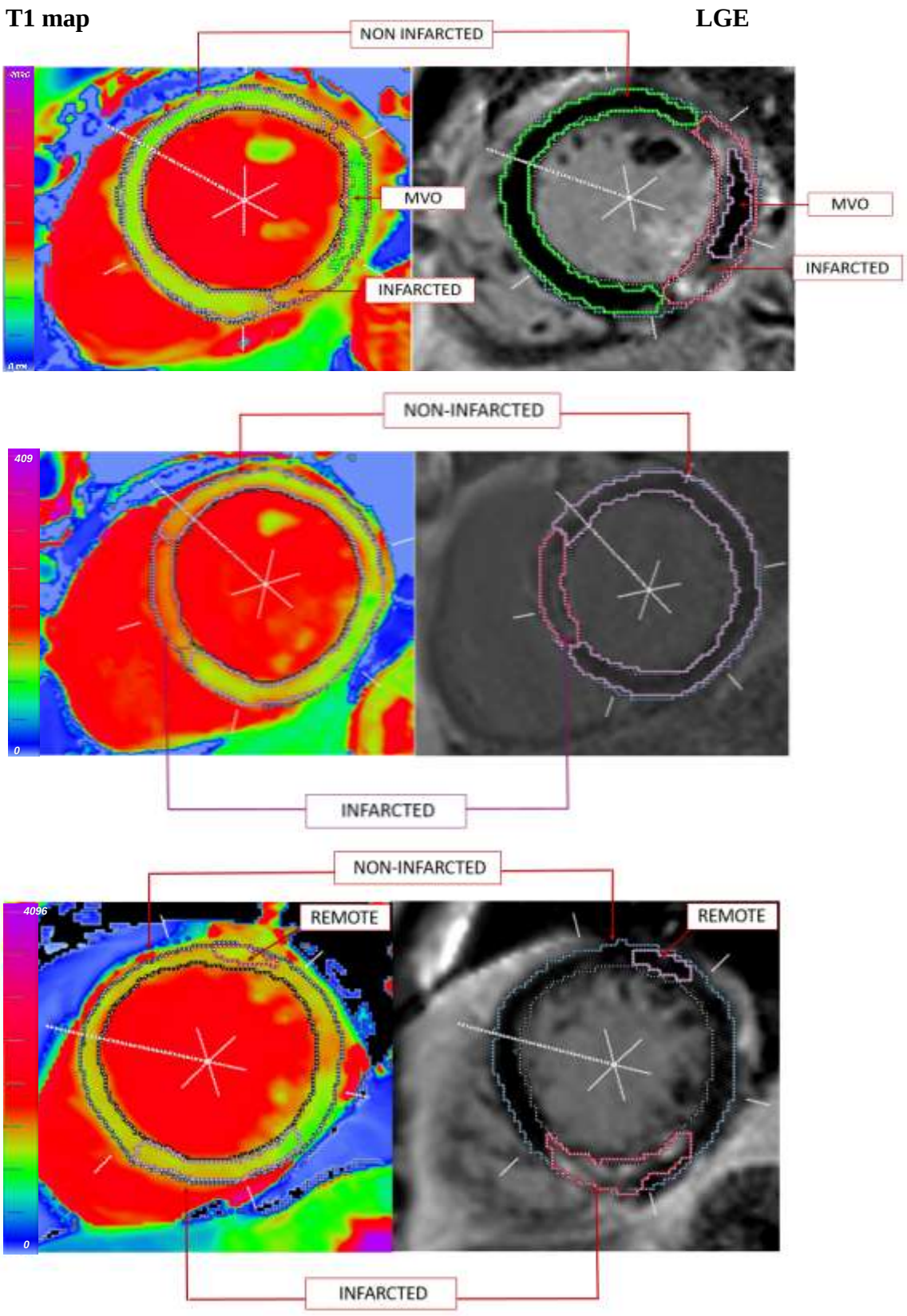


Figure 6.1 Derivation of T1 values in infarcted, non-infarcted and remote myocardium. A: Case with MVO and 'lower infarct T1.' Infarct T1 was relatively lower (<1300 ms) in patients with large MVO (>1.55% of entire myocardium). In this case, MVO represented 8.94% of the entire myocardium. Mean T1 in the entire infarcted area was low at 1242 ms whilst T1 in the entire MVO area was much lower 1166 ms. B: High non-infarct T1 (1330 ms). C: High remote T1 (1249 ms). LGE = late gadolinium enhancement.

6.2.4. Major adverse cardiac events (MACE)

Clinical outcomes data were prospectively collected from patients at their research visits, annual telephone calls, from electronic patient records (EPR) and General Practitioners (GP). Major adverse cardiac events (MACE) were defined as a composite endpoint consisting of cardiac death, new diagnosis of heart failure (HF), survived cardiac arrest and sustained ventricular arrhythmia requiring therapy. Heart failure was defined as the new occurrence of symptomatic fluid overload for which diuretics were administered in patients with LVEF<50% and/or raised levels of natriuretic peptides (92). Any events prior to the acute CMR scan were excluded from analysis.

6.2.5. Statistical analysis

Normality of data was determined using Kolmogorov-Smirnov test. Normally distributed data are presented as mean ± SD; nonparametric data as median with interquartile ranges (IQRs). Statistical comparisons for paired and unpaired samples were performed using student's t-test, Wilcoxon signed rank test, or the Mann-Whitney U test as appropriate. Categorical data and frequencies were compared with chi-square or Fisher's test as appropriate. Segmental analysis was averaged on a per-subject basis before any inter-individual and group comparisons to remove bias from clustering of segments within each subject. Correlation between variables was assessed using Pearson's product-moment correlation coefficient (r) or Spearman's rank correlation coefficient (ρ) as appropriate, depending on the normality assumption.

Survival analysis and endpoint comparison between groups were performed with the Cox regression analysis for the calculation of hazard ratio (HR) with 95% confidence interval. Kaplan Meier curves with log-rank test were constructed. Multicollinearity of variables included in the final model used was assessed using variance inflation factor analysis. The proportional-hazards assumption was met. Models of Cox-regression multivariate analysis were created to explore the incremental predictive value of different CMR indices. CMR variables and clinical factors found

to be significant univariate predictors of MACE with and without the novel T1 indices were included in the baseline model. The goodness of fit, predictive performance, discrimination and risk classification of models with T1 indices were tested with 1) concordance statistic (C-statistic) 2) Brier score 3) Net- Reclassification Index (NRI) and 4) Integrated Discrimination Index (IDI) for censored data.

Statistical analyses were performed using SPSS (version 25, IBM Inc, USA), Stata (version*16*, StataCorp LLC, TX, USA) and R statistical software (Version 4.0.5, RStudio, Inc., version 1.3, Boston, MA). *SurvIDINRI* package was used by Dr Rafail Kotronias on R Studio for the calculation of C-statistic, Brier score, NRI and IDI. All statistical tests were two-tailed, with p values <0.05 considered significant.

6.3. Results

6.3.1. Baseline clinical characteristics

221 patients with acute STEMI (age 61±11 years; 87% male) were prospectively recruited (**Figure 6.2**). 5.4% of patients had a history of myocardial infarction. Pain-to-balloon (ischaemic) time was median 193 (IQR 123-298) minutes. TIMI 3 flow was achieved after PPCI in 86% of patients.

Patients underwent an acute CMR scan at a median of 2 (IQR 1-2) days after PPCI. Patients suffered significant myocardial injury, with a median peak troponin rise of 50ng/dl (normal <0.04ng/dl) and a mean LVEF of 47±9% (**Table 6. 1**). The majority of patients were treated with optimal medical treatment, with >98% of patients receiving dual anti-platelet therapy, statin and either one of angiotensin-converting enzyme inhibitor or angiotensin receptor blocker, whilst 93% of patients were discharged on a beta blocker (**Table 6.2**). 152 (69%) patients returned for a follow-up CMR scan and blood sampling at 6 months.

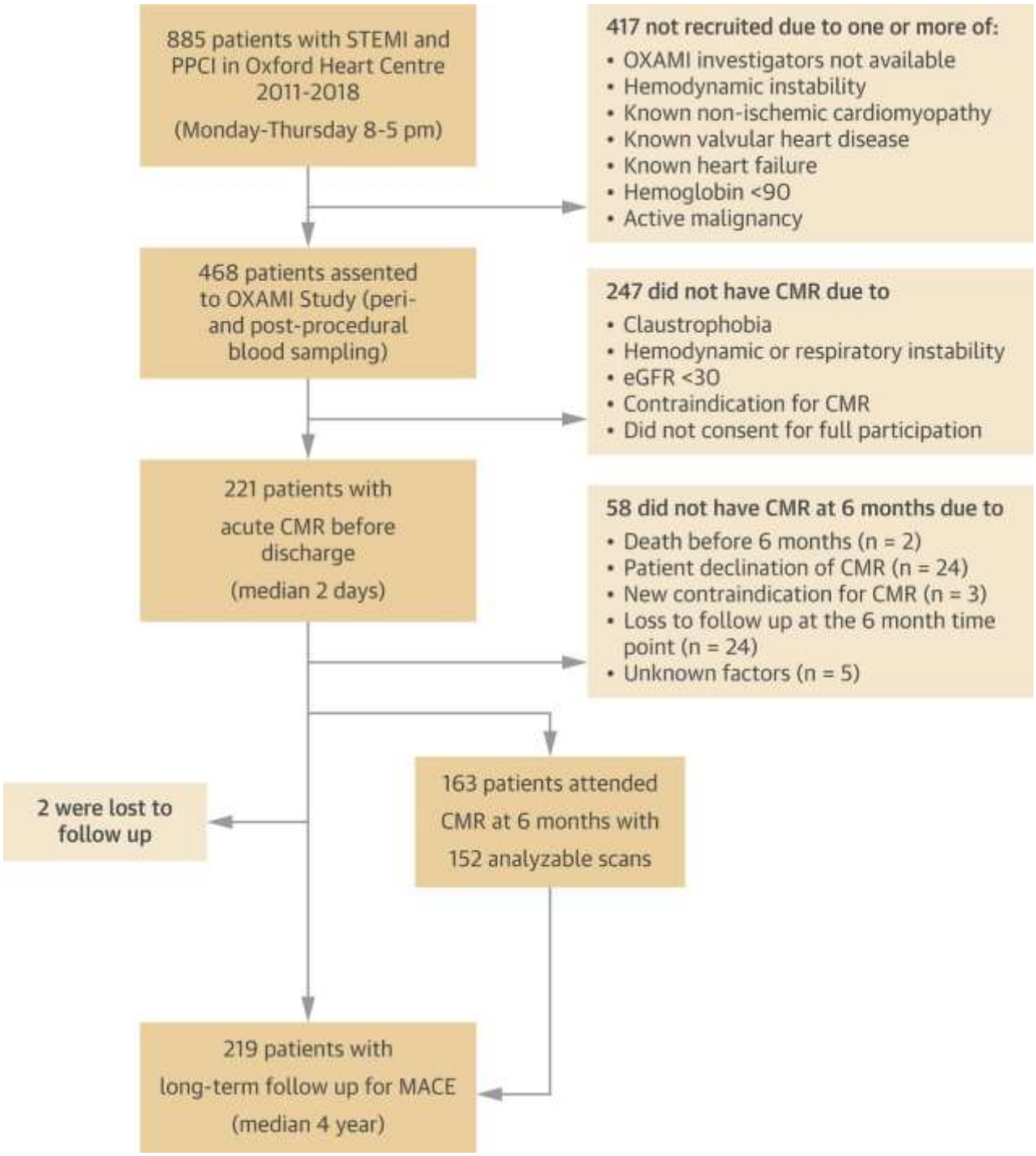


Figure 6.2 Study Flowchart. Patients with STEMI were prospectively recruited between 2011 and 2018. CMR = cardiac magnetic resonance; eGFR = estimated glomerular filtration rate; MACE = major adverse cardiac events; OXAMI = Oxford Acute Myocardial Infarction Study; PPCI = primary percutaneous coronary intervention; STEMI = ST-segment elevation myocardial infarction.

Table 6. 1 Baseline demographics, procedural, angiographic and investigations data

Factors	**All cohort (n = 219)**	**High non-infarct T1 (n = 100)**	**Normal non-infarct T1 (n = 119)**	**p-value**
Age (years)	61 ± 11	61 ± 11	61 ± 11	0.669
Male sex	86.9%	82%	90.8%	0.072
BMI (kg/m^2)	27.6 ± 4.1	27.7 ± 4.2	27.5 ± 4	0.817
TIMI risk score	2 (1-4)	3 (2-6)	2 (1-6)	0.215
Smoking history	66.1%	64%	67.2%	0.669
Hypertension	43.9%	41%	46.2%	0.495
Diabetes	18.6%	19%	17.6%	0.861
Hypercholesterolemia	38.0%	40%	36.1%	0.578
Family history of CAD	41.6%	36%	46.2%	0.133
Previous myocardial infarction	5.4%	3.0%	7.6%	0.232
Previous PCI	4.5%	2.0%	6.7%	0.115
Peripheral vascular disease	1.8%	1%	2.5%	0.627
COPD or Asthma	10.9%	11%	10.9%	1.000
ACEi or ARB use before STEMI	21.7%	24.0%	20.2%	0.516
Beta blocker use before STEMI	9.5%	8.0%	10.1%	0.644
Statin use before STEMI	20.8%	20.0%	21.0%	0.869
Systolic BP on admission (mmHg)	131 ± 26	126 ± 25	136 ± 26	**0.010**
Heart rate on admission (beats per minute)	79 ± 19	82 ± 19	76 ± 18	**0.023**
Ischaemic time (minutes)	193 (123-298)	174 (110-293)	196 (138-298)	0.175
Late presenter (6-12 hours)	19.5%	19.2%	19.3%	1.000
Aspirin pre PPCI	99.1%	98.0%	99.9%	0.207
LAD culprit	46.6%	60%	35.3%	**<0.001**
MVD (>1 vessel disease)	30.3%	23%	37%	**0.028**
TIMI flow pre PPCI = 0	70.1%	73%	68.1%	0.460
Thrombus score >2	83.3%	85.6%	79.9%	0.451
TIMI flow post PPCI = 3	86.0%	85%	87.4%	0.694
Myocardial blush grade <2	17.2%	17.6%	17.1%	1.000
Troponin peak level (ng/l)	50 (21-131)	59 (35-216)	45 (16-106)	**0.012**
Creatinine level on admission (umol/l)	78 ± 19	75 ± 18	81 ± 19	**0.033**
Peak monocyte count ($x10^9/L$)	0.91 (0.68-1.20)	0.94 (0.73-1.21)	0.87 (0.65-1.20)	0.188
Peak neutrophil count ($x10^9/L$)	8.4 ± 2.6	8.6 ± 2.5	8.2 ± 2.6	0.303
CRP (mg/L)	5.9 (2.4-15.8)	7.2 (2.8-19.1)	5.2 (1.9-13.2)	0.187
ST segment resolution >70% on ECG	75.7%	74%	76.8%	0.747

Table 6.1 abbreviations: BMI - Body Mass Index, BP -blood pressure, CAD – Coronary artery disease, COPD – Chronic obstructive pulmonary disease, ACEi – Angiotensin Converting

Enzyme inhibitor, ARB – Angiotensin Receptor Blocker, PPCI – primary percutaneous coronary intervention. GPIIb/IIIa – Glycoprotein IIb/IIIa inhibitors. LAD – left anterior descending artery. MVD – multi-vessel disease. TIMI – Thrombolysis in myocardial infarction. ng/L and ul/L – nanograms, micromoles and milligrams per litre respectively. CRP – C-Reactive Protein

Table 6.2 Cardiac medications on hospital discharge and at 6 months.

Medications	**Frequency on discharge (%)**	**Frequency at 6 months (%)**
Aspirin	98	95
Clopidogrel or Ticagrelor	99	96
Beta blocker	93	88
ACE-i or ARB	99	95
Statin	99	96

Table 6.2 abbreviations: ACE-i = Angiotensin converting enzyme inhibitor, ARB = Angiotensin receptor blocker

6.3.2. Acute tissue characteristics of the infarcted myocardium

The median infarct size (IS) was 22% (IQR 13-33%). MVO and/or IMH were present in 53% of cases. Infarct T1 was available in 90% of the cohort and the mean was significantly elevated at 1366±68ms. Infarct T1 was lower in patients with large MVO (>1.55% of myocardium): (1355±63 vs 1376±70ms, p=0.032). The area of MVO had a significantly lower T1 than the surrounding infarcted area (1293±74 vs 1369±63ms, p<0.001).

6.3.2.1. Acute tissue characteristics of the non-infarcted myocardium

Overall, 46% of patients had significantly elevated mean T1 >1250ms in the entire non-infarcted myocardium. When compared to the patients with normal mean T1 in the non-infarcted myocardium, those with high non-infarct T1 had significantly lower LVEF (50±7 vs 44±9%, p<0.001), larger IS (median 20% vs 28%, p<0.001), larger AAR (36±12 vs 47±13%, p<0.001) and larger MVO volume (median 0% vs 1.2%, p<0.007), as well as a numerically higher prevalence of IMH (47% vs 60%, p=0.109) (**Table 6.3**). In terms of clinical characteristics, patients with high non-infarct T1 had a significantly higher proportion of LAD infarctions (35 vs 60%, p<0.001) but lower prevalence of multi-vessel disease (37 vs 23%, p = 0.028).

6.3.2.2. Acute tissue characteristics of the remote zone *within* the non-infarcted myocardium

The mean T1 value in the remote zone within the non-infarcted myocardium was 1203±46ms (**Table 6.3**), which is significantly higher than the normal T1 values (1184±30ms, p<0.001). 12% of patients had high remote T1 (>1250ms).

Table 6.3 Acute CMR findings stratified according to higher and lower T1 in infarcted and non-infarcted myocardium

Acute CMR findings (median 2 days)	Patients (n = 219)	Infarct T1			Non-infarct T1		
		Higher T1 (≥1300ms) (87% of cohort)	Lower T1 (<1300ms) (13% of cohort)	p-value	High T1 (>1250ms) (46 % of cohort)	Normal T1 (≤1250ms) (54 % of cohort)	p-value
Acute LVEDVi (ml/m^2)	80 ± 17	81 ± 15	82 ± 19	ns	83 ± 17	78 ± 16	**0.016**
Acute LVESVi (ml/m^2)	43 ± 13	44 ± 12	44 ± 16	ns	47 ± 14	39 ± 11	**<0.0001**
Acute LVEF (%)	47 ± 9	47 ± 9	47 ± 9	ns	44 ± 9	50 ± 7	**<0.00001**
Acute RVEDVi (ml/m^2)	65 ± 14	65 ± 14	67 ± 17	ns	63 ± 13	67 ± 15	ns
Acute RVESVi (ml/m^2)	29 ± 10	29 ± 10	30 ± 12	ns	28 ± 9	30 ± 11	0.082
Acute RVEF (%)	56 ± 8	56 ± 8	56 ± 9	ns	57 ± 9	56 ± 8	ns
Acute AAR (% of LV mass)	41 ± 14	44 ± 13	35 ± 14	**0.005**	47 ± 13	36 ± 12	**<0.00001**
Acute IS (% of LV mass)	22 (13-33)	24 (16-34)	22 (13-29)	ns	28 (16-38)	20 (11-27)	**<0.00001**
MVO (% of LV mass)	0.57 (0.00-1.19)	0.86 (0.00-3.38)	1.23 (0.00-6.31)	ns	1.16 (0-5.22)	0 (0-2.17)	**0.007**
MVO presence (% of patients)	52.8%	57.9%	59.3%	ns	60.2%	47.4%	0.080
IMH presence (% of patients)	52.3%	58.8%	56%	ns	59.7%	47.1%	ns
RV infarct (% of patients)	25.5%	26.9%	25.9%	ns	26.2%	24.7%	ns
Global T1 (ms)	1273 ± 50	1287 ± 43	1227 ± 29	**<0.00001**	1311 ± 38	1242 ± 36	**<0.00001**
Infarct T1 (ms)	1366 ± 68	1384 ± 55	1262 ± 36	**<0.0001**	1387 ± 62	1349 ± 69	**<0.00001**
Infarct T1 adjusted for large MVO (ms)	1372 ± 67	1389 ± 56	1271 ± 33	**<0.00001**	1394 ± 59	1352 ± 68	**<0.00001**
Non-infarct T1 (ms)	1245 ± 43	1253 ± 39	1217 ± 38	**<0.00001**	1283 ± 28	1214 ± 25	**<0.00001**
Remote T1 (ms)	1203 ± 46	1209 ± 45	1182 ± 43	**0.003**	1232 ± 41	1179 ± 34	**<0.00001**

LV – left ventricle. i – indexed to body surface area. LVEDVi – indexed LV end-diastolic volume. LVESVi – indexed LV end-systolic volume. RV – Right ventricle. RVEDVi – indexed RV end-diastolic volume. RVESVi – indexed RV end-systolic volume. IS – infarct size. MVO – microvascular obstruction. IMH – intramyocardial haemorrhage. ns= non-significant p value.

6.1.1. LV characteristics at 6-month follow-up

Mean LVEF improved significantly from baseline (47% to 53%, p <0.001) and the final IS was significantly smaller (22% to 16%, p<0.001) at 6-months post-STEMI. The myocardial salvage index (MSI) was 61±21%. (**Table 6.4**).

Table 6.4 CMR findings and NT-proBNP levels at 6 months post-STEMI stratified according to higher and lower T1 in the non-infarcted myocardium on the acute scan.

CMR findings at 6 months	Patients with follow-up CMR (n=152)	Acute non-infarct T1		
		High (>1250ms) (47 % of cohort)	Normal (≤1250ms) (53 % of cohort)	p-value
LVEDVi (ml/m^2)	84 ± 19$^{\#}$	86 ± 20	81 ± 18	0.115
LVESVi (ml/m^2)	40 ± 15$^{\#}$	44 ± 16	38 ± 14	**0.015**
LVEF (%)	53 ± 9$^{\#}$	51 ± 8	55 ± 9	**0.002**
RVEDVi (ml/m^2)	71 ± 14$^{\#}$	70 ± 14	71 ± 14	0.541
RVESVi (ml/m^2)	29 ± 9$^{\#}$	29 ± 8	29 ± 9	0.649
RVEF (%)	60 ± 7$^{\#}$	60 ± 7	60 ± 6	0.899
Final infarct size (%)	16 (8-24)$^{\#}$	19 (10-28)	13 (8-25)	**0.005**
Myocardial salvage index (%)	61 (45-76)	58 (42-72)	64 (46-78)	0.258
Change in LVEDV vs baseline (%)	1.6 (-8.1-11.2)	2.8 (-8.3-14)	0.9 (-5.4-4.4)	0.267
Significant adverse remodelling (frequency in %)	14%	9%	15%	0.226
Absolute change in LVEF	5 (0-10)	7 (2-12)	3 (-1-8)	**0.011**
Blood test findings at 6 months				
NT-proBNP (pg/ml)	198 (88-398)	290 (103-523)	170 (61-312)	**0.008**

Abbreviations for Table 6.4: NT-proBNP: N-terminal pro B type natriuretic peptide. pg/ml: picograms per millilitre. $^{\#}$p<0.001 when compared to acute CMR scan findings in Table 6.3. Significant adverse remodelling is defined as ≥20% increase in LVEDV. Other abbreviations as per Table 6.3**.**

6.1.1.1. Predictive power of acute T1 indices for short-term (6-month) outcomes

Acute infarct T1 was not significantly correlated with LVEF or NT-proBNP at 6 months. In contrast, acute non-infarct T1 and remote T1 significantly correlated with LVEF (r= -0.30, r= -0.35, respectively; both p<0.001) and NT-pro-BNP levels (r=0.27, p=0.002; r=0.24, p=0.007, respectively) at 6 months (**Figure 6.3**). When compared with patients with normal non-infarct T1, those with high non-infarct T1 on the acute scan had lower LVEF (55±9% vs 51±8%, p=0.005), larger final IS (13% vs 19% p=0.005) and higher NT-pro-BNP levels (median 170 vs 290 pg/ml, p=0.008) at 6 months (**Table 6.4**). Similarly, patients with high remote T1 also had lower LVEF (54±9% vs 47±8%, p=0.001), larger final IS (13% vs 27%, p<0.001) and higher NT-pro-BNP levels (median 186 vs 319 pg/ml, p=0.022) at 6 months.

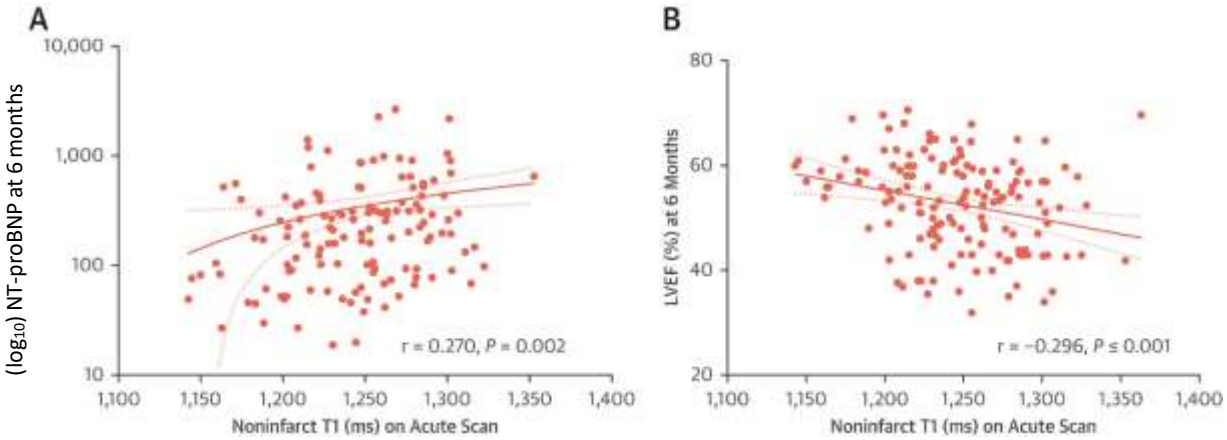


Figure 6.3 Correlation of Non-infarct T1 on acute CMR scan With LV Systolic Function and Natriuretic Peptide Levels at 6 Months. Correlation between non-infarct T1 on acute scan with (A) N-terminal pro–B-type natriuretic peptide (NT-proBNP) (pg/L) and (B) left ventricular ejection fraction (LVEF) (%) at 6 months. LV = left ventricular; other abbreviation as in Figure 6.2

6.1.2. Long-term MACE and Cox regression analysis

Two patients were lost to follow up. Median follow-up duration was 4 (IQR 2.5-6) years. Outcome analysis was censored to 2700 days, as very few patients had a greater follow-up duration. During the follow-up period, n=22 patients (10%) experienced a MACE; new diagnosis of heart failure occurred in n=20 and ventricular arrhythmia and cardiac death in n=1 each.

6.1.2.1. Univariate Cox regression analysis of long-term MACE

Clinical and procedural factors: Previous myocardial infarction, longer ischaemic time, and higher peak troponin were significantly associated with MACE (all p<0.01), whilst peak monocyte count trended towards significance (p=0.087) (**Table 6.5**).

Conventional CMR markers: LVEF (HR=0.951 per 1% increase in LVEF, p=0.048), IS (HR=1.028 per 1% increase in IS, p=0.08) and MVO (HR = 1.109 per 1% increase in MVO, p = 0.005) were associated with MACE. When dichotomised, LVEF <40% (HR=3.554, p=0.004), IS >17% (HR=3.529, p=0.044) and the presence of MVO (HR =3.714, p=0.018) were associated with MACE (**Table 6.5**).

T1 indices: Infarct T1 was significantly inversely associated with MACE (HR=0.993 per 1ms increase, p=0.035). The majority (87%) of patients had a significantly high infarct T1 (≥1300ms), whereas 13% of patients had an average infarct T1 <1300ms, referred to as 'lower infarct T1' from hereon. Lower infarct T1 was associated with a 3-fold increased risk of MACE (HR=3.114; CI 1.192-8.133, p=0.020). Non-infarct T1 (HR=1.009 per 1ms increase, p=0.056) and remote T1 (HR=1.008 per 1ms increase, p=0.083) were associated with MACE. A high non-infarct T1 was associated with a 2.5-fold increased risk of MACE (HR=2.534; CI 1.033-6.219, p=0.042). (**Table 6.5**).

Table 6.5 Univariate Cox regression analysis

	Hazard Ratio (95% CI)	p
Clinical factors and angiographic indices at admission		
Age	1.029 (0.989-1.070)	0.158
Smoking history	0.595 (0.257-1.070)	0.226
Hypertension	1.400 (0.606-3.237)	0.431
Diabetes	0.897 (0.303-2.652)	0.844
Previous history of MI	5.653 (1.867-17.114)	**0.002**
Ischaemic time per minute	1.001 (1.000-1.003)	**0.008**
LAD culprit	1.068 (0.461-2.474)	0.878
Multi-vessel disease (>1 vessel)	0.706 (0.26-1.914)	0.494
Thrombus score >2	1.107 (0.326-3.763)	0.871
TIMI flow post PPCI <3	1.513 (0.555-4.122)	0.418
Myocardial blush grade post PPCI <2	1.199 (0.403-3.565)	0.744
Peak troponin rise, per unit increase	1.002 (1.001-1.003)	**0.005**
Peak monocyte count, per unit increase	1.993 (0.904-4.391)	**0.087**
>70% ST segment resolution at discharge	0.516 (0.216-1.230)	0.136
Prescription of GDMT at discharge	0.536 (0.158- 1.182)	0.353
Prescription of GDMT at 6 months	3.359 (0.448 – 25.17)	0.238
Prescription of GDMT at final follow up	0.889 (0.375-2.112)	0.791
Acute CMR markers		
LVEF per 1 % increase	0.951 (0.905-1.00)	**0.048**
LVEF ≤40%	3.554 (1.506-8.385)	**0.004**
RVEF per 1 % increase	1.028 (0.971-1.088)	0.339
Area at risk per 1 % increase	1.035 (0.996-1.077)	**0.083**
Infarct size per 1 % increase	1.028 (0.997-1.060)	**0.082**
Infarct size >17%	3.529 (1.033-12.055)	**0.044**
RV infarct presence	0.876 (0.289-5.623)	0.114
MVO presence	3.734 (1.248-11.172)	**0.018**
IMH presence	2.161 (0.830-5.623)	0.114
Acute T1 indices		
Global T1	1.002 (0.994-1.011)	0.580
Infarct T1 per ms	0.993 (0.986-0.999)	**0.035**
Infarct T1 <1300ms	3.114 (1.192-8.133)	**0.020**
Non-infarct T1 per ms	1.009 (1.000-1.018)	**0.056**
Non-infarct T1 per 10ms	1.094 (1.000-1.195)	**0.056**
Non-infarct T1 >1250ms (>2SD)	2.534 (1.033 -6.219)	**0.042**
Remote T1 per ms	1.008 (0.999-1.017)	**0.083**
Remote T1 >1250ms (>2SD)	2.223 (0.818-6.037)	0.112

Table 6.5: Univariate Cox regression analysis of clinical, routine CMR indices and T1 biomarkers. CI – Confidence Interval. GDMT = Guideline directored medical therapy (Beta blocker and Angiotensin converting enzyme inhibitor or Angiotensin receptor blocker). Other abbreviations as per Table 2. Variables in bold had a p value <0.10 and subsequently included in the multivariate Cox regression.

6.1.2.2. Multivariate Cox regression analysis of MACE

CMR model

Both acute infarct T1 and non-infarct T1 showed incremental value beyond conventional CMR markers (LVEF, IS, MVO) in predicting long-term MACE. When these T1 indices were added to a model of multivariate Cox regression (both non-stepwise and stepwise), only MVO (p=0.038), infarct T1 (p=0.001) and non-infarct T1 (p=0.001) remained as independent predictors of MACE (**Table 6.6** for summary and **Table 6.7** for detailed analysis). When dichotomised, lower infarct T1 (p=0.001) and high non-infarct T1 (p=0.027) were the only independent predictors of MACE). Remote myocardial T1 also demonstrated a similar but weaker ability to predict MACE in such models (as continuous variable: p=0.019; but when dichotomised: p = 0.234; (**Table 6.7**).

Table 6.6 Multivariate Cox regression analysis of conventional CMR and novel T1 biomarker

Model 1		
Variable	**Hazard Ratio (HR) (95% CI)**	**p value**
Acute LVEF (per 1% increase)	1.017 (0.954-1.084)	0.608
MVO presence	2.829 (0.898-8.909)	0.076
Non-infarct T1 (per 1 ms)	1.024 (1.010-1.039)	**0.001**
Infarct T1 (per 1 ms)	0.987 (0.979-0.994)	**0.001**
Model 2		
Variable	**HR (CI)**	**p value**
Acute LVEF ≤40%	1.482 (0.538-4.083)	0.447
MVO presence	2.470 (0.799-7.630)	0.116
Non-infarct T1 (per 1 ms)	1.020 (1.006-1.034)	**0.005**
Infarct T1 (per 1 ms)	0.988 (0.981-0.995)	**0.001**
Model 3		
Variable	**HR (CI)**	**p value**
Acute LVEF ≤40%	2.347 (0.899-6.127)	0.081
MVO presence	2.013 (0.646-6.273)	0.228
Non-infarct T1 >1250ms	3.643 (1.169 -11.357)	**0.026**
Infarct T1 <1300ms	5.982 (2.077-17.277)	**0.001**

Table 6.6: Multivariate cox regression analysis to establish CMR variables predictive of clinical outcomes. Abbreviations as before. Models 1-2 contain T1 as continuous variable. Model 3 uses T1 cut-off as a categorical variable. Variables in bold had a p value <0.05 and were considered to be independent predictors of clinical outcomes. See Table 6.7 for further multivariate Cox regression models.

Table 6.7 Multivariate Cox-regression analysis of CMR variables

Model 1:		
Variable	**Hazard Ratio (HR) (CI)**	**p-value**
Acute LVEF (per 1% increase)	0.948 (0.890-1.010)	0.099
Acute infarct size (per 1% increase)	0.983 (0.938-1.030)	0.471
MVO presence	**3.803 (1.050-13.769)**	**0.042**
Model 2:		
Variable	**HR (CI)**	**p-value**
Acute LVEF (per 1% increase)	0.971 (0.909-1.039)	0.395
Acute infarct size (per 1% increase)	0.977 (0.931-1.050)	0.347
MVO presence	**4.295 (1.182-15.607)**	**0.027**
Non-infarct T1 (per 1 ms)	**1.013 (1.000-1.025)**	**0.042**
Model 3:		
Variable	**HR (CI)**	**p-value**
Acute LVEF (per 1% increase)	1.001 (0.931-1.076)	0.984
Acute infarct size (per 1% increase)	0.977 (0.932-1.023)	0.317
MVO presence	**3.747 (1.073-13.0847)**	**0.038**
Non-infarct T1 (per 1 ms)	**1.025 (1.010-1.040)**	**0.001**
Infarct T1 (per 1 ms)	**0.986 (0.979-0.994)**	**0.001**
Model 5:		
Variable	**HR (CI)**	**p-value**
Acute infarct size (per 1% increase)	0.978 (0.934-1.025)	0.353
Acute LVEF ≤40%	**3.802 (1.357-10.654)**	**0.011**
MVO presence	**3.834 (1.052-13.979)**	**0.042**
Model 6:		
Variable	**HR (CI)**	**p-value**
Acute infarct size >17%	1.314 (0.292-5.911)	0.722
MVO presence	2.521 (0.711-8.938)	0.152
Acute LVEF ≤40%	**2.852 (1.093-7.442)**	**0.032**
Model 7:		
Variable	**HR (CI)**	**p-value**
Acute LVEF ≤40%	2.134 (0.742-6.487)	0.181
Acute infarct size (per 1% increase)	0.962 (0.916-1.010)	0.122
MVO presence	**4.173 (1.073-13.0847)**	**0.029**
Non-infarct T1 (ms)	**1.022 (1.008-1.037)**	**0.002**
Infarct T1 (ms)	**0.987 (0.979-0.995)**	**0.001**
Model 8:		
Variable	**HR (CI)**	**p-value**
Acute LVEF<40%	1.482 (0.538-4.083)	0.447
MVO presence	2.470 (0.799-7.630)	0.116

Non-infarct T1 (ms)	**1.020 (1.005-1.034)**	**0.005**
Infarct T1 (ms)	**0.988 (0.981-0.995)**	**0.001**
Model 9:		
Variable	**HR (CI)**	**p-value**
Acute infarct size >17%	0.910 (0.190-4.361)	0.907
MVO presence	2.096 (0.567-7.750)	0.267
Acute LVEF ≤40%	2.389 (0.866-6.591)	0.093
Non-infarct T1 >1250ms	**3.651 (1.162-11.471)**	**0.027**
Infarct T1 <1300ms	**5.988 (2.071-17.310)**	**0.001**
Model 10:		
Variable	**HR (CI)**	**p-value**
Acute infarct size (per 1% increase)	0.962 (0.916-1.010)	0.118
MVO presence	3.350 (0.925-12.138)	0.066
Acute LVEF ≤40%	**3.328 (1.160-9.546)**	**0.025**
Non-infarct T1 >1250ms	**4.361 (1.381-13.776)**	**0.012**
Infarct T1 <1300ms	**6.251 (2.142-18.237)**	**0.001**
Model 11:		
Variable	**HR (CI)**	**p-value**
MVO presence	2.013 (0.646-6.273)	0.228
Acute LVEF ≤40%	2.347 (0.899-6.127)	0.081
Non-infarct T1 >1250ms	**3.643 (1.169-11.357)**	**0.026**
Infarct T1 <1300ms	**5.982 (2.077-17.227)**	**0.001**
Model 12:		
Variable	**HR (CI)**	**p-value**
Acute LVEF (per 1% increase)	0.977 (0.912-1.047)	0.507
Acute infarct size (per 1% increase)	0.974 (0.929-1.022)	0.289
MVO presence	3.572 (0.975-13.081)	0.055
Remote T1 (per 1 ms)	**1.015 (1.002-1.028)**	**0.019**
Infarct T1 (per 1 ms)	**0.990 (0.983-0.997)**	**0.008**
Model 13		
Variable	**HR (CI)**	**p-value**
Acute LVEF (per 1% increase)	0.958 (0.897-1.023)	0.199
Acute infarct size (per 1% increase)	0.981 (0.935-1.029)	0.981
MVO presence	3.099 (0.869-11.050)	0.081
Remote T1 >1250ms	1.996 (0.639-6.231)	0.234
Infarct T1 <1300ms	**3.560 (1.332-9.516)**	**0.011**

Holistic model incorporating clinical and CMR characteristics

Both infarct T1 and non-infarct T1 remained as significant independent predictors of MACE in multivariate Cox-regression models consisting of clinical variables (age, previous MI, ischaemic time and peak troponin) and conventional CMR indices (**Table 6.8**, **Table 6.9**).

Table 6.8 Multivariate backward step-wise Cox-regression analysis of clinical factors and T1 indices

Model 1		
Variables entered: Age, past history of MI, ischaemic time, Troponin, infarct T1 and non-infarct T1		
Variables in the equation at the final step of regression		
Variable	**Hazard Ratio (CI)**	**p-value**
Age (y)	1.046 (1.004-1.091)	**0.033**
Ischaemic time per 1 minute	1.002 (1.000-1.003)	**0.005**
Troponin (peak) per ng/l	1.002 (1.000-1.004)	**0.020**
Non-infarct T1 per 1ms increase	1.027 (1.013-1.041)	**<0.001**
Infarct T1 per 1ms increase	0.988 (0.980-0.996)	**0.003**

Backward step-wise multivariate Cox-regression analysis results. Abbreviation as before.

Table 6.9 Multivariate backward step-wise Cox-regression analysis of clinical factors, conventional CMR indices and T1 indices

Model 2		
Variables entered: Age, past history of MI, ischaemic time, Troponin, infarct T1 and non-infarct T1, LVEF ≤40%, Infarct size >17% and MVO.		
Variables in the equation at the final step of regression		
Variable	**Hazard Ratio (CI)**	**p-value**
Age (y)	1.050 (1.006-1.096)	**0.024**
Ischaemic time per 1 minute	1.002 (1.000-1.002)	**0.008**
Troponin (peak) per ng/l	1.002 (1.000-1.004)	**0.022**
Non-infarct T1 per 1ms increase	1.027 (1.013-1.040)	**<0.001**
Infarct T1 per 1ms increase	0.987 (0.980-0.995)	**0.001**

Backward step-wise multivariate Cox-regression analysis results. Abbreviation as before.

6.1.2.3. Discrimination and risk reclassification for MACE using novel T1 indices

Beyond the conventional CMR model, the addition of infarct T1 and non-infarct T1 significantly improved the prediction and reclassification of MACE. When added to a CMR model consisting of LVEF, IS and MVO, the C-statistic improved from 0.67±0.07 to 0.76±0.06 and the integrated Brier score improved from 0.076 to 0.064. In a reclassification analysis, the inclusion of non-infarct T1 and infarct T1 resulted in a net-classification index (NRI) of 40% (95% CI: 12-64, p=0.007) and an integrated discrimination index (IDI) of 16% (95% CI: 7-31, p<0.001), all indicating improved predictive performance of the T1 indices (**Table 6.10**). Similarly, non-infarct T1 and infarct T1 significantly improved the reclassification performance of a holistic model consisting of clinically important factors and conventional CMR markers (**Table 6.11**).

Table 6.10 Comparisons of the Predictive Power of Long-term MACE after STEMI Using Models Incorporating Conventional Cardiac Indices with and without Novel T1 Biomarkers

Comparison of the ability of models with conventional CMR indices (A, C) and models with T1 indices added (B,D) to predict clinical outcomes. C-statistic – concordance index. Other abbreviations as per before.

Model	Predictors	C-statistic	Integrated Brier score	Comparison of models		Net Reclassification Index NRI)		Integrated discrimination Improvement Index (IDI)	
				χ^2 difference	p	index	p	index	p
A	Acute LVEF MVO presence Infarct size	0.67 ± 0.07	0.076	N/A					
B	Acute LVEF MVO presence Infarct size Infarct T1 Non-infarct T1	0.76 ± 0.06	0.064	Model A vs B					
				15.52	<0.001	39.8% (CI 12.2-64.4%)	0.007	16.4% (CI 6.8-30.9%)	<0.001
C	Acute LVEF <40% MVO presence Infarct size	0.69 ± 0.06	0.075	N/A					
D	Acute LVEF <40% MVO presence Infarct size Infarct T1 Non-infarct T1	0.77 ± 0.06	0.064	Model A vs D					
				17.32	<0.001	50.4% (CI 17.7-68.3%)	0.013	18.7% (CI 6.5-32.4%)	<0.001
				Model C vs D					
				13.21	0.001	42.3% (CI 1.4-66.2%)	0.027	16.1% (CI 4.7-30.1%)	<0.001

Table 6.11 Comparison of the ability of models containing conventional clinical and conventional CMR indices with and without novel T1 biomarkers to predict MACE

Model	Predictors	C-statistic	Integrated Brier score	Comparison of models		Net Reclassification Index (NRI)		Integrated discrimination Improvement Index (IDI)	
				χ^2 difference	p	index	p	index	p
A	Previous MI, Ischaemic time, troponin peak	0.67 ± 0.07	0.068						
B	Previous MI, ischaemic time, troponin peak, MVO presence, LVEF <40%	0.71 ± 0.07	0.063	Model A vs B					
				7.78	0.02	30% (CI -9.1-56.8%)	ns	5.6% (CI -1.6-19.9%)	ns
C	Previous MI, ischaemic time, troponin peak, MVO presence, LVEF <40%, non-infarct T1, infarct T1	0.77 ± 0.06	0.055	Model A vs C					
				19.03	<0.001	54% (CI 0.6-71.3%)	0.047	18.5% (CI 4-35.6%)	0.013
				Model B vs C					
				11.25	0.004	26.4% (CI -3.2-60.1%)	0.086	12.9% (CI 1.5-24.8%)	0.02

Comparison of the ability of models with conventional clinical risk factors (A) with conventional CMR indices added (B) and model with T1 indices added (C) to predict clinical outcomes. Abbreviations as before.

6.4. Discussion

This study is the first to assess the long-term prognostic value of the acute changes in both the non-infarcted and infarcted myocardium immediately after STEMI. My novel contributions are:

1. A significant acute response in the non-infarcted myocardium, defined as high T1 values on CMR, was associated with significantly lower LVEF and higher levels of natriuretic peptides at 6 months and long-term MACE.
2. Non-infarct and infarct T1 are significant independent predictors of long-term MACE and offer better reclassification and significantly improved predictive performance beyond conventional CMR markers (LVEF, IS and MVO).

Infarcted myocardial tissue undergoes a high degree of inflammatory changes and exhibits significantly increased T1 times, secondary to the expansion of both intracellular and extracellular volume from myocardial necrosis, oedema and the ensuing inflammation (44,52,74,155). The core of the infarcted segment often has a lower T1 value due to the presence of MVO and/or IMH, and has been shown to be associated with poor outcomes at a median of 2.3 years post-STEMI (153). I extended this finding by showing that a lower T1 in the entire infarcted segment is predictive of long-term MACE at a median of 4 years. For every 10ms decrease in infarcted myocardial T1, there is a 7% increased risk of adverse outcomes, while an overall lower infarct T1 (<1300ms) was associated with a 3-fold increase in risk of MACE (**Table 6.5**, **Figure 6.4**). Infarct T1 indices offered significant improvement in risk-prediction beyond conventional markers, such as IS and presence of MVO (**Table 6.7**).

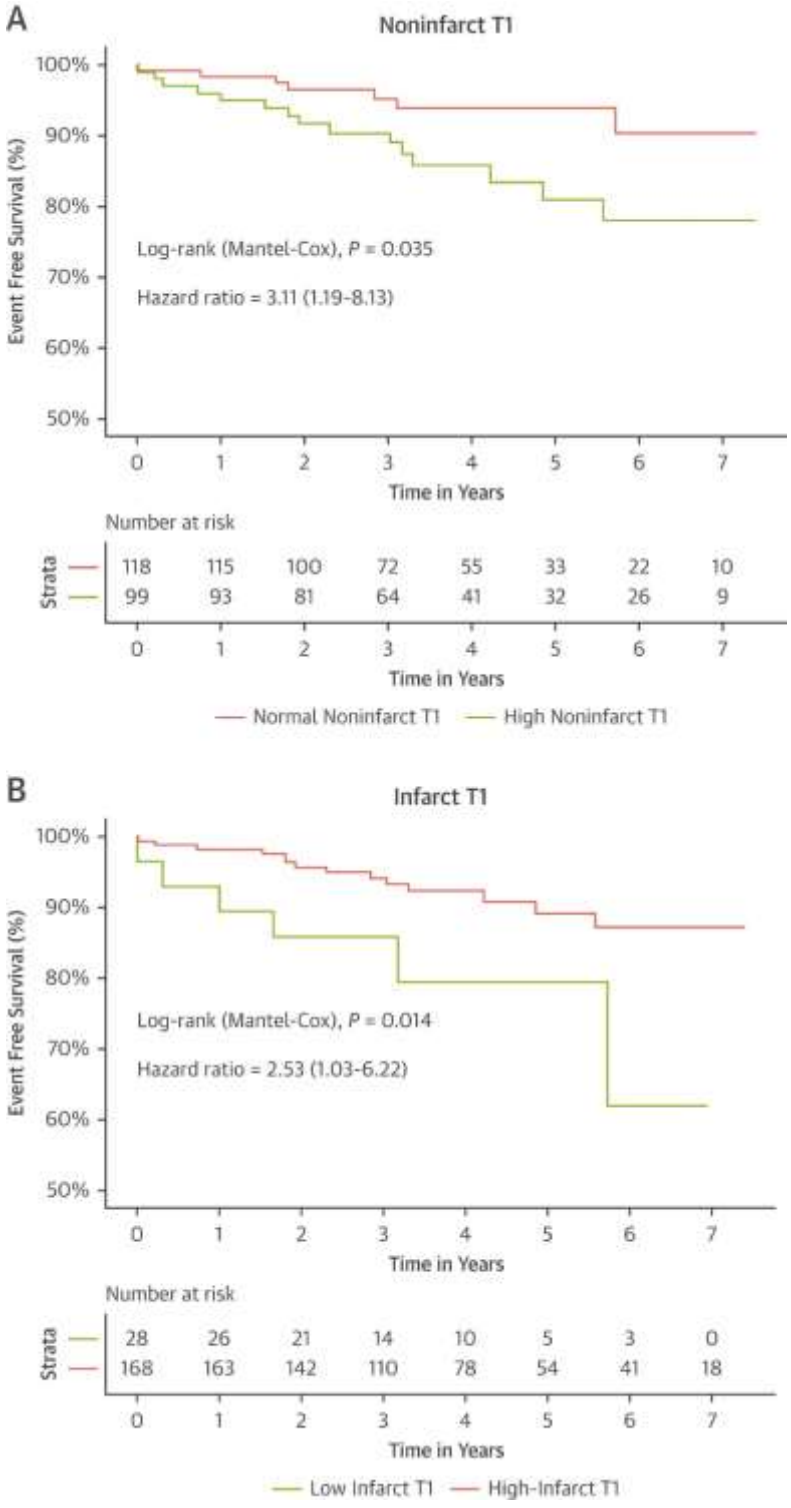


Figure 6.4 Noninfarct T1 and Infarct T1 on Acute CMR Scan Predict Long-Term MACE. Kaplan-Meier survival curves showing the differences in survival from MACE between (A) patients with high T1 (>1,250 ms) and normal T1 (<1,250 ms) in the noninfarcted myocardium, (B) patients with lower (<1,300 ms) and high (≥1,300 ms) T1 values in the infarcted myocardium. Abbreviations as before.

More interestingly, beyond the infarcted territory, remote myocardial injury and dysfunction post-MI have been described in animal and human studies (21,65,66,149–151). The proposed mechanisms include activation of the innate immune system and inflammation (21). Remote myocardial inflammation is believed to be mediated mainly by a 5-6 fold increase in leucocytes, and is coupled with an upregulation of inflammatory mediators including cytokines, adhesion molecules and matrix metalloproteinases (21,65). These may result in adverse LV remodelling, fibrosis and systolic dysfunction (151).

Increased remote myocardial T1 post-STEMI is known to be associated with adverse short-term outcomes, which I have also confirmed in this study, but its long-term prognostic implication had remained unclear (66,150). I have now shown that whilst the remote myocardial T1 is weakly associated with long-term MACE, a more complete assessment of the entire non-infarcted myocardium with T1-mapping provides a more powerful and independent prediction of long-term MACE (**Table 6.5, Table 6.6**). In particular, for every 10ms increase in non-infarct myocardial T1 the risk of long-term MACE increased by 9%. This suggests that the assessment of just a small remote zone of the non-infarcted myocardium is less comprehensive. Equally, neither the acute IS nor AAR (which relies on the assumption that remote myocardium is normal) were independent predictors of MACE in multivariate Cox regression models containing the non-infarct and infarct T1.

An acutely high remote T1 may be a surrogate marker for a large insult to the LV myocardium in STEMI. In my study, the abnormal response in the non-infarcted myocardium was associated more frequently with LAD infarctions, larger acute infarct size and higher peak troponin level (**Table 6. 1**, **Table 6.3**). Multi-vessel disease was not a predictor of clinical outcomes and more-interestingly was more prevalent amongst those with normal non-infarct T1 than in those with high non-infarct T1 (37% v 23%, p = 0.028). Thus, it is

unlikely that resting ischaemia from non-culprit vessel contributed significantly to the severely elevated observed in the non-infarcted myocardium.

Whilst the fraction of global myocardium with high T1 is positively correlated with inflammatory biomarkers, only remote T1 showed weak relationship with neutrophil counts and trend correlations with monocytes and C-reactive protein level post-PPCI (**Table 6.12**). The lack of correlations within either the infarct and non-infarct tissue T1 is likely due to the heterogeneity of these tissue classes characterised by various competing mechanisms affecting the measured T1 (e.g. MVO core in the infarcted area). In contrast, the remote myocardium T1 changes were found to be a better overall indicator of the systemic inflammatory burden. This is in keeping with pre-clinical and clinical observations that remote myocardial injury is related to the ischaemic insult and the ensuing immune-response and inflammation (21,65,150,156).

Table 6.12 Relationship between peak blood monocyte and neutrophil counts and CRP levels and T1 indices and infarct size acutely after STEMI.

	Peak monocyte count (10^9/L)	**Peak neutrophil count (10^9/L)**	**Peak CRP (mg/L)**
	Correlation (p value)		
Area of injured tissue			
Infarct size measured on LGE (%)	**0.353 (p<0.001)**	**0.271 (p=0.001)**	**0.303 (p<0.001)**
Area-at-risk measured on T1 mapping (%)	**0.261 (p<0.001)**	**0.226 (p=0.001)**	**0.195 (p=0.020)**
Fraction of myocardium with high T1>1250ms (%)	**0.158 (p=0.024)**	**0.189 (p=0.017)**	**0.157 (p=0.046)**
T1 values within tissue			
Infarct T1(ms)	0.012 (p=0.875)	-0.138 (p=0.102)	-0.033 (p=0.685)
Non-infarct T1(ms)	0.059 (p=0.406)	0.079 (p=0.328)	0.092 (p=0.246)
Remote T1(ms)	0.117 (p=0.096)	**0.166 (p=0.038)**	0.139 (p=0.079)

Table 6.12: Blood results were obtained from serial blood tests performed in the first 48 hours after PPCI for clinical purposes and the peak values were used in this analysis. Spearman (rho) and Pearson (r) correlations were performed as appropriate depending on the distribution of data. Abbreviations as per before.

The novelty of establishing the prognostic power of non-infarcted myocardial injury is best seen in the multivariate Cox regression analysis. In all the models consisting of conventional CMR indices (LVEF, IS, MVO), non-infarct myocardial T1 was an independent predictor of outcomes (**Table 6.6 Multivariate Cox regression analysis of conventional CMR and novel T1 biomarkerTable 6.6**). Indeed, when the models include both infarct and non-infarct myocardial T1, the performance of CMR in predicting adverse outcomes improved significantly (**Table 6.10**). Furthermore, the T1 indices significantly improved the predictive ability of a model containing conventional CMR indices and traditional clinical factors (**Table 6.9**). These findings challenge the current consensus that IS and LVEF should be the main prognostic indices in patients after STEMI (14), and make a case to also include the assessment of the pan-myocardial response. For instance, in my study 9/45 (20%) patients with LVEF <40% and 12/174 (7%) patients with LVEF ≥40% developed a long-term MACE. However, high non-infarct T1 was present in 7/12 (58%) of the patients with LVEF>40% who experienced a MACE; thus, if confirmed in larger trials, novel T1 indices may be used to reclassify patients otherwise labelled as low-risk, to aggressively treat and maintain optimal medical therapy to reduce the risk of long-term MACE.

My new findings build on previous reports of an association between remote myocardial changes after STEMI and adverse LV remodelling and the expansion of extracellular matrix at short-term follow-up (66,150,152), and demonstrate a strong association with the development of heart failure at long-term. Interestingly in my study, whilst the significantly abnormal T1 values in either infarcted or non-infarcted territories immediately after STEMI predicted the development of heart failure at long-term, they were not associated with adverse LV remodelling at 6 months (**Table 6.4**). Further work is required to test the performance of native T1 indices against other acute CMR indices in predicting outcomes post-STEMI,

including remote extracellular volume (152) and remote myocardial strain (157), which currently remain exploratory end-points (14). Similarly, the influence of infarcted myocardium on the functional recovery of the peri-infarcted area (non-infarcted myocardium) and may provide further insights (158).

I propose that T1-mapping could be included for a more holistic and directly quantitative assessment of the global myocardial response and risk-prediction post-STEMI. It would therefore be of clinical interest to test the prognostic benefit of identifying such at-risk patients early after STEMI and offering them aggressive optimization of existing medical therapy as well as trials of immunomodulation.

6.4.1. Limitations

This is a single centre study of patients with a lower-risk clinical profile on admission (no cardiogenic shock) and only those who were stable for a CMR scan on day 2 and therefore carries a potential selection bias. However, I believe that the discovery of novel T1 indices to further stratify the long-term risk of such patients is of significance. Scanning at day 2 may miss detecting the bimodal intensity in oedema associated with post-reperfusion (first few hours) and inflammatory response (days 4-7). However, CMR scanning of post-STEMI patients at around 2 days was an accepted practice at the time of my study protocol design and remains the most practical and clinically relevant time point for patients in UK as it coincides with their hospital discharge (153,159). Capturing T1 signals at either peak of the bimodal oedema may provide stronger associations with outcomes, but awaits further research. Although T1 maps were acquired at 3T, the use of thresholding to establish an abnormal T1(>2SD) can be performed in 1.5T scanners since ShMOLLI sequences have been validated in both settings (46). A higher number of events would be needed to firmly conclude associations with CMR imaging markers; however, the strength of my study lies in

its prospective design with serial and timely long-term follow-up of each patient (median 4 years). Moreover, I studied clinical outcomes of significance (heart failure, ventricular arrhythmias or cardiac arrest, cardiac death), and the rate of events is in line with real world data, revealing strong statistical associations with CMR markers in univariate and multivariate Cox regression models. High multicollinearity was excluded by my analysis (**Table 6. 13**). However, some degree of collinearity between the CMR variables in these models may reduce the accuracy of my findings and thus reproducibility studies with larger samples sizes and longer follow up are needed.

Table 6. 13 Multicollinearity analysis of variables used in the Cox regression analysis

Variable	**Variation Inflation Factor (VIF)**
Left ventricular ejection fraction (LVEF)	1.64
Infarct size	1.94
MVO presence	1.55
Non-infarct T1 (ms)	1.54
Infarct T1 (ms)	1.29
Mean VIF	**1.59**

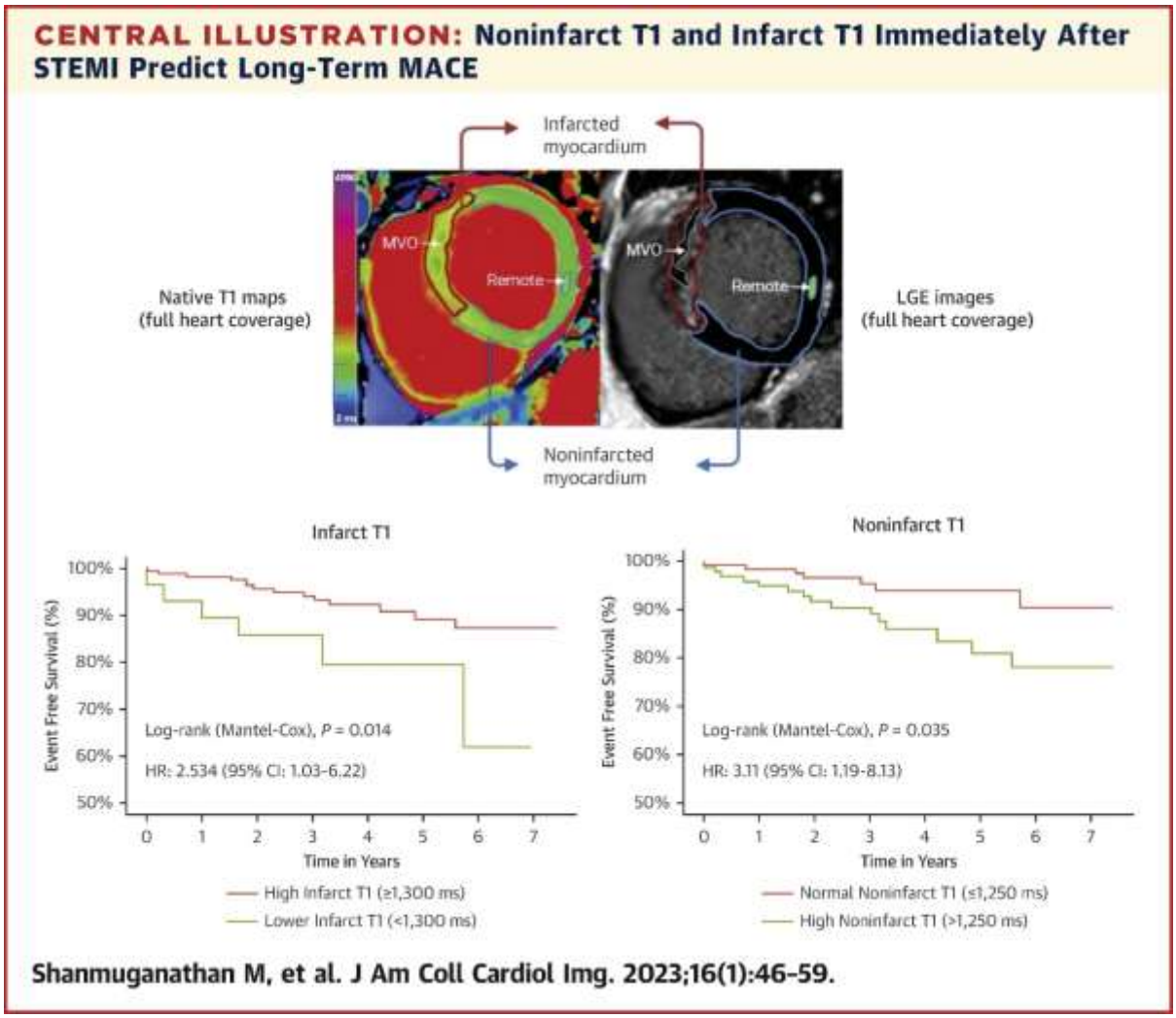
Variable	**Variation Inflation Factor (VIF)**
Left ventricular ejection fraction (LVEF) <40%	1.29
Infarct size >17%	1.33
MVO presence	1.26
Non-infarct T1 >1250ms	1.19
Infarct T1 <1300ms	1.05
Mean VIF	**1.22**

Multicollinearity of variables in the two main models was assessed with variation inflation factor (VIF). VIF <5 is considered to be reflect low level of multicollinearity, whilst VIF 5-10 and >10 indicate moderate and high levels of multicollinearity respectively (160,161). Abbreviations as before.

It is impossible to exactly match LGE and T1 images. However, in order to minimise the differences, T1-maps and LGE images were obtained at the same slice position in the scanner and analysed by experienced operators. Non-infarcted myocardium, defined as the area without LGE, includes both the salvageable myocardium as well as the myocardium supplied by non-culprit arteries. I did not differentiate the T1 changes in these two compartments for two reasons. First, it is impossible to accurately delineate the true myocardial area subtended by a coronary artery. Second, since I observed that the remote T1 is elevated and is associated with outcomes, the derivation of area at risk assuming a normal remote region is prone to errors. The exact pathophysiology behind the alterations in infarct and non-infarct T1 in these patients cannot be ascertained without direct histopathology correlates; however, it is widely considered to represent acute myocardial oedema in this setting, likely associated with myocardial necrosis and the resulting inflammation (44,52,162). Although the calculation of non-infarct T1 requires the manual matching of T1-maps and LGE images, it has the potential to be made fully-automated with the use of artificial intelligence in CMR (163). My study did not use T2-mapping, which has been shown to detect subtle oedema in the remote myocardium post-STEMI (164) but there is strong evidence that T1-mapping is a suitable alternative to detect myocardial oedema (52,72).

6.5. Conclusion

The global acute responses post-STEMI in both infarcted and non-infarcted myocardium quantified on CMR T1-mapping are independent predictors of long-term MACE, beyond conventional markers such as LVEF, infarct-size and microvascular obstruction. These insights may provide new opportunities for treatment and risk-stratification of patients with acute STEMI (***Central Illustration 6.1***).



Central Illustration 6.1 **- Non-infarct T1 and Infarct T1 Immediately After STEMI Predict Long-Term MACE.** Current assessment of myocardial tissue in patients with STEMI focuses on the infarcted myocardium, which is the area with late gadolinium enhancement (LGE) on cardiac magnetic resonance (CMR). This study describes, for the first time, the prognostic significance of myocardial injury in the entire heart using CMR T1-mapping, in both infarcted and non-infarcted myocardium (area without LGE, which includes the remote myocardium). A "lower" infarct T1 (≤1,300 ms, reflecting the presence of microvascular injury such as MVO) and a high non-infarct T1 (>1,250 ms) measured at 2 days after STEMI are associated with long-term MACE (new diagnosis of symptomatic heart failure or sustained ventricular arrhythmia or cardiac death). Abbreviations as before.

7. Conclusions and Future Directions

Diagnostic work-up and prognostication of acute myocardial injury in contemporary clinical practice is generally performed with echocardiography and ICA. Although superior in the assessment of cardiac function and characterisation of myocardial pathologies, the clinical use of CMR remains largely in stable outpatients in most centres at present. This Thesis provides fresh evidence for multi-parametric CMR's clinical utility in the acute inpatient setting, by studying four cohorts of hospitalised patients with acute myocardial injury.

Firstly, in a prospective single cohort study of hospitalised patients with suspected NSTEMI scheduled for ICA, I found that a CMR-first strategy is highly feasible, safe, offered high diagnostic yield, and demonstrated the potential to change the clinical management of up to thirty percent of patients. Such an approach can offer precision medicine as it can: a) obviate the need for ICA in patients with non-ischaemic pathologies; b) eliminate clinical uncertainty in patients with confirmed MI and multivessel coronary artery disease by identifying the infarct related artery; and c) enable the prescription of the most appropriate pharmaceutical and non-pharmaceutical therapy for each patient, according to a more confident clinical diagnosis. Given that these benefits are likely to translate to clinical and incremental cost effectiveness, my findings justify an appropriately powered randomised control trial comparing a CMR-first strategy with an ICA-first strategy, to formally test the aforementioned hypotheses.

Secondly, in a prospective case-control study of unvaccinated patients hospitalised for acute COVID-19, with or without mild acute myocardial injury, during the early part of the

pandemic, I demonstrated that acute COVID-19 was associated with mild myocardial oedema in some patients, irrespective of acute myocardial injury, when compared to matched asymptomatic uninfected controls from the community. This was the first such study of acutely ill, hospitalised COVID-19 patients, with appropriate controls. The myocardial oedema appeared to resolve during recovery, by six months after hospitalisation, without significant impact on biventricular structure and function in the acute and short-term. These findings raise the possibility that the reversible myocardial oedema observed during the acute illness may be in part due to a systemic inflammation, and is conceivable that it is also present in other systemic viral illnesses and sepsis – a hypothesis that merits investigation in the future.

Thirdly, in a prospective single cohort study of patients with late-presenting STEMI, I found that CMR pre-ICA was feasible and safe, and showed large infarct sizes, with a high CMR imaging prevalence of microvascular obstruction (MVO). By comparing the pre-ICA findings with a repeat CMR 3 days after revascularisation, I found no significant change in ventricular function or scar, but a reduction in the size of MVO. The results of this study reinforced findings from previous studies that late-presenting STEMI is associated with often irreversible and large myocardial injury, but that it is perfectly feasible to judge this using an urgent CMR-first strategy before proceeding with an urgent ICA in appropriately-selected patients. Future trials should test the clinical benefit of a CMR-first strategy in late-presenting STEMI in guiding revascularisation strategies, an approach that is akin to intracranial imaging before thrombolysis in acute stroke.

Finally, in a study of patients who had received timely reperfusion for STEMI, I found evidence of injury to both non-infarcted and infarcted myocardium on CMR T1 mapping, which, when compared to conventional CMR indices, including MVO and infarct size,

provided independent and incremental prediction of long-term risk of heart failure. This is highly supportive of the ability of native T1 mapping to detect subtle but prognostically relevant pathophysiological pan-myocardial changes in acute MI beyond conventionally-used diagnostic tools, and makes a case for recommending it as a powerful biomarker in STEMI, alongside MVO, infarct size and left ventricular ejection fraction. Moreover, by being the first body of work to show the prognostic relevance of non-infarcted myocardial injury in acute MI, it offers a potential new therapeutic target, and justifies further research, including that of the benefits of immunomodulation to enhance the long-term clinical outcomes in survivors of acute MI.

Overall, my Thesis presents new and important evidence for the potential clinical utility of non-invasive testing using acute CMR to provide more precise diagnostic and prognostic information, by differentiating the causes and assessing the extent of acute myocardial injury in hospitalised patients. This body of work supports a shift in paradigm towards a more systematic application of CMR in acute settings.

List of Tables

Table 3.1 Characteristics for All Patients and Patients Stratified by diagnosis made on Cardiovascular Magnetic Resonance performed before Invasive Coronary Angiogram 72

Table 3.2 ICA and CMR findings.....75
Table 3.3 Reclassification of clinical diagnosis with ICA using CMR 77
Table 3.4 Agreement on IRA when both CMR and ICA diagnosed MI.....80
Table 4. 1 Baseline characteristics and blood test results 91
Table 4. 2 CMR and blood test findings in controls, acute COVID-19 patients and at follow up.....93
Table 5. 1 Baseline characteristics, ICA and CMR findings.....112
Table 5.2 Absolute change in CMR indices after ICA+/-PCI in patients with paired scans. 119
Table 5.3 Absolute change in CMR indices after PCI in patients with paired scans; stratified by post-PCI TIMI-flow......120
Table 5.4 Paired analysis of CMR characteristics in patients who had PCI to culprit artery 120
Table 5.5 Paired analysis of CMR characteristics in patients with no PCI to culprit artery 120
Table 6. 1 Baseline demographics, procedural, angiographic and investigations data 138
Table 6.2 Cardiac medications on hospital discharge and at 6 months. 139
Table 6.3 Acute CMR findings stratified according to higher and lower T1 in infarcted and non-infarcted myocardium 141
Table 6.4 CMR findings and NT-proBNP levels at 6 months post-STEMI stratified according to higher and lower T1 in the non-infarcted myocardium on the acute scan. 142
Table 6.5 Univariate Cox regression analysis 145
Table 6.6 Multivariate Cox regression analysis of conventional CMR and novel T1 biomarker 146
Table 6.7 Multivariate Cox-regression analysis of CMR variables 147
Table 6.8 Multivariate backward step-wise Cox-regression analysis of clinical factors and T1 indices 149
Table 6.9 Multivariate backward step-wise Cox-regression analysis of clinical factors, conventional CMR indices and T1 indices 149
Table 6.10 Comparisons of the Predictive Power of Long-term MACE after STEMI Using Models Incorporating Conventional Cardiac Indices with and without Novel T1 Biomarkers 151
Table 6.11 Comparison of the ability of models containing conventional clinical and conventional CMR indices with and without novel T1 biomarkers to predict MACE 152
Table 6.12 Relationship between peak blood monocyte and neutrophil counts and CRP levels and T1 indices and infarct size acutely after STEMI. 156
Table 6. 13 Multicollinearity analysis of variables used in the Cox regression analysis 159

List of Figures

Figure 1. 1 Causes of acute myocardial injury. Differentiating between myocardial infarction and non-ischaemic causes is crucial to the timely and precise management of patients with acute myocardial injury. 25
Figure 1.2 Incidence of Type 1 and Type 2 AMI and non-ischaemic acute myocardial injury in hospitalized patients with cardiac symptoms and rise in high-sensitive troponin in Lothian, Scotland. Source: Shah et al AJC 2015 (2), reproduced with permission (under Creative Comms) 26
Figure 1.3 A model for interpreting myocardial injury. Ischaemic thresholds vary substantially in relation to the magnitude of the stressor and the extent of underlying cardiac disease. MI indicates myocardial infarction; URL, upper reference limit. Source: Thygesen et al; Fourth Universal Definition of Myocardial Infarction (2018). reproduced with permission (under Creative Commons CC-BY)..... 29
Figure 1.4 T2 weighted (T2W) and T1-weighted Late Gadolinium Enhancement (LGE) demonstrate myocardial oedema and necrosis in a patient with transmural inferior ST-segment Elevation Myocardial Infarction (STEMI). Adapted from Dall'Armellina, E., Piechnik, S.K., Ferreira, V.M. et al. J Cardiovas Man Reson 2012 (42). Reproduced with permission under Creative Commons CC-BY) 35
Figure 1.5 Typical appearance of T1, T2, T2*, and ECV maps in healthy subjects and in patients with myocardial disease. Arrows denote relative change in respective parametric maps**.** Source: Messroghli et al 2017 (43); Clinical recommendations for cardiovascular magnetic resonance mapping of T1, T2, T2* and extracellular volume: A consensus statement by the Society for Cardiovascular Magnetic Resonance (SCMR) endorsed by the European Association for Cardiovascular Imaging (EACVI) reproduced with permission (under Creative Commons CC-BY)..... 36
Figure 1 6 CMR's current role in the work-up of patients with MINOCA to identify non-ischaemic and ischaemic causes of acute myocardial injury. European Society of Cardiology (ESC) guideline. Source: Collet et al Eur Heart J 2021(38). ULN = Upper Limit of Normal, CAD = Coronary artery disease, MINOCA = Myocardial Infarction With Non Obstructive Coronary Arteries, IVUS = Intravascular Ultrasound, OCT = Optical Coherent Tomography, SCAD = Spontaneous Coronary Artery Dissection 39
Figure 1.7 Recommended CMR endpoints in research involving patients post-STEMI. 44

Figure 3.1 Study flow chart. NSTEMI = Non-ST-segment Elevation Myocardial Infarction. ICA = Invasive Coronary Angiogram. MI = Myocardial Infarction. MINOCA = MI with non-obstructive coronary arteries (suspected)..... 71
Figure 3.2 Break down (dot-plot) of diagnoses made on Cardiovascular Magnetic Resonance Imaging (CMR) performed prior to the Invasive Coronary Angiogram (ICA). DCM = dilated cardiomyopathy, HCM = hypertrophic cardiomyopathy 73
Figure 3.3 Reclassification of diagnosis by CMR in patients treated for MI on ICA (n=73) and NOCA on ICA (n=27). Non-ischaemic causes include myocarditis, dilated cardiomyopathy, hypertrophic cardiomyopathy, Takotsubo cardiomyopathy and right ventricular failure. NAD = No significant abnormality detected. 78

Figure 3. 4 Change in clinical management of patients with CMR prior to ICA. Such a strategy has the potential to change clinical management in 30% of the patients.....80
Figure 4.1 Photo showing a patient admitted to John Radcliffe Hospital with acute COVID-19 infection being placed in the bore of the 3T scanner in Acute Vascular Imaging Centre (AVIC) for the purposes of this research study. All the healthcare professionals involved in the research scan wore level 2 or 3 personal protection equipment (PPE) in line with their role in the care of the patient during the CMR scan and the local infection control policies of that time (this scan took place on 3rd August 2020).. 89
Figure 4.2 Myocardial tissue characteristics on CMR during acute COVID-19 in hospitalized patients compared to controls without COVID-19 from the community matched for cardiovascular risk factors. *Comparison of global myocardial T1, T2SI (T2 signal intensity) ratio and extracellular volume (ECV) fraction between outpatient controls without COVID-19 and patients with acute COVID-19 during their hospitalization. Green dotted line in the graphs denote the upper limit of normal ranges for T1, T2SI ratio and ECV in the 3T MR scanner used for this study.*.....95
Figure 4.3 Myocardial oedema as measured by CMR T1 and T2SI during acute COVID-19 and at follow up (at 6 months). Out of 23 patients scanned during acute COVID-19, 12 returned for follow up during the pandemic. All patients had normal T1 and T2SI ratio at follow up. Green dotted line in the graphs as per **Figure 4. 1**.....96
Figure 4.4 Myocardial tissue characteristics on CMR during acute COVID-19 in hospitalized patients with and without mild cardiac Troponin (CTnI) rise. Green dotted line in the graphs as per **Figure 4. 1**. Out of 23 patients, 8 had mildly elevated CTnI levels (on average 2.4-fold above normal range). Green dotted line in the graphs denote the upper limit of normal range for T1 and T2SI ratio in the 3T MR scanner used for this study.*.....*97
Figure 4.5 Multiparametric CMR imaging in 3T MRI scanner comparing acute COVID-19 patient during their hospitalization with matched control without COVID-19 from the community. *T2SI = T2 signal intensity ratio (myocardium : skeletal muscle). LGE = Late Gadolinium Enhancement. ECV = Extra cellular volume fraction. Normal values: T1<1244ms, T2<1.4. All values correspond to single slice have been shown. *100
Figure 5.1 Left and right ventricular function pre and post ICA. *24 patients underwent CMR pre-ICA and 18 underwent CMR post-ICA. Of the 18 who underwent the second CMR, 16 had had a percutaneous coronary intervention (PCI) to the culprit artery. LVEF was quantified in all patients using Short axis or long axis (biplanar) cine images. RVEF was quantified only in patients with interpretable short axis cine images. *117
Figure 5.2 Area at risk pre and post ICA. *Abbreviations and explanations as per Figure 5.1 .....*117
Figure 5.3 Infarct size pre and post ICA. *Abbreviations and explanations as per Figure 5.1 .....*118
Figure 5.4 Microvascular obstruction (MVO) size (% of total myocardial mass) pre and post ICA. *Abbreviations and explanations as per Figure 5.1 .....*118
Figure 5.5 Change in MVO size*, derived by subtracting MVO size on the pre-ICA CMR from the MVO size on the post-ICA CMR. Analysis was restricted to patients with MVO on the 1st CMR scan. Abbreviations and explanations as per Figure 5.1 .....*119
Figure 5.*6* Correlation with chest pain duration and LVEF on CMR pre-ICA. (r=-0.515; p=0.014). Abbreviations and explanations as per Figure 5.*1* 121

Figure 5.7 Correlation with chest pain duration and infarct size on CMR pre-ICA. (r=0.459; p = 0.037). Abbreviations and explanations as per Figure 5.1 121
Figure 5.8 Multiparametric CMR in a patient with late presenting STEMI with images just before and 5 days after PCI. In this example, pre-contrast T1 maps and T2w imaging show evidence of significant myocardial edema pre and post PCI. The degree of edema appears to have increased after PCI (T1 and T2 mapping and T2w imaging). The infarct size (LGE) did not change pre- and post-PCI. There was evidence of microvascular obstruction (red arrows on LGE imaging) which became smaller on the second CMR scan post-PCI on day 5. There is imaging evidence of intramyocardial haemorrhage (hypo intensity indicated by blue arrows on T2w imaging and the pink ROI on T2* mapping) at both time points. ...123

Figure 6.1 Derivation of T1 values in infarcted, non-infarcted and remote myocardium. A: Case with MVO and 'lower infarct T1.' Infarct T1 was relatively lower (<1300 ms) in patients with large MVO (>1.55% of entire myocardium). In this case, MVO represented 8.94% of the entire myocardium. Mean T1 in the entire infarcted area was low at 1242 ms whilst T1 in the entire MVO area was much lower 1166 ms. B: High non-infarct T1 (1330 ms). C: High remote T1 (1249 ms). LGE = late gadolinium enhancement.....133
Figure 6.2 Study Flowchart. Patients with STEMI were prospectively recruited between 2011 and 2018. CMR = cardiac magnetic resonance; eGFR = estimated glomerular filtration rate; MACE = major adverse cardiac events; OXAMI = Oxford Acute Myocardial Infarction Study; PPCI = primary percutaneous coronary intervention; STEMI = ST-segment elevation myocardial infarction. 137
Figure 6.3 Correlation of Non-infarct T1 on acute CMR scan With LV Systolic Function and Natriuretic Peptide Levels at 6 Months. Correlation between non-infarct T1 on acute scan with (A) N-terminal pro–B-type natriuretic peptide (NT-proBNP) (pg/L) and (B) left ventricular ejection fraction (LVEF) (%) at 6 months. LV = left ventricular; other abbreviation as in Figure 6.2.....143
Figure 6.4 Noninfarct T1 and Infarct T1 on Acute CMR Scan Predict Long-Term MACE. Kaplan-Meier survival curves showing the differences in survival from MACE between (A) patients with high T1 (>1,250 ms) and normal T1 (<1,250 ms) in the noninfarcted myocardium, (B) patients with lower (<1,300 ms) and high (≥1,300 ms) T1 values in the infarcted myocardium. Abbreviations as before.....154
Central Illustration 6.1 **- Non-infarct T1 and Infarct T1 Immediately After STEMI Predict Long-Term MACE.** Current assessment of myocardial tissue in patients with STEMI focuses on the infarcted myocardium, which is the area with late gadolinium enhancement (LGE) on cardiac magnetic resonance (CMR). This study describes, for the first time, the prognostic significance of myocardial injury in the entire heart using CMR T1-mapping, in both infarcted and non-infarcted myocardium (area without LGE, which includes the remote myocardium). A "lower" infarct T1 (≤1,300 ms, reflecting the presence of microvascular injury such as MVO) and a high non-infarct T1 (>1,250 ms) measured at 2 days after STEMI are associated with long-term MACE (new diagnosis of symptomatic heart failure or sustained ventricular arrhythmia or cardiac death). Abbreviations as before. 162

References

1. Chapman AR., Adamson PD., Mills NL. Assessment and classification of patients with myocardial injury and infarction in clinical practice. Heart 2017;103(1):10–8. Doi: 10.1136/heartjnl-2016-309530.
2. Shah ASV., McAllister DA., Mills R., et al. Sensitive Troponin Assay and the Classification of Myocardial Infarction. Am J Med 2015;128(5):493-501.e3. Doi: 10.1016/j.amjmed.2014.10.056.
3. Thygesen K., Alpert JS., Jaffe AS., et al. Fourth universal definition of myocardial infarction (2018). Eur Heart J 2019;40(3):237–69. Doi: 10.1093/eurheartj/ehy462.
4. Singh T., Chapman AR., Dweck MR., Mills NL., Newby DE. MINOCA: a heterogenous group of conditions associated with myocardial damage. Heart 2021. Doi: 10.1136/heartjnl-2020-318269.
5. Fanning JP., Nyong J., Scott IA., Aroney CN., Walters DL. Routine invasive versus conservative strategies for unstable angina and non-ST elevation myocardial infarction in the stent era. Cochrane Database of Systematic Reviews 2016;(5). Doi: 10.1002/14651858.CD004815.pub4.
6. Heitner JF., Senthilkumar A., Harrison JK., et al. Identifying the Infarct-Related Artery in Patients With Non–ST-Segment–Elevation Myocardial Infarction. Circ Cardiovasc Interv 2019;12(5):e007305. Doi: 10.1161/CIRCINTERVENTIONS.118.007305.
7. van Cauteren YJM., Smulders MW., Theunissen RALJ., et al. Cardiovascular magnetic resonance accurately detects obstructive coronary artery disease in suspected non-ST elevation myocardial infarction: a sub-analysis of the CARMENTA Trial. J Cardiovasc Magn Reson 2021;23(1):40. Doi: 10.1186/s12968-021-00723-6.
8. Smulders MW., Kietselaer BLJH., Wildberger JE., et al. Initial Imaging-Guided Strategy Versus Routine Care in Patients With Non–ST-Segment Elevation Myocardial Infarction. J Am Coll Cardiol 2019;74(20):2466–77. Doi: 10.1016/j.jacc.2019.09.027.
9. Bellenger NG., Burgess MI., Ray SG., et al. Comparison of left ventricular ejection fraction and volumes in heart failure by echocardiography, radionuclide ventriculography and cardiovascular magnetic resonance. Are they interchangeable? Eur Heart J 2000;21(16):1387–96. Doi: 10.1053/euhj.2000.2011.
10. Khan JN., McCann GP. Cardiovascular magnetic resonance imaging assessment of outcomes in acute myocardial infarction. World J Cardiol 2017;9(2):109–33. Doi: 10.4330/wjc.v9.i2.109.
11. Leiner T., Bogaert J., Friedrich MG., et al. SCMR Position Paper (2020) on clinical indications for cardiovascular magnetic resonance. J Cardiovasc Magn Reson 2020;22(1):76. Doi: 10.1186/s12968-020-00682-4.
12. Karamitsos TD., Arvanitaki A., Karvounis H., Neubauer S., Ferreira VM. Myocardial Tissue Characterization and Fibrosis by Imaging. JACC Cardiovasc Imaging 2020;13(5):1221–34. Doi: 10.1016/j.jcmg.2019.06.030.
13. Keenan NG., Captur G., McCann GP., et al. Regional variation in cardiovascular magnetic resonance service delivery across the UK. Heart 2021. Doi: 10.1136/heartjnl-2020-318667.
14. Ibanez B., Aletras AH., Arai AE., et al. Cardiac MRI Endpoints in Myocardial Infarction Experimental and Clinical Trials: JACC Scientific Expert Panel. J Am Coll Cardiol 2019;74(2):238–56. Doi: 10.1016/j.jacc.2019.05.024.

15. Kramer CM. Potential for Rapid and Cost-Effective Cardiac Magnetic Resonance in the Developing (and Developed) World. J Am Heart Assoc 2018;7(17):e010435. Doi: 10.1161/JAHA.118.010435.
16. Zhang Q., Burrage MK., Lukaschuk E., et al. Towards Replacing Late Gadolinium Enhancement with Artificial Intelligence Virtual Native Enhancement for Gadolinium-Free Cardiovascular Magnetic Resonance Tissue Characterization in Hypertrophic Cardiomyopathy. Circulation n.d.;0(0). Doi: 10.1161/CIRCULATIONAHA.121.054432.
17. Kali A., Choi E-Y., Sharif B., et al. Native T1 Mapping by 3-T CMR Imaging for Characterization of Chronic Myocardial Infarctions. JACC Cardiovasc Imaging 2015;8(9):1019–30. Doi: 10.1016/j.jcmg.2015.04.018.
18. Wang G., Lee S-E., Yang Q., et al. Multicenter Study on the Diagnostic Performance of Native-T1 Cardiac Magnetic Resonance of Chronic Myocardial Infarctions at 3T. Circ Cardiovasc Imaging 2020;13(6):e009894. Doi: 10.1161/CIRCIMAGING.119.009894.
19. Dastidar AG., McAlindon E., Rodrigues JC., et al. Remote myocardium is also affected in acute myocardial infarction: evidence from advanced CMR relaxometry. J Cardiovasc Magn Reson 2016;18(1):P219. Doi: 10.1186/1532-429X-18-S1-P219.
20. Katrukha IA., Katrukha AG. Myocardial Injury and the Release of Troponins I and T in the Blood of Patients. Clin Chem 2021;67(1):124–30. Doi: 10.1093/clinchem/hvaa281.
21. Ruparelia N., Digby JE., Jefferson A., et al. Myocardial infarction causes inflammation and leukocyte recruitment at remote sites in the myocardium and in the renal glomerulus. Inflamm Res 2013;62(5):515–25. Doi: 10.1007/s00011-013-0605-4.
22. McCarthy C., Murphy S., Cohen JA., et al. Misclassification of Myocardial Injury as Myocardial Infarction: Implications for Assessing Outcomes in Value-Based Programs. JAMA Cardiol 2019;4(5):460. Doi: 10.1001/jamacardio.2019.0716.
23. Mehta SR., Wang J., Wood DA., et al. Complete Revascularization vs Culprit Lesion–Only Percutaneous Coronary Intervention for Angina-Related Quality of Life in Patients With ST-Segment Elevation Myocardial Infarction: Results From the COMPLETE Randomized Clinical Trial. JAMA Cardiol 2022;7(11):1091–9. Doi: 10.1001/jamacardio.2022.3032.
24. Sanz-Sánchez J., Stefanini GG. Timing and completeness of revascularisation in acute coronary syndromes. Heart 2022;108(8):648–56. Doi: 10.1136/heartjnl-2020-316743.
25. Mathieu E., Ritchie H., Rodés-Guirao L., et al. Coronavirus Pandemic (COVID-19). Our World Data 2020.
26. Gray WK., Navaratnam AV., Day J., Wendon J., Briggs TWR. COVID-19 hospital activity and in-hospital mortality during the first and second waves of the pandemic in England: an observational study. Thorax 2022;77(11):1113–20. Doi: 10.1136/thoraxjnl-2021-218025.
27. Guo T., Fan Y., Chen M., et al. Cardiovascular Implications of Fatal Outcomes of Patients With Coronavirus Disease 2019 (COVID-19). JAMA Cardiol 2020;5(7):811–8. Doi: 10.1001/jamacardio.2020.1017.
28. Wei J-F., Huang F-Y., Xiong T-Y., et al. Acute myocardial injury is common in patients with COVID-19 and impairs their prognosis. Heart 2020;106(15):1154–9. Doi: 10.1136/heartjnl-2020-317007.
29. Lala A., Johnson KW., Januzzi JL., et al. Prevalence and Impact of Myocardial Injury in Patients Hospitalized With COVID-19 Infection. J Am Coll Cardiol 2020;76(5):533–46. Doi: 10.1016/j.jacc.2020.06.007.
30. Friedrich MG., Cooper LT. What we (don’t) know about myocardial injury after COVID-19. Eur Heart J 2021;42(19):1879–82. Doi: 10.1093/eurheartj/ehab145.

31. Metkus TS., Sokoll LJ., Barth AS., et al. Myocardial Injury in Severe COVID-19 Compared With Non–COVID-19 Acute Respiratory Distress Syndrome. Circulation 2021;143(6):553–65. Doi: 10.1161/CIRCULATIONAHA.120.050543.
32. Puntmann VO., Carerj ML., Wieters I., et al. Outcomes of Cardiovascular Magnetic Resonance Imaging in Patients Recently Recovered From Coronavirus Disease 2019 (COVID-19). JAMA Cardiol 2020;5(11):1265–73. Doi: 10.1001/jamacardio.2020.3557.
33. Kotecha T., Knight DS., Razvi Y., et al. Patterns of myocardial injury in recovered troponin-positive COVID-19 patients assessed by cardiovascular magnetic resonance. Eur Heart J 2021;42(19):1866–78. Doi: 10.1093/eurheartj/ehab075.
34. Joy G., Artico J., Kurdi H., et al. Prospective Case-Control Study of Cardiovascular Abnormalities 6 Months Following Mild COVID-19 in Healthcare Workers. JACC Cardiovasc Imaging 2021. Doi: 10.1016/j.jcmg.2021.04.011.
35. Kadesjö E., Roos A., Siddiqui A., Desta L., Lundbäck M., Holzmann MJ. Acute versus chronic myocardial injury and long-term outcomes. Heart 2019;105(24):1905–12. Doi: 10.1136/heartjnl-2019-315036.
36. DeFilippis AP., Chapman AR., Mills NL., et al. Assessment and Treatment of Patients With Type 2 Myocardial Infarction and Acute Nonischemic Myocardial Injury. Circulation 2019;140(20):1661–78. Doi: 10.1161/CIRCULATIONAHA.119.040631.
37. Tavakol M., Ashraf S., Brener SJ. Risks and Complications of Coronary Angiography: A Comprehensive Review. Glob J Health Sci 2012;4(1):65–93. Doi: 10.5539/gjhs.v4n1p65.
38. National Tarrif Workbook 2021.
39. Tamis-Holland JE., Jneid H., Reynolds HR., et al. Contemporary Diagnosis and Management of Patients With Myocardial Infarction in the Absence of Obstructive Coronary Artery Disease: A Scientific Statement From the American Heart Association. Circulation 2019;139(18):e891–908. Doi: 10.1161/CIR.0000000000000670.
40. Collet J-P., Thiele H., Barbato E., et al. 2020 ESC Guidelines for the management of acute coronary syndromes in patients presenting without persistent ST-segment elevation: The Task Force for the management of acute coronary syndromes in patients presenting without persistent ST-segment elevation of the European Society of Cardiology (ESC). Eur Heart J 2021;42(14):1289–367. Doi: 10.1093/eurheartj/ehaa575.
41. Fox K., Achenbach S., Bax J., et al. Multimodality imaging in cardiology: a statement on behalf of the Task Force on Multimodality Imaging of the European Association of Cardiovascular Imaging. Eur Heart J 2019;40(6):553–8. Doi: 10.1093/eurheartj/ehy669.
42. Westbrook C., Kaut Roth C., Talbot J. MRI in practice. 3rd ed. Blackwell; 2005.
43. Ismail TF., Strugnell W., Coletti C., et al. Cardiac MR: From Theory to Practice. Front Cardiovasc Med 2022;9.
44. Dall'Armellina E., Piechnik SK., Ferreira VM., et al. Cardiovascular magnetic resonance by non contrast T1-mapping allows assessment of severity of injury in acute myocardial infarction. J Cardiovasc Magn Reson 2012;14(1):15. Doi: 10.1186/1532-429X-14-15.
45. Messroghli DR., Moon JC., Ferreira VM., et al. Clinical recommendations for cardiovascular magnetic resonance mapping of T1, T2, T2* and extracellular volume: A consensus statement by the Society for Cardiovascular Magnetic Resonance (SCMR) endorsed by the European Association for Cardiovascular Imaging (EACVI). J Cardiovasc Magn Reson 2017;19(1):75. Doi: 10.1186/s12968-017-0389-8.
46. Piechnik SK., Ferreira VM., Dall'Armellina E., et al. Shortened Modified Look-Locker Inversion recovery (ShMOLLI) for clinical myocardial T1-mapping at 1.5 and 3 T

within a 9 heartbeat breathhold. J Cardiovasc Magn Reson 2010;12(1):69. Doi: 10.1186/1532-429X-12-69.
47. Ferreira VM., Schulz-Menger J., Holmvang G., et al. Cardiovascular Magnetic Resonance in Nonischemic Myocardial Inflammation: Expert Recommendations. J Am Coll Cardiol 2018;72(24):3158–76. Doi: 10.1016/j.jacc.2018.09.072.
48. Pohost GM. The History of Cardiovascular Magnetic Resonance. JACC Cardiovasc Imaging 2008;1(5):672–8. Doi: 10.1016/j.jcmg.2008.07.009.
49. Friedrich MG. Myocardial edema—a new clinical entity? Nat Rev Cardiol 2010;7(5):292–6. Doi: 10.1038/nrcardio.2010.28.
50. Friedrich MG., Marcotte F. Cardiac Magnetic Resonance Assessment of Myocarditis. Circ Cardiovasc Imaging 2013;6(5):833–9. Doi: 10.1161/CIRCIMAGING.113.000416.
51. Pelliccia F., Kaski JC., Crea F., Camici PG. Pathophysiology of Takotsubo Syndrome. Circulation 2017;135(24):2426–41. Doi: 10.1161/CIRCULATIONAHA.116.027121.
52. Ferreira VM., Piechnik SK., Dall'Armellina E., et al. Non-contrast T1-mapping detects acute myocardial edema with high diagnostic accuracy: a comparison to T2-weighted cardiovascular magnetic resonance. J Cardiovasc Magn Reson 2012;14(1):42. Doi: 10.1186/1532-429X-14-42.
53. Ferreira VM., Piechnik SK., Dall'Armellina E., et al. T(1) mapping for the diagnosis of acute myocarditis using CMR: comparison to T2-weighted and late gadolinium enhanced imaging. JACC Cardiovasc Imaging 2013;6(10):1048–58. Doi: 10.1016/j.jcmg.2013.03.008.
54. Dall'Armellina E., Karia N., Lindsay AC., et al. Dynamic Changes of Edema and Late Gadolinium Enhancement After Acute Myocardial Infarction and Their Relationship to Functional Recovery and Salvage Index. Circ Cardiovasc Imaging 2011;4(3):228–36. Doi: 10.1161/CIRCIMAGING.111.963421.
55. Luetkens JA., Homsi R., Dabir D., et al. Comprehensive Cardiac Magnetic Resonance for Short-Term Follow-Up in Acute Myocarditis. J Am Heart Assoc 2016;5(7):e003603. Doi: 10.1161/JAHA.116.003603.
56. Mileva N., Paolisso P., Gallinoro E., et al. Diagnostic and Prognostic Role of Cardiac Magnetic Resonance in MINOCA. JACC Cardiovasc Imaging 2023;16(3):376–89. Doi: 10.1016/j.jcmg.2022.12.029.
57. Dastidar AG., Baritussio A., De Garate E., et al. Prognostic Role of CMR and Conventional Risk Factors in Myocardial Infarction With Nonobstructed Coronary Arteries. JACC Cardiovasc Imaging 2019;12(10):1973–82. Doi: 10.1016/j.jcmg.2018.12.023.
58. Kwong RY., Schussheim AE., Rekhraj S., et al. Detecting acute coronary syndrome in the emergency department with cardiac magnetic resonance imaging. Circulation 2003;107(4):531–7. Doi: 10.1161/01.cir.0000047527.11221.29.
59. Cury RC., Shash K., Nagurney JT., et al. Cardiac Magnetic Resonance With T2-Weighted Imaging Improves Detection of Patients With Acute Coronary Syndrome in the Emergency Department. Circulation 2008;118(8):837–44. Doi: 10.1161/CIRCULATIONAHA.107.740597.
60. Luetkens JA., Isaak A., Öztürk C., et al. Cardiac MRI in Suspected Acute COVID-19 Myocarditis. Radiol Cardiothorac Imaging 2021;3(2):e200628. Doi: 10.1148/ryct.2021200628.
61. Luetkens JA., Isaak A., Zimmer S., et al. Diffuse Myocardial Inflammation in COVID-19 Associated Myocarditis Detected by Multiparametric Cardiac Magnetic

Resonance Imaging. Circ Cardiovasc Imaging 2020;13(5):e010897. Doi: 10.1161/CIRCIMAGING.120.010897.
62. Petersen SE., Friedrich MG., Leiner T., et al. Cardiovascular Magnetic Resonance for Patients With COVID-19. JACC Cardiovasc Imaging 2021. Doi: 10.1016/j.jcmg.2021.08.021.
63. Ferreira VM., Plein S., Wong TC., et al. Cardiovascular magnetic resonance for evaluation of cardiac involvement in COVID-19: recommendations by the Society for Cardiovascular Magnetic Resonance. J Cardiovasc Magn Reson 2023;25(1):21. Doi: 10.1186/s12968-023-00933-0.
64. Basso C., Thiene G. The pathophysiology of myocardial reperfusion: a pathologist's perspective. Heart 2006;92(11):1559–62. Doi: 10.1136/hrt.2005.086959.
65. Lee WW., Marinelli B., van der Laan AM., et al. PET/MRI of inflammation in myocardial infarction. J Am Coll Cardiol 2012;59(2):153–63. Doi: 10.1016/j.jacc.2011.08.066.
66. Reinstadler SJ., Stiermaier T., Liebetrau J., et al. Prognostic Significance of Remote Myocardium Alterations Assessed by Quantitative Noncontrast T1 Mapping in ST-Segment Elevation Myocardial Infarction. JACC Cardiovasc Imaging 2018;11(3):411–9. Doi: 10.1016/j.jcmg.2017.03.015.
67. About OxAMI. Available at: https://oxami.org.uk/about-oxami/. Accessed April 9, 2023.
68. WMA - The World Medical Association-WMA Declaration of Helsinki – Ethical Principles for Medical Research Involving Human Subjects n.d. Available at: https://www.wma.net/policies-post/wma-declaration-of-helsinki-ethical-principles-for-medical-research-involving-human-subjects/. Accessed April 11, 2023.
69. Alkhalil M., Borlotti A., De Maria GL., et al. Dynamic changes in injured myocardium, very early after acute myocardial infarction, quantified using T1 mapping cardiovascular magnetic resonance. J Cardiovasc Magn Reson 2018;20(1):82. Doi: 10.1186/s12968-018-0506-3.
70. Alkhalil M., Borlotti A., De Maria GL., et al. Hyper-acute cardiovascular magnetic resonance T1 mapping predicts infarct characteristics in patients with ST elevation myocardial infarction. J Cardiovasc Magn Reson 2020;22(1):3. Doi: 10.1186/s12968-019-0593-9.
71. Scarsini R., Shanmuganathan M., De Maria GL., et al. Coronary Microvascular Dysfunction Assessed by Pressure Wire and CMR After STEMI Predicts Long-Term Outcomes. JACC Cardiovasc Imaging 2021;14(10):1948–59. Doi: 10.1016/j.jcmg.2021.02.023.
72. Bulluck H., White SK., Rosmini S., et al. T1 mapping and T2 mapping at 3T for quantifying the area-at-risk in reperfused STEMI patients. J Cardiovasc Magn Reson 2015;17(1):73. Doi: 10.1186/s12968-015-0173-6.
73. Bondarenko O., Beek AM., Hofman MBM., et al. Standardizing the definition of hyperenhancement in the quantitative assessment of infarct size and myocardial viability using delayed contrast-enhanced CMR. J Cardiovasc Magn Reson Off J Soc Cardiovasc Magn Reson 2005;7(2):481–5. Doi: 10.1081/jcmr-200053623.
74. Liu D., Borlotti A., Viliani D., et al. CMR Native T1 Mapping Allows Differentiation of Reversible Versus Irreversible Myocardial Damage in ST-Segment-Elevation Myocardial Infarction: An OxAMI Study (Oxford Acute Myocardial Infarction). Circ Cardiovasc Imaging 2017;10(8):e005986. Doi: 10.1161/CIRCIMAGING.116.005986.

75. Klem I., Heiberg E., Van Assche L., et al. Sources of variability in quantification of cardiovascular magnetic resonance infarct size - reproducibility among three core laboratories. J Cardiovasc Magn Reson 2017;19(1):62. Doi: 10.1186/s12968-017-0378-y.
76. Carrick D., Haig C., Ahmed N., et al. Temporal Evolution of Myocardial Hemorrhage and Edema in Patients After Acute ST-Segment Elevation Myocardial Infarction: Pathophysiological Insights and Clinical Implications. J Am Heart Assoc Cardiovasc Cerebrovasc Dis 2016;5(2):e002834. Doi: 10.1161/JAHA.115.002834.
77. Triadyaksa P., Oudkerk M., Sijens PE. Cardiac T2* mapping: Techniques and clinical applications. J Magn Reson Imaging 2020;52(5):1340–51. Doi: 10.1002/jmri.27023.
78. Ganame J., Messalli G., Dymarkowski S., et al. Impact of myocardial haemorrhage on left ventricular function and remodelling in patients with reperfused acute myocardial infarction. Eur Heart J 2009;30(12):1440–9. Doi: 10.1093/eurheartj/ehp093.
79. White SK., Sado DM., Fontana M., et al. T1 Mapping for Myocardial Extracellular Volume Measurement by CMR. JACC Cardiovasc Imaging 2013;6(9):955–62. Doi: 10.1016/j.jcmg.2013.01.011.
80. Scarsini R., De Maria GL., Shanmuganathan M., et al. Pressure-bounded coronary flow reserve to assess the extent of microvascular dysfunction in patients with ST-elevation acute myocardial infarction. EuroIntervention 2021;16(17):1434–43. Doi: 10.4244/EIJ-D-19-00674.
81. TIMI Study Group The Thrombolysis in Myocardial Infarction (TIMI) trial. Phase I findings. N Engl J Med 1985;312(14):932–6. Doi: 10.1056/NEJM198504043121437.
82. Sianos G., Papafaklis MI., Serruys PW. Angiographic thrombus burden classification in patients with ST-segment elevation myocardial infarction treated with percutaneous coronary intervention. J Invasive Cardiol 2010;22(10 Suppl B):6B-14B.
83. Angiographic Assessment of Myocardial Reperfusion in Patients Treated With Primary Angioplasty for Acute Myocardial Infarction | Circulation. Available at: https://www.ahajournals.org/doi/10.1161/01.CIR.97.23.2302. Accessed April 12, 2023.
84. Amsterdam EA., Wenger NK., Brindis RG., et al. 2014 AHA/ACC Guideline for the Management of Patients With Non–ST-Elevation Acute Coronary Syndromes. Circulation 2014;130(25):e344–426. Doi: 10.1161/CIR.0000000000000134.
85. Bueno H. Epidemiology of acute coronary syndromes. In: James S, Camm AJ, Lüscher TF, Maurer G, and Serruys PW, editors. The ESC Textbook of Cardiovascular Medicine. Oxford University Press; 2018. p. 0.
86. NICOR | Myocardial Ischaemia/MINAP (Heart Attack audit) n.d. Available at: https://www.nicor.org.uk/myocardial-ischaemia-minap-heart-attack-audit/. Accessed April 17, 2023.
87. Sörensson P., Ekenbäck C., Lundin M., et al. Early Comprehensive Cardiovascular Magnetic Resonance Imaging in Patients With Myocardial Infarction With Nonobstructive Coronary Arteries. JACC Cardiovasc Imaging 2021;14(9):1774–83. Doi: 10.1016/j.jcmg.2021.02.021.
88. Liang K., Nakou E., Del Buono MG., Montone RA., D'Amario D., Bucciarelli-Ducci C. The Role of Cardiac Magnetic Resonance in Myocardial Infarction and Non-obstructive Coronary Arteries. Front Cardiovasc Med 2022;8:821067. Doi: 10.3389/fcvm.2021.821067.
89. Niccoli G., Scalone G., Crea F. Acute myocardial infarction with no obstructive coronary atherosclerosis: mechanisms and management. Eur Heart J 2015;36(8):475–81. Doi: 10.1093/eurheartj/ehu469.
90. Ibrahim H., Sharma PK., Cohen DJ., et al. Multivessel Versus Culprit Vessel–Only Percutaneous Coronary Intervention Among Patients With Acute Myocardial Infarction:

Insights From the TRANSLATE-ACS Observational Study. J Am Heart Assoc n.d.;6(10):e006343. Doi: 10.1161/JAHA.117.006343.
91. Treibel TA., White SK., Moon JC. Myocardial Tissue Characterization: Histological and Pathophysiological Correlation. Curr Cardiovasc Imaging Rep 2014;7(3):9254. Doi: 10.1007/s12410-013-9254-9.
92. Scarsini R., Shanmuganathan M., De Maria GL., et al. Coronary Microvascular Dysfunction Assessed by Pressure Wire and CMR After STEMI Predicts Long-Term Outcomes. JACC Cardiovasc Imaging 2021. Doi: 10.1016/j.jcmg.2021.02.023.
93. Troponin I - Clinical Biochemistry. Available at: https://www.ouh.nhs.uk/biochemistry/tests/tests-catalogue/troponin-1.aspx. Accessed April 17, 2023.
94. Schulz-Menger J., Bluemke DA., Bremerich J., et al. Standardized image interpretation and post-processing in cardiovascular magnetic resonance - 2020 update. J Cardiovasc Magn Reson 2020;22(1):19. Doi: 10.1186/s12968-020-00610-6.
95. null null., Cerqueira MD., Weissman NJ., et al. Standardized Myocardial Segmentation and Nomenclature for Tomographic Imaging of the Heart. Circulation 2002;105(4):539–42. Doi: 10.1161/hc0402.102975.
96. Gudenkauf B., Hays AG., Tamis-Holland J., et al. Role of Multimodality Imaging in the Assessment of Myocardial Infarction With Nonobstructive Coronary Arteries: Beyond Conventional Coronary Angiography. J Am Heart Assoc 2022;11(1):e022787. Doi: 10.1161/JAHA.121.022787.
97. van Cauteren YJM., Smulders MW., Theunissen RALJ., et al. Cardiovascular magnetic resonance accurately detects obstructive coronary artery disease in suspected non-ST elevation myocardial infarction: a sub-analysis of the CARMENTA Trial. J Cardiovasc Magn Reson 2021;23(1):40. Doi: 10.1186/s12968-021-00723-6.
98. Smulders MW., Bekkers SCAM., Kim HW., Van Assche LMR., Parker MA., Kim RJ. Performance of CMR Methods for Differentiating Acute From Chronic MI. JACC Cardiovasc Imaging 2015;8(6):669–79. Doi: 10.1016/j.jcmg.2014.12.030.
99. Eitel I., Desch S., Sareban M., et al. Prognostic significance and magnetic resonance imaging findings in aborted myocardial infarction after primary angioplasty. Am Heart J 2009;158(5):806–13. Doi: 10.1016/j.ahj.2009.08.025.
100. Williams MGL., Liang K., De Garate E., et al. Peak Troponin and CMR to Guide Management in Suspected ACS and Nonobstructive Coronary Arteries. JACC Cardiovasc Imaging 2022;15(9):1578–87. Doi: 10.1016/j.jcmg.2022.03.017.
101. Zhang Q., Burrage MK., Shanmuganathan M., et al. Artificial Intelligence for Contrast-free MRI: Scar Assessment in Myocardial Infarction Using Deep Learning-based Virtual Native Enhancement (VNE). Circulation n.d.;0(0). Doi: 10.1161/CIRCULATIONAHA.122.060137.
102. Nazir MS., Bustin A., Hajhosseiny R., et al. High-resolution non-contrast free-breathing coronary cardiovascular magnetic resonance angiography for detection of coronary artery disease: validation against invasive coronary angiography. J Cardiovasc Magn Reson 2022;24(1):26. Doi: 10.1186/s12968-022-00858-0.
103. Shafiabadi Hassani N., Talakoob H., Karim H., Mozafari Bazargany MH., Rastad H. Cardiac Magnetic Resonance Imaging Findings in 2954 COVID-19 Adult Survivors: A Comprehensive Systematic Review. J Magn Reson Imaging JMRI 2021. Doi: 10.1002/jmri.27852.
104. Petersen SE., Friedrich MG., Leiner T., et al. Cardiovascular Magnetic Resonance for Patients With COVID-19. JACC Cardiovasc Imaging 2021. Doi: 10.1016/j.jcmg.2021.08.021.

105. Ng M-Y., Ferreira VM., Leung ST., et al. Patients Recovered From COVID-19 Show Ongoing Subclinical Myocarditis as Revealed by Cardiac Magnetic Resonance Imaging. JACC Cardiovasc Imaging 2020;13(11):2476–8. Doi: 10.1016/j.jcmg.2020.08.012.
106. Joy G., Artico J., Kurdi H., et al. Prospective Case-Control Study of Cardiovascular Abnormalities 6 Months Following Mild COVID-19 in Healthcare Workers. JACC Cardiovasc Imaging 2021;14(11):2155–66. Doi: 10.1016/j.jcmg.2021.04.011.
107. Siddiqui Y., Crouser ED., Raman SV. Nonischemic Myocardial Changes Detected by Cardiac Magnetic Resonance in Critical Care Patients with Sepsis. Am J Respir Crit Care Med 2013;188(8):1037–9. Doi: 10.1164/rccm.201304-0744LE.
108. World Health Organization Use of chest imaging in COVID-19: a rapid advice guide, 11 June 2020. World Health Organization; 2020.
109. Carapella V., Puchta H., Lukaschuk E., et al. Standardized image post-processing of cardiovascular magnetic resonance T1-mapping reduces variability and improves accuracy and consistency in myocardial tissue characterization. Int J Cardiol 2020;298:128–34. Doi: 10.1016/j.ijcard.2019.08.058.
110. Burrage MK., Shanmuganathan M., Zhang Q., et al. Cardiac stress T1-mapping response and extracellular volume stability of MOLLI-based T1-mapping methods. Sci Rep 2021;11(1):13568. Doi: 10.1038/s41598-021-92923-4.
111. Carbone I., Childs H., Aljizeeri A., Merchant N., Friedrich MG. Importance of Reference Muscle Selection in Quantitative Signal Intensity Analysis of T2-Weighted Images of Myocardial Edema Using a T2 Ratio Method. BioMed Res Int 2015;2015:232649. Doi: 10.1155/2015/232649.
112. Chung MK., Zidar DA., Bristow MR., et al. COVID-19 and Cardiovascular Disease. Circ Res 2021;128(8):1214–36. Doi: 10.1161/CIRCRESAHA.121.317997.
113. Pollack A., Kontorovich AR., Fuster V., Dec GW. Viral myocarditis—diagnosis, treatment options, and current controversies. Nat Rev Cardiol 2015;12(11):670–80. Doi: 10.1038/nrcardio.2015.108.
114. Nakamori S., Fahmy A., Jang J., et al. Changes in Myocardial Native T1 and T2 After Exercise Stress: A Noncontrast CMR Pilot Study. JACC Cardiovasc Imaging 2020;13(3):667–80. Doi: 10.1016/j.jcmg.2019.05.019.
115. Nickander J., Themudo R., Thalén S., et al. The relative contributions of myocardial perfusion, blood volume and extracellular volume to native T1 and native T2 at rest and during adenosine stress in normal physiology. J Cardiovasc Magn Reson 2019;21(1):73. Doi: 10.1186/s12968-019-0585-9.
116. Chen B-H., Shi N-N., Wu C-W., et al. Early cardiac involvement in patients with acute COVID-19 infection identified by multiparametric cardiovascular magnetic resonance imaging. Eur Heart J - Cardiovasc Imaging 2021;22(8):844–51. Doi: 10.1093/ehjci/jeab042.
117. Shi S., Qin M., Shen B., et al. Association of Cardiac Injury With Mortality in Hospitalized Patients With COVID-19 in Wuhan, China. JAMA Cardiol 2020;5(7):802–10. Doi: 10.1001/jamacardio.2020.0950.
118. Mitacchione G., Schiavone M., Gasperetti A., Forleo GB. Ventricular tachycardia storm management in a COVID-19 patient: a case report. Eur Heart J Case Rep 2020;4(FI1):1–6. Doi: 10.1093/ehjcr/ytaa217.
119. Coromilas EJ., Kochav S., Goldenthal I., et al. Worldwide Survey of COVID-19–Associated Arrhythmias. Circ Arrhythm Electrophysiol 2021;14(3):e009458. Doi: 10.1161/CIRCEP.120.009458.

120. Raman B., Cassar MP., Tunnicliffe EM., et al. Medium-term effects of SARS-CoV-2 infection on multiple vital organs, exercise capacity, cognition, quality of life and mental health, post-hospital discharge. EClinicalMedicine 2021;31:100683. Doi: 10.1016/j.eclinm.2020.100683.
121. Cassar MP., Tunnicliffe EM., Petousi N., et al. Symptom Persistence Despite Improvement in Cardiopulmonary Health – Insights from longitudinal CMR, CPET and lung function testing post-COVID-19. EClinicalMedicine 2021;41:101159. Doi: 10.1016/j.eclinm.2021.101159.
122. Satterfield BA., Bhatt DL., Gersh BJ. Cardiac involvement in the long-term implications of COVID-19. Nat Rev Cardiol 2021:1–10. Doi: 10.1038/s41569-021-00631-3.
123. Pagnesi M., Baldetti L., Beneduce A., et al. Pulmonary hypertension and right ventricular involvement in hospitalised patients with COVID-19. Heart 2020;106(17):1324–31. Doi: 10.1136/heartjnl-2020-317355.
124. LATE Investigators. Late Assessment of Thrombolytic Efficacy (LATE) study with alteplase 6-24 hours after onset of acute myocardial infarction. The Lancet 1993;342(8874):759–66. Doi: 10.1016/0140-6736(93)91538-W.
125. Ndrepepa G., Kastrati A., Mehilli J., Antoniucci D., Schömig A. Mechanical Reperfusion and Long-term Mortality in Patients With Acute Myocardial Infarction Presenting 12 to 48 Hours From Onset of Symptoms. JAMA 2009;301(5):487–8. Doi: 10.1001/jama.2009.32.
126. Hochman JS., Lamas GA., Buller CE., et al. Coronary Intervention for Persistent Occlusion after Myocardial Infarction. N Engl J Med 2006;355(23):2395–407. Doi: 10.1056/NEJMoa066139.
127. Cho KH., Han X., Ahn JH., et al. Long-Term Outcomes of Patients With Late Presentation of ST-Segment Elevation Myocardial Infarction. J Am Coll Cardiol 2021;77(15):1859–70. Doi: 10.1016/j.jacc.2021.02.041.
128. Schömig A., Mehilli J., Antoniucci D., et al. Mechanical reperfusion in patients with acute myocardial infarction presenting more than 12 hours from symptom onset: a randomized controlled trial. JAMA 2005;293(23):2865–72. Doi: 10.1001/jama.293.23.2865.
129. Cohen M., Boiangiu C., Abidi M. Therapy for ST-Segment Elevation Myocardial Infarction Patients Who Present Late or Are Ineligible for Reperfusion Therapy. J Am Coll Cardiol 2010;55(18):1895–906. Doi: 10.1016/j.jacc.2009.11.087.
130. Ibanez B., James S., Agewall S., et al. 2017 ESC Guidelines for the management of acute myocardial infarction in patients presenting with ST-segment elevation: The Task Force for the management of acute myocardial infarction in patients presenting with ST-segment elevation of the European Society of Cardiology (ESC). Eur Heart J 2018;39(2):119–77. Doi: 10.1093/eurheartj/ehx393.
131. de Waha S., Patel MR., Granger CB., et al. Relationship between microvascular obstruction and adverse events following primary percutaneous coronary intervention for ST-segment elevation myocardial infarction: an individual patient data pooled analysis from seven randomized trials. Eur Heart J 2017;38(47):3502–10. Doi: 10.1093/eurheartj/ehx414.
132. Reinstadler SJ., Stiermaier T., Reindl M., et al. Intramyocardial haemorrhage and prognosis after ST-elevation myocardial infarction. Eur Heart J - Cardiovasc Imaging 2019;20(2):138–46. Doi: 10.1093/ehjci/jey101.

133. Ghugre NR., Ramanan V., Pop M., et al. Quantitative tracking of edema, hemorrhage, and microvascular obstruction in subacute myocardial infarction in a porcine model by MRI. Magn Reson Med 2011;66(4):1129–41. Doi: 10.1002/mrm.22855.
134. Kumar A., Green JD., Sykes JM., et al. Detection and Quantification of Myocardial Reperfusion Hemorrhage Using T2*-Weighted CMR. JACC Cardiovasc Imaging 2011;4(12):1274–83. Doi: 10.1016/j.jcmg.2011.08.016.
135. Carrick D., Haig C., Ahmed N., et al. Myocardial Hemorrhage After Acute Reperfused ST-Segment–Elevation Myocardial Infarction. Circ Cardiovasc Imaging 2016;9(1):e004148. Doi: 10.1161/CIRCIMAGING.115.004148.
136. Shanmuganathan M., Masi A., Burrage MK., et al. Acute Response in the Noninfarcted Myocardium Predicts Long-Term Major Adverse Cardiac Events After STEMI. JACC Cardiovasc Imaging 2023;16(1):46–59. Doi: 10.1016/j.jcmg.2022.09.015.
137. Sahan KM., Channon KM., Choudhury RP., Kharbanda RK., Lee R., Sheehan M. Refining the Enrolment Process in Emergency Medicine Research. Eur J Cardiovasc Med 2016;4(1):506–10. Doi: 10.5083/ejcm.20424884.147.
138. Zhang Q., Werys K., Popescu IA., et al. Quality assurance of quantitative cardiac T1-mapping in multicenter clinical trials - A T1 phantom program from the hypertrophic cardiomyopathy registry (HCMR) study. Int J Cardiol 2021;330:251–8. Doi: 10.1016/j.ijcard.2021.01.026.
139. Guan X., Chen Y., Yang H-J., et al. Assessment of intramyocardial hemorrhage with dark-blood T2*-weighted cardiovascular magnetic resonance. J Cardiovasc Magn Reson 2021;23:88. Doi: 10.1186/s12968-021-00787-4.
140. Keeley EC., Boura JA., Grines CL. Primary angioplasty versus intravenous thrombolytic therapy for acute myocardial infarction: a quantitative review of 23 randomised trials. The Lancet 2003;361(9351):13–20. Doi: 10.1016/S0140-6736(03)12113-7.
141. Ki Y-J., Kang J., Yang H-M., et al. Immediate Compared With Delayed Percutaneous Coronary Intervention for Patients With ST-Segment–Elevation Myocardial Infarction Presenting ≥12 Hours After Symptom Onset Is Not Associated With Improved Clinical Outcome. Circ Cardiovasc Interv 2021;14(5):e009863. Doi: 10.1161/CIRCINTERVENTIONS.120.009863.
142. Nepper-Christensen L., Lønborg J., Høfsten DE., et al. Benefit From Reperfusion With Primary Percutaneous Coronary Intervention Beyond 12 Hours of Symptom Duration in Patients With ST-Segment–Elevation Myocardial Infarction. Circ Cardiovasc Interv 2018;11(9):e006842. Doi: 10.1161/CIRCINTERVENTIONS.118.006842.
143. Kloner RA. Does reperfusion injury exist in humans? J Am Coll Cardiol 1993;21(2):537–45. Doi: 10.1016/0735-1097(93)90700-B.
144. Busk M., Kaltoft A., Nielsen SS., et al. Infarct size and myocardial salvage after primary angioplasty in patients presenting with symptoms for <12 h vs. 12–72 h. Eur Heart J 2009;30(11):1322–30. Doi: 10.1093/eurheartj/ehp113.
145. Alkhalil M., Choudhury RP. Reperfusion Treatment in Late Presentation Acute Myocardial Infarction. Circ Cardiovasc Interv 2018;11(9):e007287. Doi: 10.1161/CIRCINTERVENTIONS.118.007287.
146. Wu KC. CMR of microvascular obstruction and hemorrhage in myocardial infarction. J Cardiovasc Magn Reson 2012;14(1):68. Doi: 10.1186/1532-429X-14-68.
147. De Maria GL., Alkhalil M., Wolfrum M., et al. Index of Microcirculatory Resistance as a Tool to Characterize Microvascular Obstruction and to Predict Infarct Size Regression in Patients With STEMI Undergoing Primary PCI. JACC Cardiovasc Imaging 2019;12(5):837–48. Doi: 10.1016/j.jcmg.2018.02.018.

148. Szummer K., Jernberg T., Wallentin L. From Early Pharmacology to Recent Pharmacology Interventions in Acute Coronary Syndromes. J Am Coll Cardiol 2019;74(12):1618–36. Doi: 10.1016/j.jacc.2019.03.531.
149. Thackeray JT., Hupe HC., Wang Y., et al. Myocardial Inflammation Predicts Remodeling and Neuroinflammation After Myocardial Infarction. J Am Coll Cardiol 2018;71(3):263–75. Doi: 10.1016/j.jacc.2017.11.024.
150. Carrick D., Haig C., Rauhalammi S., et al. Pathophysiology of LV Remodeling in Survivors of STEMI: Inflammation, Remote Myocardium, and Prognosis. JACC Cardiovasc Imaging 2015;8(7):779–89. Doi: 10.1016/j.jcmg.2015.03.007.
151. Guerra MS., Roncon-Albuquerque R., Lourenço AP., Falcão-Pires I., Cibrão-Coutinho P., Leite-Moreira AF. Remote myocardium gene expression after 30 and 120 min of ischaemia in the rat. Exp Physiol 2006;91(2):473–80. Doi: 10.1113/expphysiol.2005.032557.
152. Bulluck H., Rosmini S., Abdel-Gadir A., et al. Automated Extracellular Volume Fraction Mapping Provides Insights Into the Pathophysiology of Left Ventricular Remodeling Post–Reperfused ST-Elevation Myocardial Infarction. J Am Heart Assoc n.d.;5(7):e003555. Doi: 10.1161/JAHA.116.003555.
153. Carrick D., Haig C., Rauhalammi S., et al. Prognostic significance of infarct core pathology revealed by quantitative non-contrast in comparison with contrast cardiac magnetic resonance imaging in reperfused ST-elevation myocardial infarction survivors. Eur Heart J 2016;37(13):1044–59. Doi: 10.1093/eurheartj/ehv372.
154. Carapella V., Puchta H., Lukaschuk E., et al. Standardized image post-processing of cardiovascular magnetic resonance T1-mapping reduces variability and improves accuracy and consistency in myocardial tissue characterization. Int J Cardiol 2020;298:128–34. Doi: 10.1016/j.ijcard.2019.08.058.
155. Zhang L., Yang ZG., Xu H., et al. Histological Validation of Cardiovascular Magnetic Resonance T1 Mapping for Assessing the Evolution of Myocardial Injury in Myocardial Infarction: An Experimental Study. Korean J Radiol 2020;21(12):1294–304. Doi: 10.3348/kjr.2020.0107.
156. Biesbroek PS., Amier RP., Teunissen PaulFA., et al. Changes in remote myocardial tissue after acute myocardial infarction and its relation to cardiac remodeling: A CMR T1 mapping study. PLoS ONE 2017;12(6):e0180115. Doi: 10.1371/journal.pone.0180115.
157. Eitel I., Stiermaier T., Lange T., et al. Cardiac Magnetic Resonance Myocardial Feature Tracking for Optimized Prediction of Cardiovascular Events Following Myocardial Infarction. JACC Cardiovasc Imaging 2018;11(10):1433–44. Doi: 10.1016/j.jcmg.2017.11.034.
158. Mewton N., Croisille P., Revel D., Weber O., Higgins CB., Saeed M. Left ventricular postmyocardial infarction remodeling studied by combining MR-tagging with delayed MR contrast enhancement. Invest Radiol 2008;43(4):219–28. Doi: 10.1097/RLI.0b013e318161613e.
159. Eitel I., Wöhrle J., Suenkel H., et al. Intracoronary Compared With Intravenous Bolus Abciximab Application During Primary Percutaneous Coronary Intervention in ST-Segment Elevation Myocardial Infarction: Cardiac Magnetic Resonance Substudy of the AIDA STEMI Trial. J Am Coll Cardiol 2013;61(13):1447–54. Doi: 10.1016/j.jacc.2013.01.048.
160. Arezoo B., Midi H. Robust Estimations as a Remedy for Multicollinearity Caused by Multiple High Leverage Points. J Math Stat 2009;5. Doi: 10.3844/jmssp.2009.311.321.
161. Stephanie Variance Inflation Factor. Statistics How To. Available at: https://www.statisticshowto.com/variance-inflation-factor/. Accessed May 9, 2022.

162. Higgins CB., Herfkens R., J. Lipton M., et al. Nuclear magnetic resonance imaging of acute myocardial infarction in dogs: Alterations in magnetic relaxation times. Am J Cardiol 1983;52(1):184–8. Doi: 10.1016/0002-9149(83)90093-0.
163. Zhang Q., Burrage MK., Lukaschuk E., et al. Toward Replacing Late Gadolinium Enhancement With Artificial Intelligence Virtual Native Enhancement for Gadolinium-Free Cardiovascular Magnetic Resonance Tissue Characterization in Hypertrophic Cardiomyopathy. Circulation 2021;144(8):589–99. Doi: 10.1161/CIRCULATIONAHA.121.054432.
164. Fernández-Jiménez R., Barreiro-Pérez M., Martin-García A., et al. Dynamic Edematous Response of the Human Heart to Myocardial Infarction. Circulation 2017;136(14):1288–300. Doi: 10.1161/CIRCULATIONAHA.116.025582.